Spectroscopic studies of proteins in reversed micelles

Promotor : dr. C. Veeger, hoogleraar in de Biochemie

Co-promotor: dr. A.J.W.G. Visser, universitair hoofddocent

C.H.W. Vos

Spectroscopic studies of proteins in reversed micelles

Proefschrift

ter verkrijging van de graad van
doctor in de landbouwwetenschappen,
op gezag van de rector magnificus,
dr. H.C. van der Plas,
in het openbaar te verdedigen
op woensdag 19 oktober 1988
des namiddags te vier uur in de aula
van de Landbouwuniversiteit te Wageningen.

ISN: 437061

STELLINGEN

1. Meier en Luisi presenteren fluorescentie emissiespectra van paardelever alcohol dehydrogenase in Aerosol-OT omgekeerde micellen zonder daarbij essentiele parameters als de excitatiegolflengte en de eiwitconcentratie te vermelden. Dit doet veel, zo niet alles, af aan de bruikbaarheid en de reproduceerbaarheid van de resultaten.

   Meier,P. & Luisi,P.L. (1980) J. Solid-Phase Biochem. **5**, 269-282.

2. Pileni *et al.* baseren de conclusie, dat cytochroom c zich in het grensvlak van Aerosol-OT micellen bevindt, op onvoldoende experimentele gegevens.

   Pileni,M.P., Zemb,T. & Petit,C. (1985) Chem. Phys. Lett. **118**, 414-420.

3. Het observeren van een derde fluorescentie levensduur bij paardelever alcohol dehydrogenase door Demmer *et al.* kan worden veroorzaakt door het feit, dat zij hun metingen bij een constante ionsterkte van 0.3 M hebben gedaan.

   Demmer,D.R., James,D.R., Steer,R.P. & Verrall,R.E. (1987) Photochem. Photobiol. **45**, 39-48.

4. Berekeningen van secondaire structuurkenmerken van eiwitmoleculen door het fitten van circulair dichroisme spectra met een lineaire combinatie van een set basisspectra zijn, vanwege de instabiliteit van het stelsel vergelijkingen, zeer gevoelig voor experimentele onnauwkeurigheden.

   Provencher,S.W. & Glockner,J. (1981) Biochemistry **20**, 33-37.

5. Ondanks de toegenomen beschikbaarheid van computers is, bij de interpretatie van kinetische gegevens van enzymreacties, het gebruik van Lineweaver-Burk plots nog niet uit te bannen.

6. Het op voorhand vastleggen van een functie, bij de berekening van de verdeling van adsorptie-energieen, moet worden afgewezen, omdat er methoden bestaan, die tot goede resultaten komen zonder beperking aan de vorm van deze verdeling.

   Vos,K. & Koopal,L.K. (1985) J. Colloid Interface Sci. **105**, 183-196.

7. Bij de huidige toename van het luchtverkeer valt binnen afzienbare tijd een tekort aan luchtruim te verwachten.

8. In mei 1988 is in Nederland een poging gedaan om de gemiddelde snelheid op de autosnelwegen te verlagen door de maximum snelheid te verhogen.

9. Veel uitlaatgaskatalysatoren zullen na de buitenlandse vakantie alleen nog maar dienen als herinnering aan het genoten belastingvoordeel bij de aanschaf van de auto.

10. Promovendi doen het met artikelen.

Stellingen bij het proefschrift
"Spectroscopic Studies of Proteins in Reversed Micelles"
Kees Vos, 19 oktober 1988.

"Misschien is niets geheel waar en zelfs dat niet."

Multatuli

Voor Miranda
en mijn ouders.

VOORWOORD

Dit proefschrift beschrijft het onderzoek, dat ik in de periode januari 1985 tot april 1987 heb uitgevoerd bij de vakgroep Biochemie van de Landbouwuniversiteit.

Uiteraard zijn meerdere mensen hierbij betrokken geweest. Enkelen daarvan wil ik hier noemen. Allereerst is dat Ton Visser, die vanaf november 1984, tijdens de laatste fase van mijn doctoraalstudie, hard heeft meegewerkt aan mijn wetenschappelijke vorming. Ook Prof. Dr. C. Veeger en Colja Laane hebben grote invloed gehad op het verloop van het onderzoek.

Van buiten de vakgroep Biochemie wil ik nog noemen Arie van Hoek (vakgroep Moleculaire Fysica) en Daniel Lavalette (Institut Curie, Orsay).

Iedereen die betrokken is geweest bij de totstandkoming van dit proefschrift wil ik hier hartelijk bedanken.

Kees Vos
oktober 1988

CONTENTS

1 INTRODUCTION

Overview

The spectroscopic characterization of some protein-containing reversed micellar systems has been investigated. The concept of protein solubilization in hydrocarbon media via reversed micelles was first introduced by Gitler and Montal [1]. Their system consisted of proteolipids, solubilized in an apolar solvent, with phospholipids as surfactant. Some years later Wells introduced the term "enzymes in reversed micelles" based on a study of phospholipase in diethylether/methanol mixtures with phosphatidylcholine as the surfactant [2]. In this case the enzyme was already soluble in some organic solvents and the surfactant acted also as the substrate of the enzyme.

One of the first hydrophilic enzymes, incorporated into reversed micelles, was chymotrypsin. Detailed activity and spectroscopic data were reported by the groups of Martinek [3], Luisi [4] and Menger [5].

In the following years, numerous publications, dealing with reversed micellar enzymological subjects, appeared. Three partially overlapping fields of interest can be distinguished. The first one is the study of enzymatic activity in reversed micellar solutions. Among this belongs the work done in our laboratory, which is concentrated on the optimization of biocatalytic processes in reversed micellar systems [6-9]. The second field of interest consists of structural and dynamic aspects of protein containing reversed micelles. During the last few years, several groups have reported on spectroscopic and ultracentrifugation studies. The work presented in this thesis belongs to this category. The third line of interest is the study of enzyme recovery using reversed micellar systems. This type of research has gained increasing attention during the last years. It is possible to selectively extract proteins from an aqueous phase into a hydrocarbon phase containing reversed micelles and to re-extract the protein again into a second aqueous phase. This process can be applied to the purification of proteins [10-14].

Outline of this thesis

In Chapter 2 a review is presented about spectroscopic studies performed with reversed micellar systems. In this chapter a number of techniques is described, which can be used in reversed micellar research. These techniques are both applied to "empty" and protein-containing systems.

Chapter 3 provides a detailed description of the time-resolved fluorescence technique and analysis, that we have applied to protein-containing reversed micellar systems. Examples are given of the fluorescence properties of three well characterized proteins in a normal aqueous environment. These examples illustrate the kind of information obtainable by studying time-resolved fluorescence properties.

In Chapters 4,5 and 6 investigations on protein containing reversed micellar systems are presented. Chapters 4 and 5 describe micellar systems, containing the fluorescent cytochrome c derivatives porphyrin cytochrome c or Zn-porphyrin cytochrome c. Chapter 6 reports on studies of the same micellar systems but with alcohol dehydrogenase as the guest protein instead of cytochrome c.

In the last chapter of this thesis (Chapter 7) a summarizing discussion of the results is presented.

Literature

1. Gitler,C. & Montal,M. (1972) FEBS Lett. **28**, 329-332.

2. Misiorowski,R.L. & Wells,M.W. (1974) Biochemistry **13**, 4921-4927.

3. Martinek,K., Levashov,A.V., Klyachko,N.L. & Berezin,I.V. (1977) Dokl. Akad. Nauk. SSSR **236**, 920-923.

4. Luisi,P.L., Bonner,F., Pellegrini,A., Wiget,P. & Wolf,R. (1979) Helv. Chim. Acta **62**, 740-753.

5. Menger,F.M. & Yamada,K. (1979) J. Am. Chem. Soc. **101**, 6731-6734.

6. Hilhorst,R., Laane,C. & Veeger,C. (1982) Proc. Natl. Acad. Sci. USA 79, 3927-3930.

7. Hilhorst,R., Laane,C. & Veeger,C. (1983) FEBS Lett. 159, 225-228.

8. Hilhorst,R., Spruijt,R., Laane,C. & Veeger,C. (1984) Eur. J. Biochem. 144, 459-466

9. Laane,C., Boeren,S., Vos,K. & Veeger,C. (1987) Biotechnol. Bioeng. 30, 81-87.

10. Luisi,P.L., Bonner,F.J., Pellegrini,A., Wiget,P. & Wolf,R. (1979) Helv. Chim. Acta 62, 740-753.

11. Van 't Riet,K. & Dekker,M. (1984) Proc. 3rd Eur. Congr. Biotechnol. Munich, Vol III, 541.

12. Goklen,K.E. & Hatton,T.A. (1985) Biotechnol. Progr. 1, 69-74.

13. Dekker,M., Van 't Riet,K., Weijers,S.R., Baltussen,J.W.A., Laane,C. & Bijsterbosch,B.H. (1986) Chem. Eng. J. 33, B27-B33.

14. Giovenco,S., Verheggen,F. & Laane,C. (1987) Enz. Microb. Technol. 9, 470-473.

2 SPECTROSCOPY OF REVERSED MICELLES

Kees Vos, Colja Laane and Antonie J.W.G. Visser*

Reprinted from: Photochemistry and Photobiology (1987) 45, 863-878.

Introduction

Reversed micelles are nanometer-scale water droplets, stabilized by a monolayer of surfactants in a bulk organic solvent. For the formation of these surfactant aggregates at least three components are necessary, i.e. an aqueous solution, a water-immiscible organic solvent and a surfactant. Typically stable and optically transparent solutions are formed within seconds upon mixing approximately 10% surfactant, 80–90% organic solvent and only a few percent of water. By varying the nature and concentration of its constituents, the properties of these colloidal particles can be modulated and tailored easily to meet the desired specifications. A prerequisite for the formation of reversed micelles is, that the interfacial tension between the water and the organic phase is close to zero. In a three component system this is achieved solely by the surfactant. However some surfactants are not able to lower the interfacial tension sufficiently and a cosurfactant is required to minimize the interfacial tension further (Overbeek, 1978). Well known cosurfactants are aliphatic alcohols ranging from pentanol up to dodecanol.

In reversed micelles, the surfactants are located only at the interface with their polar head groups directed towards the water pool and their tails sticking out in the continuous phase. In contrast, the cosurfactant partitions between the interface and the organic phase. An important parameter for reversed micellar media is the amount of water present per surfactant molecule. This parameter has adopted many names throughout the years but we prefer the expression w_0†.

In contrast to 'normal' micelles, reversed micelles do not repel each other because they are electrostatically neutral. As a result reversed micelles are able to collide freely in the hydrocarbon solution and with a low efficiency (about 1%) such collisions lead to the exchange of water pools (Eicke *et al.*, 1976). Reversed micelles are therefore not rigid but dynamic entities, which can communicate with each other on a μs timescale.

Originally reversed-micellar research seemed to be a privilege of scientists, having a physical-colloidal signature. To date, many other disciplines show interest as well in the unique properties of reversed micelles. Technologists and engineers regard them as a part of surfactant chemistry with important practical applications in tertiary oil recovery, lubrication, cosmetics and food industry (Luisi, 1985). Biologists and biophysicists see in these structures a similarity and hence a model for cell membranes and simple organelles (De Kruyff *et al.*, 1980; Fendler, 1982), while chemists view them as versatile microreactors, in which chemical reactions can be accelerated and shifted into the desired direction (Fendler, 1982; Kitahara, 1980; O'Connor *et al.*, 1984). Interest from biotechnologists aroused over the last few years because enzymes can be hosted in reversed micelles without loss of activity, which makes it possible to perform bioconversions of water-insoluble compounds (Luisi and Laane, 1986, and references cited therein) and to isolate intra- (Giovenco *et al.*, 1987) and extracellular (Dekker *et al.*, 1986) proteins.

In a recent article the biotechnological aspects of reversed micelles have been reviewed (Luisi and Laane, 1986). Here we will concentrate on some techniques that have been employed to obtain detailed structural information about these surfactant aggregates, either alone or in association with proteins. Among these are scattering techniques, which yield information about the size and shape of reversed micelles, as well as magnetic resonance and optical methods by which the dynamics of micellar systems can be investigated on a molecular level.

*To whom correspondence should be addressed.

†*Abbreviations*: AOT, aerosol-OT (sodium-*bis*(2-ethylhexyl)sulfosuccinate); BHDC, benzyldimethyl-n-hexadecyl ammonium chloride; C_{18}RB, rose bengal hexadecyl ester; CD, circular dichroism; CTAB, cetyl trimethyl ammonium bromide; CTACl, cetyl trimethyl ammonium chloride; D_{O_2}, oxygen diffusion coefficient; DAP, dodecylammonium propionate; DLPC, dilinoleoyl phosphatidyl choline; DPPC, dipalmitoyl phosphatidyl choline; ENDOR, electron nuclear double resonance; EPR, electron paramagnetic resonance; FMN, flavine mononucleotide; g_i, parallel component of g value; k_1, luminescence decay rate constant; k_e, bimolecular rate constant for the exchange process of different water pools; k_q, intrawater pool quenching rate constant; LS, light scattering; NMR, nuclear magnetic resonance; PADS, peroxylamine disulfonate; R_c, polar core radius; R_h, hydrodynamic radius; RB, rose bengal; SANS, small angle neutron scattering; SAXS, small angle X-ray scattering; SDBS, sodium dodecyl benzene sulfonate; SDS, sodium dodecyl sulfate; T_1, spin-lattice relaxation time; T_2, spin-spin relaxation time; w_0, $[H_2O]/[surfactant]$; WP, water pool

Previous reviews on this subject have been presented by Eicke (1980), Martinek *et al.* (1986) and Luisi and Magid (1986).

Scattering techniques

In this section the following scattering techniques, which yield macroscopic, structural information on reversed micelles, will be shortly discussed: light scattering (LS), small-angle neutron scattering (SANS) and small-angle X-ray scattering (SAXS). The three techniques have many elements in common in the treatment of scattered intensity. The expression for the intensity of neutrons scattered by monodisperse, spherical particles shows great analogy with that of the Rayleigh ratio in static LS. Instead of the difference in refractive index of droplets and organic solvent, the corresponding difference in scattering length appears in the expression for the intensity of scattered neutrons. The intensity of X-rays scattered by monodisperse *w/o* microemulsions follows a similar relationship as for SANS. In SAXS the intensity of scattered X-rays is related to the difference in electron density between particle and solvent. Scattering experiments on microemulsions are often accompanied by electrical conductivity and viscosity studies.

The majority of scattering experiments pertained to LS, which essentially probes the Brownian motion of the particles. Light scattering techniques have proven to be a powerful tool to determine sizes and diffusion coefficients of droplets and to measure intermicellar interactions. For diluted microemulsions static LS can yield the second virial coefficient of the osmotic compressibility. The dynamic counterpart of LS, also known as quasi-elastic light scattering or photon correlation spectroscopy, consists of a measurement of the autocorrelation function of the light scattered by the micelles, from which the translational diffusion coefficient can be obtained. Extrapolation to a zero volume fraction of the dispersed phase yields the diffusion coefficient and the hydrodynamic radius of the droplet (from the Stokes–Einstein relation). A virial series for the experimental translational diffusion coefficient can be developed as well. Both second virial coefficients for static and dynamic LS are related to the potential describing inter-droplet interaction. The major contribution to the interaction potential stems from hard sphere repulsion (Agterof *et al.*, 1976). Terms involving small van der Waals attraction are treated as perturbation. Detailed accounts on theoretical and experimental relationships can be found in recent literature (Cazabat and Langevin, 1981; Kaler and Prager, 1982; Roux *et al.*, 1984; Nicholson and Clarke, 1984). Generally, it can be stated that there is qualitative agreement between theory and experiment for low micellar concentrations.

The more earlier LS studies were mainly concerned with various reversed micelles of AOT in different organic solvents (Day *et al.*, 1979; Sein *et al.*, 1979; Zulauf and Eicke, 1979; Gulari *et al.*, 1980). Quaternary systems were also studied, e.g. water/SDS/cyclohexane with pentanol as cosurfactant (Cazabat *et al.*, 1980) and water/SDBS/hexadecane/pentanol (Gulari *et al.*, 1980).

In later studies the amplitude of the above mentioned interaction potential was modulated by changing the volume fraction of water, addition of salt or variation of the chemical nature of oil, cosurfactant or surfactant. Thus, Cazabat and Langevin (1981) concluded that micellar stabilisation is influenced by the polarity of the continuous phase (e.g. cyclohexane *vs* toluene) and alcohol chain length (butanol, pentanol or hexanol), whereas the droplet sizes depend mostly on w_0. Roux *et al.* (1984) introduced in the same micelles additional variations. The continuous phase consisted of, among others, decane and dodecane, cosurfactants were pentanol, hexanol or heptanol and two surfactants were used, SDS and alpha-methyl SDS. Important parameters for an adequate description of the LS data are the chain length of the alcohol and the polar head area of the surfactant, which changes after ramification. Interpenetration of the droplets was taken into account in the interaction potential. The same research group has extended the latter investigations by the use of a graded series of homologues of SDS, each compound containing a larger ramification near the polar head group (Dichristina *et al.*, 1985). Analysis of LS data indicated a constant surface area occupied by surfactant and cosurfactant. The increase in the polar head surface area of the individual surfactant molecule is compensated by a decrease in the alcohol content at the surface boundary. Proceeding through the SDS series a definite decrease of the second virial coefficient was found indicating an increase in micellar attraction and penetration length.

A system where the alcohol is not only cosurfactant, but also acts as organic solvent, was studied by Sjöblom *et al.* (1982), namely water/sodium octanoate/decanol. The micelles grow continuously with increasing w_0; the continuous phase behaves as pure decanol saturated with water.

Reversed micelles of egg lecithin were also studied with LS and electron microscopy (Kumar *et al.*, 1984). Homodisperse aggregates are formed in benzene or carbon tetrachloride, whereas anisotropic, tubular structures with aqueous canals are favoured in cyclohexane at relatively high w_0.

More complicated aggregation schemes and polydispersity were recently taken into account in order to improve the correlation between theory and experiment. Baker *et al.* (1984) have reinvestigated the quaternary system water/SDBS/*p*-xylene/hexanol. The Rayleigh ratio for certain concentrations of surfactant increases slowly with the volume fraction of water and more rapidly above a critical point reaching a maximum at another, higher critical vol-

ume fraction. The results were semi-quantitatively described using a hard sphere model for particle interactions. Not all the available cosurfactant molecules seem to be adsorbed in the interfacial region. Effects of polydispersity were introduced to improve the modeling of dynamic LS experiments on AOT reversed micelles in heptane within a large range of volume fraction of water (0.05 to 0.4) (Nicholson and Clarke, 1984).

An elegant (tracer) forced LS technique has been described for direct measurements of self-diffusion coefficients of microemulsions (Cazabat *et al.*, 1984b).

Furthermore, LS has been proven a useful technique to investigate protein encapsulation in reversed micelles. The insertion of water soluble myelin basic protein into AOT reversed micelles in isooctane has been studied with dynamic LS (Chatenay *et al.*, 1985). At low w_0 (w_0 = 5.6) the hydrodynamic radius of micelles filled with protein (R_h = 43 Å) is significantly larger than that of empty micelles (R_h = 29 Å). The results were analyzed using a water shell model, in which the protein is separated from the organic solvent by a monolayer of surfactant molecules and a shell of water (Bonner *et al.*, 1980). About three empty micelles are required to build up a filled one. At high degree of protein occupancy a small fraction of droplets contains protein aggregates. Conversely, results at higher w_0 values (w_0 = 22.4) revealed similar radii for empty and filled micelles (R_h = 50–57 Å), and the absence of protein aggregates.

Currently, there exists a lively interest in critical phenomena related to percolation thresholds and phase separation. These phenomena occur in each microemulsion. One example is the system water/SDS/toluene/butanol, which exhibits large interdroplet attraction and, in more concentrated systems, rapid exchange of micellar constituents, both mutually and between the continuous phase (Cazabat *et al.*, 1984a). Another example consists of water/AOT/isooctane mixtures near the phase separation temperature (Hilfiker *et al.*, 1985). Not only LS data, but also the results of electrical conductivity, ultrasonic absorption, dielectric spectroscopy (for example: Van Dijk *et al.*, 1986) and Kerr effect measurements (Eicke *et al.*, 1985) lead to the concept of percolation and open, infinite clusters in the description of critical behavior of microemulsions. The organization into bicontinuous structures (oil-rich and water-rich domains separated by surfactant sheets) at intermediate volume fractions of water cannot be ruled out (Kager and Prager, 1982). A manifold of other structural models has been proposed [for a survey see Lindman *et al.* (1981) and De Gennes and Taupin (1982)].

The advantage of SANS over LS is the larger range of the scattering vector (0.02–0.2 $Å^{-1}$, depending on the angle between scattered and incident monochromatic beam and the tunable wavelength), allowing more detailed information on size and size distribution of microemulsions. Elaborate descriptions of SANS applied to microemulsions have been given by Dvolaitzky *et al.* (1978), Ober and Taupin (1980), Robinson *et al.* (1984), Ravey and Buzier (1984) and Magid (1986). Since the coherent neutron scattering length of hydrogen and deuterium are widely different, heavy water usually replaces normal water in order to improve the contrast profile of the droplet.

Robinson and coworkers (1984) studied *w/o* microemulsions with 0.1 *M* AOT, D_2O instead of H_2O and alkanes of increasing chain length (hexane → dodecane). In heptane the radius of the water core, determined from the intensity pattern, follows an approximately linear relationship with respect to w_0 ($5<w_0<40$). At w_0=20 the radii of the water droplets are dependent on the alkane chain length. The experimental SANS patterns show increasing discrepancies with a fitted function based on monodisperse spheres. This effect was attributed to polydispersity and is more pronounced in the lower scattered intensity region and with longer chain length of the organic solvent. The large droplet-size distribution within these microemulsions is in agreement with the photon correlation results of Nicholson and Clarke (1984). In a second paper of the same research group critical behaviour in the same microemulsions was detected with SANS upon approaching the phase transition temperature (Toprakcioglu *et al.*, 1984). The group of Robinson (Fletcher *et al.*, 1984) found no change in scattering profile when α-chymotrypsin was incorporated in the same AOT reversed micelles (w_0=15 and 20).

A SANS study of the effect of additives (toluene, octanol, benzyl alcohol, short-chain alcohols) on the temperature-induced phase transition of AOT reversed micelles was performed by Howe *et al.* (1986). By monitoring the critical scattering component of the SANS intensity profile a decrease or increase in transition temperature, depending on the nature of the additive, was found. The results were interpreted by assuming different location and partitioning of the various additives.

A quasi-electric, incoherent neutron scattering method has been recently described to investigate the translational motion of AOT reversed micelles (Fletcher *et al.*, 1986). The results suggest, that additives like toluene and benzyl alcohol or the solubilization of chymotrypsin do not influence the translation diffusion of AOT. Substitution of water by glycerol, however, produces a significant reduction in AOT mobility. Measurements of spectra associated with water mobility revealed the presence of 5–10% of water bound to the enzyme during the experimental time scale. The mobility of the remainder of the solubilized water is unaffected by the presence of chymotrypsin.

Ravey and Buzier (1984) reported on SANS of reversed micelles of the nonionic surfactant tetra-

ethylene glycol dodecyl ether in decane. The microemulsions consist of large nonspherical water droplets inside a surfactant shell, even for volume fractions of the dispersed phase as high as 0.5.

A SAXS experiment determines a so-called radius of gyration, which is related to the polar core radius (R_c). A detailed account of SAXS theory and applications to microemulsions has been given by Kaler *et al.* (1983). The system used by the latter research group is not a standard one: a commercial surfactant mixture (TRS 10–80), tertiary amyl alcohol, various brines and octane. Depending on the composition the microemulsion is either rich in oil or water. SAXS data could be adequately modeled for increasing volume fractions of brine until a percolation threshold. Kaler and coworkers (1983) have provided arguments in favour of a bicontinuous structural model, which is in fairly good agreement with SAXS data over a wide range of brine volume fractions.

Pileni *et al.* (1985) have conducted SAXS experiments on a mixture of .water/AOT/isooctane (w_0=9), to which small amounts of different compounds were added. Relatively small solutes (ether, dioctyl viologen) do not change the radius as compared to empty micelles (R_c=34.9 Å). Solubilisation of α-chymotrypsin induces a slightly larger radius (R_c=36.8 Å), in contrast with the results of Fletcher *et al.* (1984). α-Chymotrypsin was assumed to be located in the water core. On the other hand incorporation of cytochrome c results in a slight decrease in core radius (R_c=33.6 Å) indicating a possible interfacial location of the protein.

Optical spectroscopy

Optical spectroscopy and especially fluorescence and flash photolysis techniques have been widely applied to reversed micellar systems. In most of the experiments, some probe molecule is entrapped in the water pool of the micelles and from its behaviour some properties of the interior of the micelles can be extracted.

Eicke and Zinsli (1977) used Na-fluorescein in micelles consisting of AOT in isooctane. From their time-resolved fluorescence and anisotropy measurements they concluded that this label is strongly associated with the water/surfactant interface. At low w_0 values (w_0<4) the label has no internal mobility within the micelle. The radii of the micelles, which can be calculated from the rotational correlation times *via* the Stokes-Einstein relationship, are in this case simply the sum of the radii of the empty micelles and label. At higher water contents complications arise. When the w_0 values and the [AOT] are not too high the measured correlation times are determined by the rotation of the micelles. Both at higher w_0 values and at high surfactant concentrations, the micelles tend to coagulate. The correlation times are in this case determined by the rotation of the probe within the micelles. From the decrease in the initial anisotropy with increasing w_0, Eicke and Zinsli concluded that the packing density of the interface decreases when the size of the water pools increases.

Probes which do not interact so strongly with the AOT interface were used by Keh and Valeur (1981) and Visser *et al.* (1984). Keh and Valeur used 3,4,9,10-perylene sodium tetracarboxylate and 9,10-anthracene diacetic acid. From the steady-state anisotropy they calculated the correlation times of the labels, using the well known Perrin equation. A model was proposed in which the rotation of the probe within the micelles and the one of the whole micelles are coupled. This model was used to determine the hydrodynamic volume of the micelles by measuring the correlation times in two related organic solvents of different viscosity. The results were in good agreement with values obtained by photon-correlation spectroscopy (Zulauf and Eicke, 1979).

Visser *et al.* (1984) used FMN as probe and measured the time resolved fluorescence and anisotropy of FMN in AOT, CTAB and DAP micelles. In CTAB and DAP the fluorescent properties of the FMN molecule are more influenced than in AOT. This was explained by electrostatic interactions between the negatively charged phosphate group of FMN and the head groups of the different surfactants. The anisotropy decays follow in all cases a single exponential function. Therefore Visser *et al.* assumed the rotations of the label and the micelle to be independent. Using the hydrodynamic radii of the micelles measured by other techniques it was possible to calculate the correlation times of the FMN molecule within the micelles.

Recently the same group (Visser *et al.*, 1987) employed an amphiphilic flavin to investigate the dynamic properties of the interface of AOT reversed micelles in heptane. The fluorescence anisotropy could only be fitted with a double exponential function, yielding a short correlation time (0.5 ns), which is constant at larger w_0 and a longer correlation time, that varies from 1.1 to 2.5 ns in the w_0-range studied. The contribution of the short component increases with larger w_0, providing evidence for enhanced mobility at the boundary region.

Reversed micelles of calcium alkanyl sulfonates in alkanes of increasing chain length (hexane → nonane) were probed with 1-pyrene carboxaldehyde and a graded series of pyrene carboxylic acids with varying alkyl chain length (Jao and Kreuz, 1986). 1-Pyrene carboxaldehyde is an appropriate probe for measuring micellar sizes. The other series of probes is useful for establishing polarity gradients and lateral mobility *via* the ratio of excimer to monomer fluorescence. In a previous study an oxygen concentration gradient for the same micelles and probes was found from quenching of pyrene carboxylic acid fluorescence by oxygen (Jao and Kreuz, 1984).

The H-bonding capacity of the entrapped water can be monitored *via* the fluorescent lifetimes of xanthene dyes like rose bengal (RB) (Rodgers,

1981; Rodgers, 1984). In protic solvents like water and alcohols these dyes have a very short lifetime, probably due to an efficient intersystem crossing from excited singlet to triplet. The less H-bonding capacity of the solvent the longer are the lifetimes of these labels. Besides normal RB Rodgers (1984) also used its hexadecyl ester (C_{16}RB) in a system consisting of AOT in heptane. This probe will be anchored in the interface with its apolar tail. The results show no differences between RB and C_{16}RB so it can be safely assumed that RB is also associated with the interface. At w_0=0 the H-bonding capacity of the entrapped water is in the same order of magnitude as in *t*-butanol and increases gradually until a limiting value is reached at w_0>20. At w_0>20 the lifetime of RB is still much longer than in bulk water (0.28 ns for the micelles *vs* 0.08 ns for bulk water). Nuclear magnetic resonance studies have shown, that entrapped water has the relaxation properties of bulk water at w_0>8 (Wong *et al.*, 1977) providing evidence for probe association with the interface.

Experiments with probes, which are localized in the apolar phase have also been performed (Geladé *et al.*, 1982; Geladé and De Schryver, 1984a,b). Derivatives of naphtalene with aliphatic tails of varying length were used. From measurements of the hetero-excimer formation of these probes with triethylamine and the energy transfer to terbium ions, which are localized in the water pools, conclusions could be drawn about the localization of these probes, the properties of the solvent in the vicinity of the micelles and the rate of terbium exchange between micelles by intermicellar collisions.

Extensive research has been carried out on the transfer of photo-electrons between entrapped donor and acceptor molecules. Light is used as an electron pump, promoting charge transfer from the donor to the acceptor. The microheterogeneity of the system retards the back reaction and this allows the utilization of the reduced acceptor in a chemical process. Because the charge transfer leads to quenching of the luminescence of the donor, useful information can be obtained about the system under investigation by studying the kinetics of the luminescence decay. This decay is mainly determined by the distribution of the donor and acceptor molecules among the water pools, which is best described by a Poisson distribution. With this assumption it is possible to derive the following expression, which describes the complex decays that are observed (Infelta *et al.*, 1974; Tachiya, 1975; Atik and Singer, 1978, 1979; Atik and Thomas, 1981a):

$$I(t) = I(0)\exp[-C_1 t - C_2\{1-\exp(-C_3 t)\}]$$

where

$$C_1 = k_1 + k_q k_c[Q]/(k_q + k_c[WP]),$$

$$C_2 = k_q[Q]/[WP](k_q + k_c[WP])$$

and

$$C_3 = k_q + k_c[WP].$$

The parameters in this expression are: k_1, the decay rate constant of the donor in the absence of quencher; k_q, the intrawater pool first-order quenching rate constant; k_c, the bimolecular rate constant for the exchange process of the different water pools and [WP], the water pool concentration. For the characterization of the micellar systems, the parameters k_c and [WP] are of special interest. The k_c is a good measure for the facility of the micelles to exchange their contents. The lower k_c, the more the back transfer of the electrons will be retarded. From [WP] the size of the water pools can easily be calculated.

Atik and Thomas (1981a,b) have studied AOT and CTAB reversed micellar systems using various donor–acceptor couples. The authors found radii for the water pools in AOT micelles, which are in good agreement with those found by Zulauf and Eicke (1979). The exchange rates are in the order of 10^7 M^{-1} s^{-1}. This is about 1% of the calculated collision rate of the micelles. Additives, such as benzyl alcohol increase the exchange rate, while a solute like benzene decreases it. Atik and Thomas ascribed these effects to interactions of these additives with the micellar head groups.

Experiments of the same kind have been performed by Geladé and De Schryver (1982, 1984a), by Furois *et al.* (1984), by Brochette and Pileni (1985), by Almgren *et al.* (1986) and by Handa *et al.* (1986). Geladé and De Schryver have studied DAP micelles in cyclohexane, using 1-methylnaphtalene and 2-(1-naphtyl) acetic acid as the fluorophores and potassium iodide and sodium nitrate as the quenchers.

Handa *et al.* (1986) made use of tris(2,2'-bipyridine) ruthenium(II) dichloride as fluorophore and potassium ferricyanide as quencher in reversed micelles composed of heptakis (ethylene glycol) mono-n-decylether and hexanol in decane. The partitioning of $[Ru(bipy)_3]Cl_2$ between the hydrated poly(ethylene glycol) shell and the water pool could be quantitated.

The same $Ru(bipy)_3^{2+}$ ion with methyl viologen as quencher was used by Almgren *et al.* (1986) in a study of the reversed micellar system Triton X-100/toluene/water. The rapid exchange of probes and quenchers between the droplets was assumed to follow a fusion-fission process in which two droplets merge transiently into a large drop, which splits up rapidly in two drops again.

The systems studied by Furois *et al.* (1984) and by Brochette and Pileni (1985) consisted of AOT micelles in isooctane with different porphyrins as fluorophores and three viologen derivatives as quenchers. The same micellar system was used by Pileni *et al.* (1984) in a study of the quenching of hydrated electrons, generated by pulse radiolysis, by nitrate ions. From this study it appeared, that the hydrated electrons are also Poisson distributed and therefore from these experiments the same kind of information about the system could be extracted as from the experiments described above.

In reversed micelles of benzyldimethyl-*n*-hexadecyl ammonium chloride (BHDC) interactions between excited-state zinc tetraphenyl porphyrin and quinones (duroquinone and anthraquinone-2-sulfonate) have been investigated by Costa and Brookfield (1986) using time-resolved fluorescence spectroscopy. Fluorescence quenching was presumed to be associated with intramolecular charge transfer from singlet excited porphyrin to ground-state quinone. Dynamic quenching was observed in case of duroquinone as quencher, which is solubilized in the benzene organic phase. The other quencher anthraquinone-2-sulfonate, is bound at the interface leading to biexponential fluorescence decay with average time constants, characteristic for unquenched porphyrin (1 ns) and quenched porphyrin (100 ps), respectively. The fluorescence decays were interpreted in terms of an active-sphere quenching model. In the later model only quenchers which are bound to BHDC within a certain volume around the BHDC-bound porphyrin lead to quenching. The observed lifetimes result in an estimate of the pseudo-unimolecular electron-transfer rate constant of the order of 10^{10} s^{-1}.

It is also possible to use micellar entrapped redox proteins as the electron acceptor, which has been shown by Pileni (1981) and by Visser and Fendler (1982). In the work of Pileni N-methyl-phenothiazine was used as the photoactive compound, which reduces cytochrome *c*. With a second electron donor in the system, which is able to reduce the oxidized N-methyl-phenothiazine, irreversibly reduced cytochrome *c* was observed under continuous radiation conditions. Visser and Fendler studied the reduction of cytochrome *c* and cytochrome c_3 by electrons generated by pulse radiolysis and by pyrene photoionization. With both methods of electron generation an instantaneous, reversible reduction of the proteins was observed, which means, that the proteins have maintained their native conformation within the micelles.

Reversed micelles are frequently used as models for complex biological systems. An example of this is the study of the behaviour of singlet oxygen in microheterogeneous systems as a model for the activity of singlet oxygen in the photodynamic damage in biological systems (Lee and Rodgers, 1983; Rodgers and Lee, 1984). A model was developed for the dynamic behaviour and the quenching of singlet oxygen in reversed AOT micelles. Singlet oxygen is not restricted to one of the different phases but can diffuse freely through the whole system. Based on lifetime measurements of singlet oxygen, velocity and equilibrium constants for the exchange of this probe between aqueous and organic phase could be calculated. Quenching studies with water soluble molecules yield information about the water structure in the micelles. When the azide ion was used as quencher a maximal constant quenching rate is reached at $w_0>30$. This rate is about 80% of the value in bulk water, indicating that the entrapped water under these circumstances behaves almost like normal water. Tryptophan behaves differently. The tryptophan molecule is probably associated with the interface. In this case the quenching rate is also constant at $w_0>30$ but the value is only 50% of that in bulk water. These results clearly indicate that there is a large difference between water in the neighbourhood of the interface and in the center of the micelle.

Recently, extensive research has been performed on ground and excited-state proton transfers (Kondo *et al.*, 1982; Bardez *et al.*, 1984, 1985; Politi *et al.*, 1985; Politi and Chaimovich, 1986). Used probes are pyranine (8-hydroxy-1,3,6-pyrenetrisulfonate), 2-naphtol, 2-naphtol-6-sulfonate and 2-naphtol-6,8-disulfonate. A common property of these probes is, that the pK_a value in the excited state is much lower than in the ground state. Hence upon excitation with a short light pulse a proton can dissociate from these compounds. Different fluorescence techniques have been applied to determine the rate constants for the de- and reprotonation of the probes. Pyranine has been used by: Kondo *et al.* (1982) in AOT and CTACl micelles, by Bardez *et al.* (1984) in AOT micelles and by Politi *et al.* (1985) and Politi and Chaimovich (1986) also in AOT micelles. This probe with its trianionic character is expected to be in the center of the water pools in the case of AOT micelles. In CTACl micelles pyranine will probably be located in the vicinity of the interface due to electrostatic attractions.

The rate of deprotonation in small micelles ($0<w_0<3$) was found to be much lower than in water. This is due to the fact, that in small micelles a limited number of water molecules is available to hydrate the proton. Moreover the structure of the water was assumed to be disrupted (less hydrogen bonding) (Rodgers, 1981, 1984) which also will decrease the ability to accept the proton. With increasing water pool size the rate of deprotonation also increases and reaches the same value as in water at $w_0>12$. In CTACl micelles the addition of water has almost no effect, indicating that pyranine sticks at the interface in this micelle. Reprotonation is faster in small micelles than in water. This behaviour has been explained in terms of the so-called cavity effect. The ejected protons remain in the vicinity of the pyranine molecule. Also in this case the same rate as in water is reached at $w_0>12$. These observations prove that water in the center of the water pools of AOT micelles has more or less the same properties as bulk water at $w_0>12$.

2-Naphtol and its sulfonate derivatives have been used by Bardez *et al.* (1985 and 1986) and by Politi and Chaimovich (1986). It was found that 2-naphtol shows no deprotonation in AOT micelles, whatever the water content. Apparently this probe is located in the interface where it does not 'see' any water molecules. 2-Naphtol-6-sulfonate can be deprotonated in the micelles but the rate is much lower

than in water. Only at w_0>40 the aqueous value is reached and then still the recombination rate is much faster. This behaviour has been explained in terms of localization of the probe. It was assumed to be in the vicinity of the interface where the structure of the water is also affected at high w_0 values. 2-Naphtol-6,8-disulfonate shows almost the same behaviour as pyranine and is therefore believed to be in the center of the water pools. This observation is consistent with the fact that this probe is the most hydrophilic one of the three naphtol derivatives. The change in free energy for the de- and reprotonation processes by specific localization effects can very well be compared to the situation which can occur in the active sites in enzymes.

Bardez *et al.* (1986) determined the binding constant between 2-naphtol and AOT from changes in the light absorption spectra in the absence of water. Water solubilization in AOT reversed micelles decreases the binding constant and induces changes in the probe microenvironment as a function of AOT concentration with accompanying increased polarity at higher water content. Steady-state fluorescence polarization reveals an increase in mobility of 2-naphtol at larger w_0, which was interpreted by a more loose interface.

Recently a Fourier transform infra red study on reversed micelles has been published (Holmgren *et al.*, 1986). The reversed micellar system was sodium octanoate/octanoic acid/water. Methylene and the antisymmetric carboxylate vibrational modes were monitored. Hydrogen bonding and counterion effects at the interface could be inferred from frequency shifts and band width alterations.

During the last decade, numerous publications have appeared about biopolymers and especially about proteins, which are incorporated in reversed micellar systems. For recent surveys see Luisi and Magid (1986) and Waks (1986). In this part of this review we will focus attention on optical spectroscopic techniques, which were applied to elucidate the structural properties of these kind of systems.

Among the earliest publications in this field are those of the group of Douzou (Douzou *et al.*, 1979; Balny and Douzou, 1979). In this case the reversed micellar systems were used to perform cryoenzymological studies. When the conditions are favorably chosen, it is possible to cool the micellar solutions down to subzero temperatures, without freezing of the entrapped water. Using this method it was for instance possible to record absorption spectra of entrapped cytochrome *c* at temperatures as low as −40°C. Other enzymes, which have been studied in reversed micelles at subzero temperatures are: horse radish peroxidase, catalase and bacterial cytochrome P450. With this last enzyme also some kinetic experiments have been performed.

A pioneering group, which is very active in the field of the micellar solubilization of proteins, is the one of Luisi in Switzerland. Detailed studies of entrapped ribonuclease (Wolf and Luisi, 1979), horse liver alcohol dehydrogenase (Meier and Luisi, 1980), lysozyme (Grandi *et al.*, 1981) and α-chymotrypsin (Barbaric and Luisi, 1981) have been presented.

In the case of ribonuclease UV absorption and CD spectra have been recorded in a system consisting of 50 m*M* AOT in octane, w_0=19. The spectra are virtually the same as the ones of the protein in water, except for the 240–250 nm region in the CD spectrum, where some differences occur. From these observations it was concluded, that the protein conformation in the micelles is almost the same as that in water. It is noted by the authors, that more marked differences were observed, when methyltrioctyl ammonium chloride was used as the surfactant.

The system horse liver alcohol dehydrogenase/AOT/isooctane was characterized, using CD, UV absorption and fluorescence techniques. From CD measurements in the 200–250 nm region it was concluded, that the secondary structure of the protein in the micelles is almost the same as that in water. A closer examination of the properties of the aromatic amino acids reveal some differences between a hydrocarbon and an aqueous enzyme solution. Ultraviolet-absorption spectra show, that the p*K* of a tyrosine residue in the protein is higher in the micelles than in water. In addition, the intrinsic fluorescence of the protein is quenched. This most probably means, that at least one of the tryptophans senses an altered environment. The quenching of the fluorescence by NADH was used to determine the dissociation constant of the enzyme–coenzyme complex and the concentration of active sites. The value of the dissociation constant thus obtained, is close to the 'aqueous' value when overall concentrations of the reactants are considered and much higher when water pool concentrations are used. The concentration of active sites is about 10–20% lower than in the aqueous solution. The authors ascribed this effect to denaturation of a fraction of the protein molecules during the solubilization procedure.

The spectroscopic properties of lysozyme change rather drastically upon incorporation in (AOT/isooctane) micelles. The absorption spectrum does not change too much but the CD spectrum in the far UV region show some important changes. Especially at low water contents the ellipticity between 220 and 230 nm increases, which indicates a higher helical content under these conditions. Also in the aromatic region (250–300 nm) the CD spectrum changes. The spectral properties of lysozyme in this region are predominantly determined by the six tryptophan residues. Changes in the environment of these residues can also be monitored via the protein fluorescence. Again the most dramatic changes occur at low water contents, where a blue shift of the fluorescence of about 10 nm and a marked increase of the quantum efficiency were observed. This suggests, that one of the tryptophan residues, which is

rather exposed when the protein is in normal aqueous solution, gets more buried in the protein coil in the micelles. Furthermore the lysozyme fluorescence was more accessible to acrylamide quenching in the micelles, which also indicates that conformational changes have occurred.

The properties of α-chymotrypsin also change when it is incorporated. Especially the fluorescence and CD data show, that the protein is in a more rigid conformation than in aqueous solution. This effect decreases when the size of the water pools increases. It seems contradicting, that the aqueous properties are best approximated at w_0=19 and not at w_0=22.5, which was the highest value studied. The increased rigidity was in this case observed via the CD spectra, which shows an increased ellipticity in the far UV region and via the polarization of the fluorescence, which is higher in the micelles than in water, indicating, that the fluorophores have lost mobility. These effects were observed at w_0<19. At w_0=22.5 the opposite behaviour was found. Both the ellipticity and the degree of polarization are lower than in water in this case.

The tryptophan fluorescence of the hemoproteins cytochrome *c*, cytochrome b_5 and myoglobin in AOT micelles has been studied by Erjomin and Metelitza (1984). A significant increase of the intensity of the fluorescence was observed for cytochrome *c* and myoglobin. With cytochrome b_5 this effect was also found but it was less pronounced. Apart from a change in intensity, in all proteins a blue shift of the emission maximum was observed. These results were interpreted in terms of an increased viscosity and a decreased polarity in the environment of the tryptophan residues. The fact, that the changes for cytochrome b_5 are smaller than for the other proteins was explained by the formation of protein aggregates, which do not disintegrate upon incorporation. Within an aggregate the microenvironment of much of the tryptophans is not altered and therefore the overall properties of cytochrome b_5 show only small changes. The effect of several additives on the cytochrome *c* fluorescence was tested. Aliphatic alcohols and secondary amines quench the fluorescence, whereas polar aprotic solvents like dimethylsulfoxide increase the fluorescence intensity. These results were interpreted by the effect of these additives on the properties of the water in the neighbourhood of the protein.

The integrity of an entrapped enzyme can be tested by activity measurements in reversed micelles. A luminescence assay in reversed micelles was developed to detect hydrogen peroxide, which is a product of the reaction catalyzed by glucose oxidase, *via* coupling to the well-known luminol chemiluminescence (Visser and Santema, 1984). The glucose oxidase was entrapped in CTAB reversed micelles. The sensitivity of the method enables to easily select optimum conditions for enzymatic activity, like e.g. choice of cosurfactant, organic solvent or w_0.

Membrane proteins can also be incorporated in reversed micelles as was shown with the Folch–Pi proteolipid (Delahodde *et al.*, 1984) and with the myelin basic protein (Nicot *et al.*, 1985). The Folch–Pi proteolipid is a water insoluble protein–lipid omplex, which is usually studied in solvents like 2-chloroethanol or chloroform–methanol mixtures. The maximum solubility of the complex in AOT/isooctane micelles was found to take place at a water content w_0=5.6. The tryptophan fluorescence in this system shows a marked blue shift (10 nm) as compared to a 2-chloroethanol solution of the complex, which is an indication of a more apolar environment of the tryptophan. The CD spectrum in the far UV region is consistent with a secondary structure that is substantially helical (about 55%). This is less than in 2-chloroethanol or in a chloroform-methanol mixture but these solvents are known to be helix inducers. The reversed micelles seem to form a good medium to mimic the natural environment of this proteolipid.

Myelin basic protein is a water soluble protein, which behaves like an extended, flexible polyelectrolyte with little periodic secondary structure. It is believed, that in its native environment the protein has a more structured conformation. Two different micellar media, with an anionic (AOT) and a nonionic (tetraethylene glycol mono-*n*-dodecyl ether) surfactant, were used. By CD measurements it was evident, that in both types of micelles the protein is more structured than in water. The latter effect was also indicated by measurements of the tryptophan fluorescence in the AOT micelles. Upon incorporation, the emission maximum shifts about 15 nm to the blue, which is an indication, that the single tryptophan becomes more buried in the protein coil. The latter effect is independent of the water content of the micelles. A compound like N-acetyl-L-tryptophanamide also exhibits a blue shifted emission maximum but the shift gradually increases with decreasing water content. This means, that the conformational change in the protein is induced by the interface. Time-resolved fluorescence and anisotropy measurements show, that increasing the water content of the micelles only influences the internal dynamics of the protein and not its conformation.

The secondary structure inducing capacities of reversed micellar media can be studied in detail when small model-peptides are incorporated (Gierasch *et al.*, 1984; Thompson and Gierasch, 1984; Seno *et al.*, 1984). Gierasch *et al.* (1984) and Thompson and Gierasch (1984) studied the behaviour of a cyclic pentapeptide, cyclo(Gly-Pro-Gly-D-Ala-Pro), in AOT micelles. With different spectroscopic techniques it was demonstrated, that this peptide undergoes a conformational change in the micelles, similar as in solutions with a high sodium chloride

concentration. From this fact it was concluded that the conformational change in the micelles occurs because the peptide experiences a high sodium concentration in the micelles.

The peptides studied by Seno *et al.* (1984) were poly(N^5-dihydroxyethylaminopropyl-L-glutamine) and poly(N^5-dihydroxyethyl-L-glutamine). Both peptides assume a disordered structure in pure water. Poly(N^5-dihydroxyethylaminopropyl-L-glutamine) is transformed into α-helix in AOT reversed micelles at low w_0 and in aqueous AOT solutions. The interactions of the peptide with the surfactant seem to decrease the de-stabilization of the helix, owing to the hydration shell surrounding the hydroxyl groups in the side chain. In sodium ethanesulfonate solution no helix formation could be detected. Therefore neither the sodium ion nor the sulfonate are involved in the induction of the secondary structure. Poly(N^5-dihydroxyethyl-L-glutamine) does not show any helix formation, probably because in this peptide there is steric hindrance from the bulky dihydroxy-ethylamino group, which is located near the main chain. In general it can be concluded, that forces of different nature play roles in the formation of secondary structure in peptide chains.

The feasibility has been demonstrated to solubilize nucleic acids in hydrocarbon solvents *via* reversed micelles (Imre and Luisi, 1982). RNA (mol. wt. 2000–3000) was added in solid form to AOT/isooctane solutions and the solubility was investigated as a function of the pH of the aqueous phase and of the water content of the micelles. There seems to be almost no dependence on the pH value but there is one on w_0. Solubility increases with increasing w_0 until a value of w_0=20 and then decreases with further increasing w_0. Circular dichroism measurements show, that the RNA is much more structured in the micelles than in aqueous solution. These facts indicate a strong influence of the interface on the RNA molecule.

Large pieces of DNA (mol. wt. ≈250 000) can be incorporated by injecting concentrated aqueous DNA solutions in an AOT solution. The CD spectra of these preparations are of the so called ψ-type, which means a strong increase of the ellipticity in the 240–340 nm region. A similar CD spectrum is found for the DNA in bacteriophages and is related to a strongly condensed form of the DNA. The effect can even be amplified by addition of magnesium ions, which are capable of neutralizing negative charges on the DNA molecule. These observations demonstrate again the power of reversed micellar media to mimic the interfacial properties of bioassemblies.

Magnetic resonance

In this section electron paramagnetic resonance (EPR) and nuclear magnetic resonance (NMR) applied to reversed micelles are briefly surveyed. EPR measurements are usually carried out with spin labels or probes incorporated in the micelles. Dynamic information can be obtained from analysis of line shape and width of spin labels and by comparison with EPR spectra taken with spin labels in solvents of known viscosity. Nuclear magnetic resonance measurements yield both dynamic and structural infofmation (at molecular level) and have the advantage that the intrinsic nuclear moments of micellar constituents can be utilized preventing external perturbation. Most measurements pertained to ^{1}H and ^{13}C resonances, but ^{31}P (e.g. pH determinations of phosphate buffers in reversed micelles or investigations of phospholipid reversed micelles), ^{23}Na (e.g. AOT) and ^{19}F (introduced as label in certain micelles) NMR spectroscopy have been reported as well. A spin-echo ^{1}H and ^{13}C method for simultaneous measurement of self-diffusion coefficients of all micellar components will be summarized (Lindman and Stilbs, 1984). Both EPR and NMR experiments have been mostly performed with reversed micelles from AOT in various organic solvents. These experiments will be discussed first. Reversed micelles made from other surfactants will be surveyed thereafter.

Menger and coworkers (1975) have introduced nitroxide spin labels in AOT reversed micelles in heptane. Nitroxide radicals exhibit a three-line EPR spectrum because of the hyperfine interaction between the unpaired electron spin (S=1/2) and the nuclear spin of ^{14}N (I=1). The hyperfine coupling constant is sensitive towards the polarity of the micro-environment. The line width is a measure of the rate of molecular tumbling and therefore depends on the microviscosity. Different degrees of hydration and three labels with different polar side-chains were used. The effect of pool size on the nitrogen hyperfine coupling constant and the line width of the spectral lines was explained in terms of micro-environmental changes. In small droplets the nitroxide group is located in the interfacial region of water, surfactant and continuous phase. In larger water pools (w_0>10) the spin label remains entirely within the water pool. The anionic spin label shows a splitting of the line at high field, which arises from slowly exchanging labels between the micellar interior and surfactant boundary region.

A similar exchange of the spin probe 2,2,6,6-tetramethyl-4-piperidone N-oxide in AOT reversed micelles in heptane at different w_0 in supercooled water (−32°C) was observed by Yoshioka (1981). Typical rotational correlation times for w_0=8 are 0.24 ns (0°C) and 0.08 ns (20°C). At room temperature the rotational correlation time becomes shorter with increasing w_0. The observed correlation times are composed of contributions from internal motion and micellar rotation. In two following papers (Yoshioka, 1983; Yoshioka and Kazama, 1983) the positional exchange of the same spin probe in AOT reversed micelles was examined in greater detail.

The exchange could be monitored at low temperature in relatively large water pools. A two-phase model of the water pool was proposed to fit the calculated to the observed spectra. At room temperature the rate of exchange between the two phases amounted to about 4×10^6 s^{-1}.

Belongova and coworkers (1983) have investigated (among others) α-chymotrypsin, spin labeled at the active site, in AOT reversed micelles in octane. With increasing w_0 the mobility of the label decreases first (w_0=10–15), manifested by longer correlation times, but increased gradually in the range w_0=20–80. The catalytic activity of α-chymotrypsin reaches its optimum at w_0 values when a maximum rigidity of the active site is detected.

The product of oxygen diffusion coefficient (D_{O_2}) and concentration in AOT solubilized water in heptane was measured with the paramagnetic probe peroxylaminedisulfonate (PADS, Fremy's salt) (Gandin *et al.*, 1984). The location of this ionic, hydrophilic probe in the water core is unambiguous. The effect of oxygen presence on the line width of the EPR spectrum of PADS was studied. The product $[O_2].D_{O_2}$ increases linearly with the radius of the water droplet (from 12 to 43 Å) indicating a concomitant decrease in water viscosity. Line width measurements permitted absolute viscosity determinations ranging from 5.6 cP at R_c=12 Å to 0.93 cP at R_c=43 Å. The oxygen concentration in the water pool (1.8×10^{-4} *M*) appeared to be lower than in bulk water (2.4×10^{-4} *M*). The organic solvent is the oxygen reservoir from which oxygen diffuses towards the spin probe in the water core.

Nitrogen-14-ENDOR spectra of Fremy's salt in reversed micelles of DAP and AOT in toluene at room temperature have recently been reported (Janzen *et al.*, 1986). The observation of ENDOR signals was much easier in micellar encapsulated water than in bulk water, which was ascribed to a more polar and viscous environment in the water pools as compared to that in bulk water.

Lim and Fendler (1978) utilized 2,2,5,5-tetramethylpyrrolidine-1-oxyl derivatives (neutral, cationic and anionic) in DAP reversed micelles in benzene. The neutral spin label exchanges among micellar and solvent environments. The charged compounds are preferably located in the surfactant boundary region, the cationic label probably in a less polar environment. The anionic radical can be reduced by sodium ascorbate (water soluble) and phenylhydrazine (benzene soluble). The second order rate constant for quenching by phenylhydrazine remains unaffected in the presence of DAP, but decreases in case of quenching by sodium ascorbate. The latter effect was explained by mutual electrostatic repulsion between both anionic species.

Long fatty acid spin label analogues were used in the system water/CTAB/hexanol in order to probe the dynamics of the interface (Lufimpadio *et al.*, 1984). The rotational correlation times depend strongly on the micellar composition, e.g. on the molar ratio [CTAB]/[hexanol] at constant w_0.

Seno and colleagues (1980) utilized EPR spectroscopy of Mn^{2+} solubilized in water pools of CTAB reversed micelles in chloroform. The line width of one of the hyperfine lines was measured as a function of the water content in the micelle. At low water concentrations the line width is larger than in bulk water, which was explained by a distorted structure of the Mn^{2+}–water complex. The water is used for solvation of the polar head groups and is not available for Mn^{2+} coordination.

Cupric chloride was used as a spin probe to investigate the vitrification behaviour upon cooling of water within cationic (CTACl), anionic (SDS) and nonionic (Triton X-100) reversed micelles in the presence of several short-chain alcohols as cosurfactants and in different organic solvents (octanol, toluene, cyclohexane) (Brüggeler, 1986). Only in one case ice formation was observed when a microemulsion was cooled very slowly. In all other reversed micelles the bound water vitrifies upon cooling. The $g_{\parallel}$ splitting of the Cu^{2+} ion turns out to be very sensitive to participation of alcohol/surfactant in the coordination sphere of the metal ion.

Important parameters in NMR spectroscopy are the chemical shift of the nuclei and their spin-lattice (T_1) and spin-spin (T_2) relaxation times. Good introductions in theoretical, experimental and analytical aspects of NMR applications in reversed micelles are given by Wong *et al.* (1977) (^1H, chemical shift and nuclear relaxation of entrapped water, and ^{23}Na, line width determined by quadrupole coupling), Maitra and Eicke (1981) (^1H, spin-spin coupling and AOT conformation), Martin and Magid (1981) (^{13}C, chemical shift and spin-lattice relaxation in AOT), Seelig (1984) (^{31}P polymorphism in lipids) and Smith and Luisi (1980) (^{31}P, pH of phosphate buffer in reversed micelles).

With increasing water content a downfield chemical shift in the ^1H NMR spectra of H_2O in AOT reversed micelles was observed (Wong *et al.*, 1977). Both ^1H spin-lattice and ^1H and ^{23}Na spin-spin relaxation rates decrease with increasing water content. Data were interpreted by assuming highly immobilized water in small pools. After complete hydration of the sodium ion (w_0>6) the rigidity of the micelles is greatly reduced. In large pools a considerable fraction of Na^+ is located within the core.

Maitra and Eicke (1981) have measured the temperature dependence of proton-proton coupling constants of AOT in order to assess different rotamer populations (rotational isomers or Newman projections of the monosubstituted succinic ester). An increase in temperature would increase the population of an energetically higher rotamer. A different equilibrium mixture of rotamers exists in AOT dissolved in organic solvents of decreasing polarity (methanol, chloroform and isooctane). The composition of the rotamer mixture depends on

solvent–surfactant interaction. In polar solvents there is a strong, isotropic solvent–surfactant interaction, in apolar solvents the polar heads have no interaction. Better hydration is an important property of AOT in the enhancement of surface activity and hence, its solubilization and aggregational properties. In a following paper (Maitra *et al.*, 1983) the effect of 'cosurfactants' like benzene and nitrobenzene on AOT reversed micelles in isooctane was investigated with ^{1}H NMR. It was demonstrated that the solubilized water adopts the properties of bulk water and, at increasing 'cosurfactant' concentration, the surfactant molecules are solvated by the 'cosurfactant' molecules in the interfacial region thereby reducing the solubilization power of the reversed micelles.

Martin and Magid (1981) have detected conformational and dynamic changes in AOT reversed micelles (in cyclohexane, benzene or carbon tetrachloride) at increasing water content using ^{13}C NMR spectroscopy. Conformational changes were induced throughout the AOT molecule resulting in more open, extended micellar structures. Such structures are favored at lower w_0 in benzene or carbon tetrachloride because of solvent penetration. In the latter solvents the more favorable interactions between surfactant and solvent reduce the solubilizing capacity of AOT. A distribution of correlation times affecting the nuclear relaxation of all the carbon nuclei of AOT was inferred from frequency-dependent spin-lattice relaxation times. In a following article (Magid and Martin, 1984) the presence of different rotamers has been demonstrated, in agreement with the ^{1}H NMR data of Maitra and Eicke (1981).

Fujii and colleagues (1982) have utilized ^{31}P NMR spectroscopy in order to determine the pH of phosphate buffer inside AOT reversed micelles dissolved in octane (see also Smith and Luisi, 1980). Internal consistency could be obtained by using another, spectrophotometric method with an indicator dye. The principle of pH-measurements consists of chemical shift measurement of ^{31}P in phosphate buffer as function of pH and comparison with results in reversed micelles. The pH inside the water pools turned out to be a few tenths lower than the corresponding value in aqueous buffer. The chemical shift and accordingly the true pH in the reversed micelle was dependent on w_0 for $w_0>7$. The ^{23}Na NMR results of Fujii *et al.* (1982) are not essentially different from those of Wong *et al.* (1977).

Maitra (1984) has determined the fraction of bound water in the water core, water core radius, thickness of the bound water layer (3–5 Å) and effective head-group area of AOT in reversed micelles in isooctane or cyclohexane from chemical shifts of water protons and aggregation data. The stability of the reversed micelles is governed by the rotational isomerism of AOT (internal rotation about C–C bond of the ethane part) leading to favorable surfactant packing factors, particularly in isooctane. In the low w_0-range ($w_0<10$) some AOT molecules remain outside the interface and thereby increase the surfactant layer from about 10 Å to about 15 Å. Stabilization is then obtained by insertion of solvent molecules into the surfactant monolayer. For $w_0>10$ the number of water molecules bound to an AOT molecule remains a constant number of 6.

^{1}H NMR spectra of the small pentapeptide Met-enkephalin (an opioid molecule) in AOT reversed micelles in isooctane ($w_0=20$) were reported by De Marco *et al.* (1984). Temperature coefficients of the chemical shift of the amide protons, measured in various solvents and in reversed micelles, indicate the largest folding of the peptide in the reversed micelle. Lanthanide shift reagents selectively affect ^{1}H resonances from phenylalanine and tyrosine, from which spatial information of these amino acid residues was inferred.

The ^{13}C chemical shift data and spin-lattice relaxation times of enriched glycine, solubilized in glycerol-water mixtures and in DAP reversed micelles in benzene or carbon tetrachloride, have been used to derive microviscosities of the water pool (Tsujii *et al.*, 1983). At relatively small pools the microviscosity of entrapped glycine (i.e. the viscosity of the surrounding water molecules) turns out to be similar to that of a 78% aqueous glycerol solution. Microviscosities decrease with larger w_0.

Reversed micelles of sodium octanoate and cosolubilized water in hexanol were studied by ^{23}Na and ^{13}C NMR spectroscopy (Fujii *et al.*, 1983). Line width measurements of the ^{23}Na resonance indicate mobility of sodium ions at approximately $w_0>6$. The ^{13}C chemical shift and spin-lattice relaxation measurements indicate a different dynamic behaviour of the methylene carbons, the influence of water molecules on specific methylene carbon mobilities and contact of water with hexanol.

Lufimpadio *et al.* (1984) have utilized ^{19}F NMR spectroscopy of 6-fluorohexanol to demonstrate the distribution of this label in the interface and continuous phase in CTAB reversed micelles in hexanol. Since exchange is rapid on NMR time scale the relevant chemical shift parameters could be obtained from a titration with CTAB, and from these the concentration of hexanol in the interface.

Nuclear magnetic resonance spectroscopy has also been applied to phospholipid reversed micelles. Boicelli *et al.* (1982) have studied the effect of the presence of amino acids and small peptides in the water pools on the nuclear relaxation rates of micellar constituents. The reversed micelle consisted of egg phosphatidyl choline in deuterated benzene. ^{31}P, ^{13}C and ^{1}H spin-latice relaxation times were obtained. ^{1}H Relaxation times indicate two fractions of water molecules, bound to the polar lipid head group and freely moving water. The main effect of the incorporation of the perturbing species in the

micelles is to alter the distribution and organization of the water molecules. Cross relaxation and magnetization transfer play an important role in the relaxation mechanism of the micellar nuclei. Reversed micelles of dilinoleoyl phosphatidyl choline (DLPC) and dipalmitoyl phosphatidyl choline (DPPC) in benzene were investigated with ^{31}P NMR spectroscopy in order to determine exchange rates and lifetimes of the phospholipids (Barclay *et al.*, 1986). Two exchange rates were determined, namely from one micelle to another and from single lipids in the solvent to the micelle. A magnetization transfer to a water soluble lanthanide shift reagent ensures the resolution of the signals of the two populations. The two exchange lifetimes are similar for DLPC (≈30 ms), whereas the lifetime for monomer/micelle exchange in the DPPC system is twice as long. Direct diffusion through the solvent seems a possible mechanism for intermicellar exchange.

Lindman and coworkers (1981) have described an interesting ^{1}H and ^{13}C Fourier transform pulsed-gradient spin-echo method to obtain multicomponent self-diffusion coefficients. The method was applied to a broad range of microemulsion systems involving ionic and nonionic surfactants, cosurfactants of various (alcohol) chain length, water and different hydrocarbons (Lindman *et al.*, 1981). The measurements were performed using various compositions of constituents covering a wide range in the ternary phase diagram. Two systems will be briefly discussed, namely consisting of AOT reversed micelles (Lindman *et al.*, 1981; Stilbs and Lindman, 1984; Geiger and Eicke, 1986) and the role of cosurfactants in *w/o* microemulsion structure (Lindman *et al.*, 1981; Stilbs *et al.*, 1983). Various aspects of both systems are discussed in general by Lindman and Stilbs (1984).

Self-diffusion coefficients of the system water/AOT/*p*-xylene or isooctane reveal rapid oil diffusion and slow water diffusion. The latter system is characterized by a distinct separation into hydrophilic and hydrophobic domains. In *p*-xylene the self-diffusion coefficient of AOT is similar to that of water (Stilbs and Lindman, 1984; Lindman and Stilbs, 1984). Conversely, the self-diffusion coefficients for the system water/sodium octanoate/decanol indicate a much less distinction between hydrophilic and hydrophobic domains (Lindman and Stilbs, 1984). A nonnegligible amount of water is dispersed in the continuous medium (*cf.* also Sjöblom *et al.*, 1982).

In a recent paper Geiger and Eicke (1986) have extended ^{1}H spin-echo NMR measurements on the system water/AOT/isooctane, containing selectively deuterated, different components, with temperature as variable. The self-diffusion coefficients of AOT decrease with increasing w_0 at 25°C. The latter observation was explained by geometrical considerations and the Stokes–Einstein relation for translational diffusion. Discrepancies between observed and calculated diffusion coefficients could be resolved by the presence of a small fraction of AOT molecularly dissolved in the organic solvent. A dependence of the diffusion coefficients on temperature was observed for reversed micelles with $w_0>38$. The self-diffusion coefficient of water at 25°C is similar to that of AOT under the same experimental conditions, but it increases dramatically at increasing temperature for $w_0>38$. These phenomena were interpreted in terms of the onset of phase separation and percolation. The slightly lower self-diffusion coefficient of isooctane in the presence of AOT has been ascribed to a distribution of micellar-bound isooctane and free, mobile isooctane in the bulk dispersion medium.

Quite rapid self-diffusion of virtually all components was observed in a quaternary system like water/SDS/butanol or pentanol/toluene or cyclohexane (Stilbs *et al.*, 1983; Lindman and Stilbs, 1984). The self-diffusion coefficient of water was only a factor of 2 to 3 less than the one of the hydrocarbon. These observations indicate a low degree of organization for the system. Conversely, closed water domains are distinctly separated from the organic solvent when a long alcohol like octanol acts as cosurfactant.

Conclusion

This review shows, that in contrast to 'normal' media rather sophisticated techniques are required to obtain structural and dynamic information on reversed micellar systems. In ordinary homogeneous media, parameters such as salt concentration, acidity, viscosity, dielectric constant etc. are determined easily by a variety of techniques. However in microheterogeneous media like reversed micellar solutions, the values of these parameters are strongly regio-dependent. For example in the water pool the salt concentration will be quite different from that in the interface and organic phase. Even within water pools salt-gradients do exist as induced by the surfactant head groups. This implicates, that different techniques have to be used together to probe different regions within the micelles. With the aid of spectroscopic methods, surveyed in this review, complementary information is obtained.

REFERENCES

Agterof, W. G. M., J. A. J. Van Zomeren and A. Vry (1976) On the application of hard sphere fluid theory to liquid particle dispersions. *Chem. Phys. Lett.* **43**, 363–367.

Almgren, M., J. Van Stam, S. Swarup and J.-E. Löfroth (1986) Structure and transport in the microemulsion phase of the system Triton X-100–toluene–water. *Lang-*

muir **2**, 432–438.

Atik, S. S. and L. A. Singer (1978) Nitroxyl radical quenching of the pyrene fluorescence in micellar environments. Development of a kinetic model for steady state and transient experiments. *Chem. Phys. Lett.* **59**, 519–524.

Atik, S. S. and L. A. Singer (1979) A comparison of approximate and exact statistical models for intramicellar fluorescence quenching. *Chem. Phys. Lett.* **66**, 234–237.

Atik, S. S. and J. K. Thomas (1981a) Transport of photoproduced ions in water in oil microemulsions: Movement of ions from one water pool to another. *J. Am. Chem. Soc.* **103**, 3543–3550.

Atik, S. S. and J. K. Thomas (1981b) Photoprocesses in cationic microemulsion systems. *J. Am. Chem. Soc.* **103**, 4367–4371.

Baker, R. C., A. T. Florence, R. H. Ottewil and Th. F. Tadros (1984) Investigations into the formation and characterization of microemulsions. II. Light scattering, conductivity and viscosity studies of microemulsions. *J. Colloid Interface Sci.* **100**, 332–349.

Balny, C. and P. Douzou (1979) New trends in cryoenzymology: II. Aqueous solutions of enzymes in apolar solvents. *Biochimie* **61**, 445–452.

Barbaric, S. and P. L. Luisi (1981) Micellar solubilization of biopolymers in organic solvents. 5. Activity and conformation of α-chymotrypsin in isooctane-AOT reverse micelles. *J. Am. Chem. Soc.* **103**, 4239–4244.

Barclay, L. R. C., B. J. Balcom and B. J. Forrest (1986) *Phospholipid inverted micelles. Autooxidation* kinetics and ^{31}P NMR exchange rates. *J. Am. Chem. Soc.* **108**, 761–766.

Bardez, E., B.-T. Goguillon, E. Keh and B. Valeur (1984) Dynamics of excited-state reactions in reversed micelles. 1. Proton transfer involving a hydrophylic fluorescent probe. *J. Phys. Chem.* **86**, 4826–4831.

Bardez, E., E. Monnier and B. Valeur (1985) Dynamics of excited-state reactions in reversed micelles. 2. Proton transfer involving various fluorescent probes according to their site of solubilization. *J. Phys. Chem.* **89**, 5031–5036.

Bardez, E., E. Monnier and B. Valeur (1986) Absorption and fluorescence probing of the interface of Aerosol OT reversed micelles and microemulsions. *J. Colloid Interface Sci.* **112**, 200–207.

Belonogova, O. V., G. I. Likhtenshtein, A. V. Levashov, Y. L. Khmeniltskii, N. L. Klyachko and K. Martinek (1983) Use of the spin label method to study the state of the active site and microsurroundings of α-chymotrypsin, solubilized in octane, using surfactant Aerosol-OT. *Biokhimiya* **48**, 379–386.

Boicelli, C. A., F. Conti, M. Giomini and A. M. Giuliani (1982) Interactions of small molecules with phospholipids in inverted micelles. *Chem. Phys. Lett.* **89**, 490–496.

Bonner, F. J., R. Wolf and P. L. Luisi (1980) Micellar solubilization of biopolymers in hydrocarbon solvents. I. A structural model for protein containing reverse micelles. *J. Solid-Phase Biochem.* **5**, 254–268.

Brochette, P. and M. P. Pileni (1985) Photoelectron transfer in reverse micelles: 3. Influence of sensitizer location on reactivity. *Nouv. J. Chim.* **9**, 551–555.

Brüggeller, P. (1986) Cooling of water/oil microemulsions: The cupric probe. *J. Phys. Chem.* **90**, 1830–1834.

Cazabat, A. M., D. Chatenay, P. Guering, D. Langevin, J. Meunier, O. Sorba, J. Lang, R. Zana and M. Paillette (1984a) Percolation and critical points in microemulsions. In *Surfactants in Solution III* (Edited by K. L. Mittal and B. Lindman), pp. 1737–1744. Plenum Press, New York.

Cazabat, A. M., D. Chatenay, D. Langevin, J. Meunier and L. Leger (1984b) Mutual and self diffusion coefficients of microemulsions from spontaneous and forced light scattering techniques. In *Surfactants in Solution III* (Edited by K. L. Mittal and B. Lindman), pp. 1729–1736. Plenum Press, New York.

Cazabat, A. M. and D. Langevin (1981) Diffusion of interacting particles: Light scattering study of microemulsions. *J. Chem. Phys.* **74**, 3148–3158.

Cazabat, A. M., D. Langevin and A. Pouchelon (1980) Light-scattering study of water-oil microemulsions. *J. Colloid Interface Sci.* **73**, 1–12.

Chatenay, D., W. Urbach, A. M. Cazabat, M. Vacher and M. Waks (1985) Proteins in membrane-mimetic systems. Insertion of myelin basic protein into microemulsion droplets. *Biophys. J.* **48**, 893–898.

Costa S. M. B. and R. L. Brookfield (1986) Interactions of excited-state porphyrin-quinone in reversed micelles studied by time-resolved fluorescence spectroscopy. *J. Chem. Soc. Faraday Trans. II* **82**, 991–1002.

Day, R. A., B. H. Robinson, J. H. R. Clarke and J. V. Doherty (1979) Characterization of water-containing reversed micelles by viscosity and dynamic light scattering methods. *J. Chem. Soc. Faraday Trans. I* **75**, 132–139.

De Gennes, P. G. and C. Taupin (1982) Microemulsions and the flexibility of oil/water interfaces. *J. Phys. Chem.* **86**, 2294–2304.

Dekker, M., K. Van't Riet, S. R. Weyers, J. W. A. Baltussen, B. Bijsterbosch and C. Laane (1986) Enzyme recovery by liquid/liquid extraction using reversed micelles. *Chem. Eng. J.* **33**, B27–B33.

De Kruyff, B., P. R. Cullis and A. J. Verkley (1980) *Non-bilayer lipid structures in model and biological* membranes. *Trends Biochem. Sci.* **5**, 79–81.

Delahodde, A., M. Vacher, C. Nicot and M. Waks (1984) Solubilization and insertion into reverse micelles of the major myelin transmembrane proteolipid. *FEBS Lett.* **172**, 343–347.

De Marco, A., L. Zetta, E. Menegatti and M. Guarneri (1984) ^{1}H-NMR of Met-enkephalin in AOT reverse micelles. *FEBS Lett.* **178**, 39–43.

Dichristina, T., D. Roux, A. M. Bellocq and P. Bothorel (1985) Study by light scattering of the effect of the surfactant chemical structure on micellar interactions of water/oil microemulsions. *J. Phys. Chem.* **89**, 1433–1437.

Douzou, P., E. Keh and C. Balny (1979) Cryoenzymology in aqueous media: Micellar solubilized water clusters. *Proc. Natl. Acad. Sci. USA* **76**, 681–684.

Dvolaitzky, M., M. Guyot, M. Lagues, J. P. Le Pesant, R. Ober, C. Sauterey and C. Taupin (1978) A structured description of liquid particle dispersions: Ultracentrifugation and small angle neutron scattering studies of microemulsions. *J. Chem. Phys.* **69**, 3279–3288.

Eicke, H. F. (1980) Surfactants in nonpolar solvents. Aggregation and micellization. *Top. Curr. Chem.* **87**, 85–145.

Eicke, H. F., R. Hilfiker and H. Thomas (1985) Probing order phenomena by pulsed electro-optic Kerr effect measurements. *Chem. Phys. Lett.* **120**, 272–275.

Eicke, H. F., J. C. W. Shepperd and A. Steinemann (1976) Exchange of solubilized water and aqueous electrolyte solutions between micelles in apolar media. *J. Colloid Interface Sci.* **56**, 168–176.

Eicke, H. F. and P. E. Zinsli (1978) Nanosecond spectroscopic investigations of molecular processes in *w/o* microemulsions. *J. Colloid Interface Sci.* **65**, 131–140.

Erjomin, A. N. and D. I. Metelitza (1984) Fluorescence of *hemoproteins in reversed micelles of surfactants* in octane. *Biokhimiya* **49**, 1947–1954.

Fendler, J. H. (1982) *Membrane-Mimetic Chemistry*. Wiley-Interscience, New York.

Fletcher, P. D. I., A. M. Howe, N. M. Perrins, B. H. Robinson, C. Toprakcioglu and J. C. Dore (1984) Structural and dynamic aspects of microemulsions. In

Surfactants in Solution III (Edited by K. L. Mittal and B. Lindman) pp. 1745–1758. Plenum Press, New York.

Fletcher, P. D. I., B. H. Robinson and J. Tabony (1986) A quasi-elastic neutron scattering study of water-in-oil microemulsions stabilized by Aerosol-OT. Effect of additives including solubilized protein on molecular motions. *J. Chem. Soc. Faraday Trans. 1* **82**, 2311–2321.

Fujii, H., T. Kawai, H. Nishikawa and G. Ebert (1982) Determination of pH in reversed micelles. II. Application of the method proposed previously to other reversed micellar systems. *Colloid Polymer Sci.* **260**, 697–701.

Fuji, H., T. Kawai, H. Nishikawa and G. Ebert (1983) ^{13}C- and ^{23}Na-NMR studies of sodium octanoate in reversed micelles. *Colloid Polymer Sci.* **261**, 340–345.

Furois, J. M., P. Brochette and M. P. Pileni (1984) Photoelectron transfer in reverse micelles: 2. Photooxidation of magnesium porphyrin. *J. Colloid Interface Sci.* **97**, 552–558.

Gandin, E., Y. Lion and A. Van de Vorst (1984) Diffusion-concentration product of oxygen within water pools of Aerosol-OT-heptane reversed micelles. *J. Phys. Chem.* **88**, 280–284.

Geiger, S. and H. F. Eicke (1986) The macrofluid concept versus the molecular mixture. A spin-echo-NMR study of the water/Aerosol-OT/oil system. *J. Colloid Interface Sci.* **110**, 181–187.

Geladé, E., N. Boens and F. C. De Schryver (1982) Exciplex formation in dodecylammonium propionate reversed micellar system. *J. Am. Chem. Soc.* **104**, 6288–6292.

Geladé, E. and F. C. De Schryver (1982) Fluorescence quenching in dodecylammonium propionate reversed micelles. *J. Photochem.* **18**, 223–230.

Geladé, E. and F. C. De Schryver (1984a) Fluorescence: A method to obtain information about reverse micellar systems. In *Reverse Micelles* (Edited by P. L. Luisi and B. E. Straub), pp. 143–164. Plenum, New York.

Geladé, E. and F. C. De Schryver (1984b) Energy transfer in inverse micelles. *J. Am. Chem. Soc.* **106**, 5871–5875.

Gierasch, L. M., K. F. Thompson, J. E. Lacy and A. L. Rockwell (1984) Exploring peptide interactions with interfacial water. In *Reverse Micelles* (Edited by P. L. Luisi and B. E. Straub), pp. 265–277. Plenum, New York.

Giovenco, S., F. Verheggen and C. Laane (1987) Purification of intracellular enzymes from whole bacterial cells using reversed micelles. *Enz. Microb. Technol.* Submitted.

Grandi, C., R. E. Smith and P. L. Luisi (1981) Micellar solubilization of biopolymers in organic solvents. Activity and conformation of lysozyme in isooctane reverse micelles. *J. Biol. Chem.* **256**, 837–843.

Gulari, E., B. Bedwell and S. Alkhafaji (1980) Quasi-electric light-scattering investigation of microemulsions. *J. Colloid Interface Sci.* **77**, 202–212.

Handa, T., M. Sakai and M. Nakagaki (1986) Two solubilization sites of tris(2,2'-bipyridine) ruthenium(II) dichloride in water/oil non-ionic emulsion. *J. Phys. Chem.* **90**, 3377–3380.

Hilfiker, R., H. F. Eicke, S. Geiger and G. Furler (1985) Optical studies of critical phenomena in macrofluid-like three-component microemulsions. *J. Colloid Interface Sci.* **105**, 378–387.

Holmgren, A., K. Fontell and G. Lindblom (1986) A Fourier transform-infrared study of the reversed micellar solution phase of the sodium octanoate/octanoic acid/water system. *Acta Chem. Scand.* **A40**, 299–305.

Howe, A. M., C. Toprakcioglu, J. C. Dore and B. H. Robinson (1986) Small-angle neutron scattering studies of microemulsions stabilized by Aerosol-OT. Part 3. The effect of additives on phase stability and droplet structure. *J. Chem. Soc. Faraday Trans. 1* **82**, 2411–2422.

Imre, V. E. and P. L. Luisi (1982) Solubilization and condensed packaging of nucleic acids in reversed micelles. *Biochem. Biophys. Res. Commun.* **107**, 538–545.

Infelta, P. P., M. Grätzel and J. K. Thomas (1974) Luminescence decay of hydrophobic molecules solubilized in aqueous micellar systems. A kinetic model. *J. Phys. Chem.* **78**, 190–195.

Janzen, E. G., Y. Kotake, G. A. Coulter and W. M. Oehler (1986) ENDOR in water pools of inverse micelles in toluene. *Chem. Phys. Lett.* **126**, 205–208.

Jao, T. C. and K. L. Kreuz (1984) Solubility of oxygen in inverted micelles of calcium alkylbenzene sulfonates. *J. Colloid Interface Sci.* **102**, 308–310.

Jao, T. C. and K. L. Kreuz (1986) Characterization of inverted micelles of calcium alkarylsulfonates by some pyrene fluorescence probes. In *ACS Symp. Ser. 311, Phenomena in Mixed Surfactant Systems* (Edited by J. F. Scamehorn), pp. 90–99.

Kaler, E. W., K. E. Bennet, H. T. Davis and L. E. Scriven (1983) Toward understanding microemulsion microstructure: A small-angle X-ray scattering study. *J. Chem. Phys.* **79**, 5673–5684.

Kaler, E. W. and S. Prager (1982) A model of dynamic scattering by microemulsions. *J. Colloid Interface Sci.* **86**, 359–369.

Keh, E. and B. Valeur (1981) Investigation of water-containing inverted micelles by fluorescence polarization. Determination of size and internal fluidity. *J. Colloid Interface Sci.* **79**, 465–478.

Kitahara, A. (1980) Solubilization and catalysis in reverse micelles. *Adv. Colloid Interface Sci.* **12**, 109–140.

Kondo, H., M. Ichiro and J. Sunamoto (1982) Biphasic structure for reversed micelles. Depressed acid dissociation of excited-state pyranine in the restricted reaction field. *J. Phys. Chem.* **86**, 4826–4831.

Kumar, V. V., C. Kumar and P. Raghunathan (1984) Studies on lecithin reverse micelles: Optical birefringence, viscosity, light scattering, electrical conductivity and electron microscopy. *J. Colloid Interface Sci.* **99**, 315–323.

Lee, P. C. and M. A. J. Rodgers (1983) Singlet molecular oxygen in micellar systems. 1. Distribution equilibria between hydrophobic and hydrophilic compartments. *J. Phys. Chem.* **87**, 4894–4898.

Lim, Y. Y. and J. H. Fendler (1978) Spin probes in reversed micelles. Electron paramagnetic spectra of 2,2,5,5-tetramethyl pyrrolidine-1-oxyl derivatives in benzene in the presence of dodecylammonium propionate aggregates. *J. Am. Chem. Soc.* **100**, 7490–7494.

Lindman, B. and P. Stilbs (1984) Characterization of microemulsion structure using multi-component self-diffusion data. In *Surfactants in Solution III* (Edited by K. L. Mittal and B. Lindman), pp. 1651–1662. Plenum Press, New York.

Lindman, B., P. Stilbs and M. E. Mosely (1981) Fourier transform NMR self-diffusion and microemulsion structure. *J. Colloid Interface Sci.* **83**, 569–582.

Lufimpadio, N., J. B. Nagy and E. G. Derouane (1984) Preparation of colloidal iron boride particles in the CTAB–hexanol–water reversed micellar system. In *Surfactants in Solution III* (Edited by K. L. Mittal and B. Lindman), pp. 1483–1497. Plenum Press, New York.

Luisi, P. L. (1985) Enzymes hosted in reverse micelles in hydrocarbon solution. *Angew. Chem. (Int. Ed.)* **24**, 439–460.

Luisi, P. L. and C. Laane (1986) Solubilization of

enzymes in apolar solvents via reverse micelles. *Trends Biotech.* **4**, 153–161.

Luisi, P. L. and L. J. Magid (1986) Solubilization of enzymes and nucleic acids in hydrocarbon micellar solution. *CRC Crit. Rev. Biochem.* **20**, 409–474.

Magid, L. J. (1986) The elucidation of micellar and microemulsion architecture using small-angle neutron scattering. *Colloids Surf.* **19**, 129–158.

Magid, L. J. and C. A. Martin (1984) ^{13}C NMR studies of molecular conformations and interactions in the curved surfactant monolayers of Aerosol OT water-in-oil microemulsions. In *Reverse Micelles* (Edited by P. L. Luisi and B. E. Straub), pp. 181–193. Plenum, New York.

Maitra, A. (1984) Determination of size parameters of water-Aerosol-OT-oil reverse micelles from their nuclear magnetic resonance data. *J. Phys. Chem.* **88**, 5122–5125.

Maitra, A. and H. F. Eicke (1981) Effect of rotational isomerism on the water-solubilizing properties of Aerosol-OT as studied by ^1H-NMR spectroscopy. *J. Phys. Chem.* **85**, 2687–2691.

Maitra, A., G. Vasta and H. F. Eicke (1983) Revisiting the effects of nonamphiphilic organic additives on the water solubilizing properties of Aerosol-OT within the L_2 phase. *J. Colloid Interface Sci.* **93**, 383–391.

Martin, C. A. and L. J. Magid (1981) Carbon-13 NMR investigations of Aerosol-OT water-in-oil microemulsions. *J. Phys. Chem.* **85**, 3938–3944.

Martinek, K., A. V. Levashov, N. Klyachko, Y. L. Khmelnitski and I. V. Berezin (1986) Micellar enzymology. *Eur. J. Biochem.* **155**, 453–468.

Meier, P. and P. L. Luisi (1980) Micellar solubilization of biopolymers in hydrocarbon solvents. II. The case of horse liver alcohol dehydrogenase. *J. Solid-Phase Biochem.* **5**, 269–282.

Menger, F. M., G. Saito, G. V. Sanzero and J. R. Dodd (1975) Motional freedom and polarity within water pools of different sizes. Spin label studies. *J. Am. Chem. Soc.* **97**, 909–911.

Nicholson, J. D. and J. H. R. Clarke (1984) Photon correlation techniques in the investigation of water-in-oil microemulsions. In *Surfactants in Solution III* (Edited by K. L. Mittal and B. Lindman), pp. 1663–1674. Plenum Press, New York.

Nicot, C., M. Vacher, M. Vincent, J. Gallay and M. Waks (1985) Membrane proteins in reverse micelles: Myelin basic protein in a membrane-mimetic environment. *Biochemistry* **24**, 7024–7032.

Ober, R. and C. Taupin (1980) Interactions and aggregation in microemulsions. A small-angle neutron scattering study. *J. Phys. Chem.* **84**, 2418–2422.

O'Connor, C. J., T. D. Lomax and R. E. Ramage (1984) Exploitation of reversed micelles as membrane-mimetic reagents. *Adv. Colloid Interface Sci.* **20**, 21–97.

Overbeek, J. Th. G. (1978) Microemulsions: A field at the border between lyophobic and lyophilic colloids. *Far. Discussions Chem. Soc.* **65**, 7–19.

Pileni, M. P. (1981) Photoelectron transfer in reverse micelles. Photoreduction of cytochrome *c*. *Chem. Phys. Lett.* **81**, 603–605.

Pileni, M. P., P. Brochette, B. Hickel and B. Lerebours (1984) Hydrated electrons in reverse micelles: 2. Quenching of hydrated electron by sodium nitrate. *J. Colloid Interface Sci.* **98**, 549–554.

Pileni, M. P., Th. Zemb and C. Petit (1985) Solubilization by reverse micelles: Solute localization and structure perturbation. *Chem. Phys. Lett.* **118**, 414–420.

Politi, M. J., O. Brandt and J. H. Fendler (1985) Ground and excited-state proton transfers in reversed micelles. Polarity restrictions and isotope effects. *J. Phys. Chem.* **89**, 2345–2354.

Politi, M. J. and H. Chaimovich (1986) Water activity in reversed sodium *bis*(2-ethylhexyl) sulfosuccinate micelles. *J. Phys. Chem.* **90**. 282–287.

Ravier, J. C. and M. Buzier (1984) Structure of non-ionic microemulsions by small angle neutron scattering. In *Surfactants in Solution III* (Edited by K. L. Mittal and B. Lindman), pp. 1759–1779. Plenum Press, New York.

Robinson, B. H., C. Toprakcioglu, J. C. Dore and P. Chieux (1984) Small-angle neutron scattering study of microemulsions stabilized by Aerosol-OT. Part 1. Solvent and concentration variation. *J. Chem. Soc. Faraday Trans. I* **80**, 13–27.

Rodgers, M. A. J. (1981) Picosecond fluorescence studies of xanthene dyes in anionic micelles in water and reverse micelles in heptane. *J. Phys. Chem.* **85**, 3372–3374.

Rodgers, M. A. J. (1984) Picosecond studies of rose bengal fluorescence in reverse micellar systems. In *Reverse Micelles* (Edited by P. L. Luisi and B. E. Straub), pp. 165–174. Plenum, New York.

Rodgers, M. A. J. and P. C. Lee (1984) Singlet molecular oxygen in micellar systems. 2. Quenching behaviour in AOT reverse micelles. *J. Phys. Chem.* **88**, 3480–3484.

Roux, D., A. M. Bellocq and P. Bothorel (1984) Effect of the molecular structure of components on micellar interactions in microemulsions. *Prog. Colloid Polymer Sci.* **69**, 1–11.

Seelig, J. (1984) Lipid polymorphism, reverse micelles and phophorus-31 nuclear magnetic resonance. In *Reverse Micelles* (Edited by P. L. Luisi and B. E. Straub), pp. 209–220. Plenum, New York.

Sein, E., J. R. Lalanne, J. Buchert and S. Kielich (1979) Dynamic aspect of Raleigh scattering and viscosity of the ternary system Aerosol-OT/water/carbon tetrachloride. *J. Colloid Interface Sci.* **72**, 363–366.

Seno, M., H. Noritomi, Y. Kuroyanagi, K. Iwamoto and G. Ebert (1984) Conformational studies of poly(N^5-ω-hydroxyalkyl-L-Glutamine)s in reversed micelles. *Colloid Polymer Sci.* **262**, 896–901.

Seno, M., K. Sawada, K. Araki, H. Kise and K. Iwamoto (1980) ESR spectra of Mn(II) ions in reversed micellar systems. *Bull. Chem. Soc. Jpn.* **53**, 2083–2084.

Sjöblom, J., K. Rosenqvist and P. Stenius (1982) Reversed micellar solutions in the system sodium octanoate/decanol/water: Model calculations and dynamic light scattering measurements. *Colloid Polymer Sci.* **260**, 82–88.

Smith, R. E. and P. L. Luisi (1980) Micellar solubilization of biopolymers in hydrocarbon solvents. III. Empirical definition of an acidity scale in reverse micelles. *Helv. Chim. Acta* **63**, 2302–2311.

Stilbs, P. and B. Lindman (1984) Aerosol-OT aggregation in water and hydrocarbon solution from NMR self-diffusion measurements. *J. Colloid Interface Sci.* **99**, 290–293.

Stilbs, P., K. Rapacki and B. Lindman (1983) Effect of alcohol cosurfactant length on microemulsion structure. *J. Colloid Interface Sci.* **95**, 583–585.

Tachiya, M. (1975) Application of a generating function to reaction kinetics in micelles. Kinetics of quenching of luminescent probes in micelles. *Chem. Phys. Lett.* **33**, 289–292.

Thompson, K. F. and L. M. Gierasch (1984) Conformation of a peptide solubilizate in a reversed micelle water pool. *J. Am. Chem. Soc.* **106**, 3648–3652.

Toprakcioglu, C., J. C. Dore, B. H. Robinson, A. Howe and P. Chieux (1984) Small-angle neutron-scattering studies of microemulsions stabilized by Aerosol-OT. Part 2. Critical scattering and phase stability. *J. Chem. Soc. Faraday Trans. I* **80**, 413–422.

Tsujii, K., J. Sunamoto and J. H. Fendler (1983) Microscopic viscosity of the interior

water pool in dodecylammonium propionate reversed micelles. *Bull. Chem. Soc. Jpn.* **56**, 2889–2893.

Van Dijk, M. A., G. Casteleijn, J. G. H. Joosten and Y. K. Levine (1986) Percolation in oil-continuous microemulsions. A dielectric study of Aerosol OT/water/isooctane. *J. Chem. Phys.* **85**, 626–631.

Visser, A. J. W. G. and J. H. Fendler (1982) Reaction of reversed micelle entrapped cytochrome c and cytochrome c_3 by electrons generated by pulse radiolysis or by pyrene photoionization. *J. Phys. Chem.* **86**, 947–950.

Visser, A. J. W. G. and J. S. Santema (1984) A luminol-mediated assay for oxidase reactions in reversed micellar systems. In *Analytical Applications of Bioluminescence and Chemiluminescence* (Edited by L. J. Kricka, P. E. Stanley, G. H. G. Thorpe and T. P. Whitehead), pp. 559–563. Academic Press, London.

Visser, A. J. W. G., J. S. Santema and A. Van Hoek (1984) Spectroscopic and dynamic characterization of FMN in reversed micelles entrapped water pools. *Photochem. Photobiol.* **39**, 11–16.

Visser, A. J. W. G., K. Vos, J. S. Santema, J. Bouwstra and A. Van Hoek (1987) Static and time-resolved fluorescence of an amphiphilic flavin in Aerosol OT reversed micelles. *Photochem. Photobiol.* Submitted.

Waks, M. (1986) Proteins and peptides in water-restricted environments. *Proteins: Struc. Funct. Genet.* **1**, 4–15.

Wolf, R. and P. L. Luisi (1979) Micellar solubilization of enzymes in hydrocarbon solvents. Enzymatic Activity and spectroscopic properties of ribonuclease in *n*-octane. *Biochim. Biophys. Res. Commun.* **89**, 209–217.

Wong, M., J. K. Thomas and T. Nowak (1977) Structure and state of H_2O in reversed micelles. 3. *J. Am. Chem. Soc.* **99**, 4730–4736.

Yoshioka, H. (1981) Temperature dependence of motion of a spin probe in Aerosol-OT reversed micelles. *J. Colloid Interface Sci.* **83**, 214–220.

Yoshioka, H. (1983) Exchange of the position of a spin probe in Aerosol-OT reversed micelles. *J. Colloid Interface Sci.* **95**, 81–86.

Yoshioka, H. and S. Kazama (1983) Spectral simulation study of the positional exchange of a spin probe in an Aerosol-OT reversed micelle. *J. Colloid Interface Sci.* **95**, 240–246.

Zulauf, M. and H. F. Eicke (1979) Inverted micelles and microemulsions in the ternary system H_2O/Aerosol-OT/isooctane as studied by photon correlation spectroscopy. *J. Phys. Chem.* **83**, 480–486.

3 APPLICATION OF A REFERENCE CONVOLUTION METHOD TO TRYPTOPHAN FLUORESCENCE IN PROTEINS
A REFINED DESCRIPTION OF ROTATIONAL DYNAMICS

Kees Vos, Arie van Hoek and Antonie J.W.G. Visser

Reprinted from: European Journal of Biochemistry (1987) 165, 55-63.

A reference method for the deconvolution of polarized fluorescence decay data is described. Fluorescence lifetime determinations for *p*-terphenyl, *p*-bis[2-(5-phenyloxazolyl)]benzene and *N*-acetyltryptophanamide ($AcTrpNH_2$) show that with this method more reliable fits of the decays can be made than with the scatterer method, which is most frequently used. Analysis of the $AcTrpNH_2$ decay with *p*-terphenyl as the reference compound yields an excellent fit with lifetimes of 2.985 ns for $AcTrpNH_2$ and 1.099 ns for *p*-terphenyl (20°C), whereas the $AcTrpNH_2$ decay cannot be satisfactorily fitted when the scatterer method is used. The frequency of the detected photons is varied to determine the conditions where pulse pile-up starts to affect the measured decays. At detection frequencies of 5 kHz and 15 kHz, which corresponds to 1.7% and 5% respectively of the rate of the excitation photons no effects are found. Decays measured at 30 kHz (10%) are distorted, indicating that pile-up effects play a role at this frequency.

The fluorescence and fluorescence anisotropy decays of the tryptophan residues in the proteins human serum albumin, horse liver alcohol dehydrogenase and lysozyme have been reanalysed with the reference method. The single tryptophan residue of the albumin is shown to be characterized by a triple-exponential fluorescence decay. The anisotropy decay of albumin was found to be mono-exponential with a rotational correlation time of 26 ns (20°C). The alcohol dehydrogenase has two different tryptophan residues to which single lifetimes are assigned. It is found that the rotational correlation time for the dehydrogenase changes with excitation wavelength (33 ns for λ_{ex} = 295 nm and 36 ns for λ_{ex} = 300 nm at 20°C), indicating a nonspherical protein molecule. Lysozyme has six tryptophan residues, which give rise to a triple-exponential fluorescence decay. A single-exponential decay with a rotational correlation time of 3.8 ns is found for the anisotropy. This correlation time is significantly shorter than that arising from the overall rotation and probably originates from intramolecular, segmental motion.

Time-resolved fluorescence measurements of intrinsic probes in proteins can be a powerful tool to obtain information about the molecular structure and dynamic processes taking place on the fluorescence time scale, like rotation of the whole molecule or segments of it and interactions with other molecules, present in the solution [1, 2]. One class of intrinsic probes is formed by the tryptophan residues in proteins [3].

Interpretation of tryptophan fluorescence decay is a complex matter. In many cases, multiple exponential decays are found for proteins containing a single tryptophan [4]. This anomalous behaviour has been explained by the existence of three different $\alpha-\beta$ rotamers of tryptophan. According to the so-called 'modified conformer model' (MCM) [5–7] intramolecular charge transfer from the excited indole ring to electrophilic substituents on the 3-ethyl chain can occur. In each of the three $\alpha-\beta$ rotamers the distance and orientation of the indole ring relative to these substituents can be different, leading to different amounts of intramolecular charge transfer and thus to different lifetimes. Another complicating factor is that the light absorption of indole in the near-ultraviolet region involves two overlapping transitions, ^1L_a and ^1L_b [8, 9]. The relative contribution of these two transitions to the fluorescence is dependent on the excitation and emission wavelengths. Emission at 345 nm originates solely from the ^1L_a state, but excitation at 295 nm or 300 nm elicits both the ^1L_a and ^1L_b transitions [9]. Energy transfer between the two states can occur very efficiently [10, 11] and therefore the observed fluorescence is partially the result of this process. This explains why the anisotropy of the fluorescence at zero time never reaches the theoretical value of 0.4 even in case of immobilized fluorophores [12]. Changing the excitation wavelength from 295 nm to 300 nm gives a decrease of the contribution of the ^1L_b transition and thus an increase of the initial anisotropy.

At present, the most frequently used method for the time-resolved fluorescence measurements, is time-correlated single-photon counting [13]. The observed fluorescence, $S(t)$, is then a convolution of the delta pulse response, $s(t)$, of the sample, with the impulse response profile, $P(t)$. Once $P(t)$ is known, the decay parameters of the fluorescence can be obtained from $S(t)$ by a deconvolution procedure. A method to measure $P(t)$ is to use a scatterer, but this has the serious drawback that the measurements of $P(t)$ and $S(t)$ occur at different wavelengths and since most photomultipliers show some wavelength-dependent time dependence [14, 15] the $P(t)$

Correspondence to A. J. W. G. Visser, Laboratorium voor Biochemie der Landbouwuniversiteit, De Dreijen 11, NL-6703 BC Wageningen, The Netherlands

Abbreviations. $AcTrpNH_2$, *N*-acetyl-tryptophanamide; POPOP, *p*-bis[2-(5-phenyloxazolyl)]benzene; HSA, human serum albumin; DW, Durbin-Watson parameter; LADH, horse-liver alcohol dehydrogenase; MCA, multichannel analyzer.

Enzymes. Horse liver alcohol dehydrogenase (EC 1.1.1.1); lysozyme (EC 3.2.1.17).

obtained is not the actual profile. To overcome this problem Zuker et al. [16] have recently developed a method in which the real $P(t)$ is obtained via the exponential fluorescence of a reference compound, which emits at the same wavelength as the sample under consideration. We have applied this method in a study of the tryptophan fluorescence and anisotropy decays of the proteins human serum albumin (HSA), horse liver alcohol dehydrogenase (LADH) and lysozyme, using *p*-terphenyl as reference compound and we have compared the results obtained with the 'reference method' to the ones obtained with the 'scatterer method'. Refinement of the procedure leads to a more profound interpretation of the experimental results and to new insights into the type of motions of these proteins.

MATERIALS AND METHODS

Chemicals and enzymes

(*p*-Terphenyl (scintillation grade) obtained from BDH and *p*-bis[2-(5-phenyloxazolyl)]benzene (POPOP, scintillation grade) obtained from Eastman Kodak, were dissolved in ethanol (Merck, fluorescent grade). AcTrpNH$_2$ (*N*-acetyl-L-tryptophanamide) purchased from Sigma was dissolved in 50 mM pH 7.0 potassium phosphate buffer. Oxygen quenching was prevented by bubbling the samples with oxygen-free argon. Defatted monomeric human serum albumin (HSA) was prepared as described for bovine serum albumin [17]. HSA (Sigma) was dissolved in water; charcoal was added and the pH of the solution was adjusted to 3.0 with 1 M HCl. After 2 h of stirring at room temperature, the charcoal was removed by centrifugation and the supernatant was adjusted to pH 8.0 with 1 M NaOH. Subsequently the supernatant was applied to a column (2.0 × 30 cm) of Sephadex G-150 (Pharmacia) equilibrated with 50 mM Tris, 0.2 M NaCl pH 8.0; 1-ml fractions were collected and only the last protein-containing fraction (monomer) was used for the experiments. LADH and lysozyme were obtained from Boehringer, LADH as a crystaline suspension in 20 mM potassium phosphate, 10% ethanol pH 7.0. 1 ml of the suspension was dialysed against 20 mM potassium phosphate pH 7.0 buffer for 24 h. Afterwards the undissolved material was removed by centrifugation. Lysozyme, which was supplied in a dry crystalline form, was dissolved in the same phosphate buffer and also dialysed for 24 h. All solutions were prepared with an $A_{295\,nm}$ = 0.1, except the POPOP solution, which had an $A_{295\,nm}$ of 0.05. All experiments were done at 20°C, unless otherwise indicated.

Experimental setup

The experimental setup for the polarized fluorescence decay measurements has been described previously [18, 19]. Some changes in the detection system were made to increase the sensitivity. A sheet of Polaroid (type HNP'B linear polarizer for ultraviolet radiation) was used to separate the parallel and the perpendicular components of the fluorescence. Every 10 s (controlled by the timer of the multichannel analyzer) this polarizer was rotated 90° from the original position in 0.3 s and the different components were stored in two different subgroups of the MCA (1024 channels). Typically this procedure was repeated 10 times. The detection wavelength was selected with interference filters (337, 345, 350 and 437 nm, 10-nm bandpass). The digital output of the MCA was sent to a Micro VAX II computer, where the data were evaluated.

DATA ANALYSIS

Fluorescence

The parallel, $I_{\parallel}(t)$, and the perpendicular, $I_{\perp}(t)$, polarized components of the fluorescence are measured. From these components the total fluorescence can be calculated:

$$S(t) = I_{\parallel}(t) + 2I_{\perp}(t) . \tag{1}$$

$S(t)$ is a convolution of the actual fluorescence, $s(t)$, with the impulse response profile, $P(t)$:

$$S(t) = P(t) * s(t) = \int_0^t P(t')\, s(t-t')\mathrm{d}t' . \tag{2}$$

This discussion will be restricted to (sum of) exponential decays, where:

$$s(t) = \sum_i \alpha_i \exp(-t/\tau_i) . \tag{3}$$

The τ_i's are the fluorescence lifetimes and the α_i's are a measure for the contribution of the different lifetimes to the total fluorescence decay. The fluorescence parameters α_i and τ_i must be determined from $S(t)$. The most popular among the different methods is that of least-squares fitting. In this procedure the weighted sum of squared residuals, WSSR, is minimized.

$$\mathrm{WSSR} = \sum_{k=1}^{n} w_k [S(t_k) - S_c(t_k)]^2 . \tag{4}$$

$S_c(t)$ is the calculated fit of $S(t)$, w_k is the weighting factor of data point $S(t_k)$ and n is the total number of data points. The weighting factors are given by the inverse of the variance of $S(t_k)$ [20–22].

$$w_k = 1.0/\mathrm{var}[S(t_k)] . \tag{5}$$

$$\mathrm{var}[S(t_k)] = \mathrm{var}[I_{\parallel}(t_k)] + 4\,\mathrm{var}[I_{\perp}(t_k)] . \tag{6}$$

For single-photon counting data, Poissonian noise is assumed so the variances of $I_{\parallel}(t_k)$ and $I_{\perp}(t_k)$ can be estimated as follows:

$$\mathrm{var}[I_{\parallel}(t_k)] = I_{\parallel}(t_k) . \tag{7a}$$

$$\mathrm{var}[I_{\perp}(t_k)] = I_{\perp}(t_k) . \tag{7b}$$

When background fluorescence must be subtracted $I_{\parallel}(t_k)$ and $I_{\perp}(t_k)$ are given by:

$$I_{\parallel}(t_k) = I_{s\parallel}(t_k) - I_{b\parallel}(t_k) \tag{8a}$$

$$I_{\perp}(t_k) = I_{s\perp}(t_k) - I_{b\perp}(t_k) \tag{8b}$$

where the subscripts s and b denote sample and background fluorescence respectively. In this case the Eqns (7) become:

$$\mathrm{var}[I_{\parallel}(t_k)] = I_{s\parallel}(t_k) + I_{b\parallel}(t_k) \tag{9a}$$

$$\mathrm{var}[I_{\perp}(t_k)] = I_{s\perp}(t_k) + I_{b\perp}(t_k) . \tag{9b}$$

Application of the proper weighting factors in the case of background fluorescence is very important in the fitting procedure.

As mentioned in the introduction, the use of a scatterer to measure $P(t)$ directly has serious disadvantages and therefore the use of reference compounds to obtain the impulse response profile has been proposed by several authors [16, 23–26]. Using the fluorescence, $S_r(t)$, of a reference compound with a single-exponential decay, with lifetime τ_r, the decay parameters can be obtained from:

$$S(t) = \sum_i \alpha_i S_r(t) + S_r(t) * \left\{ \sum_i \alpha_i \left(\frac{1}{\tau_r} - \frac{1}{\tau_i} \right) \exp(-t/\tau_i) \right\} . \tag{10}$$

In the weighting factors for the residues both the noise in $S(t)$ and $S_r(t)$ must be accounted for, therefore:

$$w_k = 1.0/\{\mathrm{var}[S(t_k)] + \left(\sum_i \alpha_i\right)^2 \mathrm{var}[S_r(t_k)]\}. \qquad (11)$$

Minimization of the weighted-squared residuals can be performed with τ_r fixed, if an accurate value is known for it, or with τ_r as an extra iteration variable. A number of available reference compounds is well characterized [16, 27, 28], so in most cases τ_r will be known beforehand. A limitation of the method is that in the case that one of the τ_i values equals τ_r, this component will not be found in the analysis, because of elimination of the term $(1/\tau_r - 1/\tau_i)$ in Eqn (10).

Anisotropy

The anisotropy $r(t)$ of the fluorescence, is defined as follows:

$$r(t) = \frac{i_\parallel(t) - i_\perp(t)}{i_\parallel(t) + 2i_\perp(t)}. \qquad (12)$$

Like $s(t)$, $r(t)$ can be analysed in terms of a series of exponentials:

$$r(t) = \sum_j \beta_j \exp(-t/\phi_j) \qquad (13)$$

where ϕ_j are the rotational correlation times. Experimentally one obtains $I_\parallel(t)$ and $I_\perp(t)$ and not $i_\parallel(t)$ and $i_\perp(t)$. Hence the only quantity that can be directly constructed is the so-called experimental anisotropy, $R(t)$:

$$R(t) = \frac{I_\parallel(t) - I_\perp(t)}{I_\parallel(t) + 2I_\perp(t)}. \qquad (14)$$

The relationship between $R(t)$ and $r(t)$ is:

$$R(t) = \frac{P(t) * \{s(t)r(t)\}}{S(t)}. \qquad (15)$$

When the α_i's and the τ_i's are known the anisotropy parameters can be obtained by fitting $R(t)$ to Eqn (15) (cf. [19]) but it is also possible to derive the expressions for $I_\parallel(t)$ and $I_\perp(t)$ and fit these quantities simultaneously with one set of parameters [29, 30].

Combination of Eqn (14) with Eqn (15) gives:

$$I_\parallel(t) = P(t) * \left\{\frac{2}{3}r(t)s(t) + \frac{1}{3}s(t)\right\} \qquad (16a)$$

$$I_\perp(t) = P(t) * \left\{\frac{1}{3}s(t) - \frac{1}{3}r(t)s(t)\right\}. \qquad (16b)$$

The weighting factors for the residuals, $w_{k\parallel}$ and $w_{k\perp}$, are in this case given by the inverse of the variances of $I_\parallel(t_k)$ and $I_\perp(t_k)$. The Eqns (15) and (16) can be used in the case that $P(t)$ is measured directly with a scatterer. When a reference is used the expressions for $I_\parallel(t)$ and $I_\perp(t)$ are (cf. [26]):

$$I_\parallel(t) = \frac{1}{3}\left(\sum_i \alpha_i + 2\sum_i\sum_j \alpha_i\beta_j\right) S_r(t) + \frac{1}{3}S_r(t) * \sum_i \left\{\alpha_i\left(\frac{1}{\tau_r} - \frac{1}{\tau_i}\right)\exp(-t/\tau_i)\right. \qquad (17a)$$
$$\left. + \frac{2}{3}S_r(t) * \sum_i\sum_j \left\{\alpha_i\beta_j\left(\frac{1}{\tau_r} - \frac{1}{\tau_i} - \frac{1}{\phi_j}\right)\exp(-t/\tau_i - t/\phi_j)\right\}\right.$$

$$I_\perp(t) = \frac{1}{3}\left(\sum_i \alpha_i - \sum_i\sum_j \alpha_i\beta_j\right) S_r(t) + \frac{1}{3}S_r(t) * \sum_i \left\{\alpha_i\left(\frac{1}{\tau_r} - \frac{1}{\tau_i}\right)\exp(-t/\tau_i)\right. \qquad (17b)$$
$$\left. - \frac{1}{3}S_r(t) * \sum_i\sum_j \left\{\alpha_i\beta_j\left(\frac{1}{\tau_r} - \frac{1}{\tau_i} - \frac{1}{\phi_j}\right)\exp(-t/\tau_i - t/\phi_j)\right\}\right.$$

and the weighting of the residues:

$$w_{k\parallel} = 1/\left\{\mathrm{var}[I_\parallel(t_k)] + \left(\frac{1}{3}\sum_i \alpha_i + \frac{2}{3}\sum_i\sum_j \alpha_i\beta_j\right)^2 \mathrm{var}[S_r(t_k)]\right\} \qquad (18a)$$

$$w_{k\perp} = 1/\left\{\mathrm{var}[I_\perp(t_k)] + \left(\frac{1}{3}\sum_i \alpha_i - \frac{1}{3}\sum_i\sum_j \alpha_i\beta_j\right)^2 \mathrm{var}[S_r(t_k)]\right\}. \qquad (18b)$$

$S_r(t)$ can be measured with the polarizer set at 54.74° to the vertical or as $I_{r\parallel}(t) + 2I_{r\perp}(t)$.

In the derivation of the Eqns (17) and (18), it is assumed that when $s(t)$ and $r(t)$ are multiple exponential all the cross terms for the different lifetimes τ_i and correlation times ϕ_j must be accounted for. Physically this means that every lifetime component is coupled with every rotation. For instance, in the case of a mixture of two fluorescence compounds with each a single lifetime and correlation time, these lifetimes must only be associated with one of the correlation times. Hence, the model has to be adapted and some of the cross terms have to be omitted.

Computer programs

Two Fortran-77 computer programs were developed to analyse the polarized fluorescence decay data. In the first one $S(t)$ can be fitted with Eqn (2) or Eqn (10) yielding the fluorescence decay parameters α_i and τ_i. The fitting routine is according to the finite difference Levenberg-Marquardt algorithm, provided by the IMSL subroutine ZXSSQ [31]. The second program uses the α_i's and the τ_i's as input parameters and fits $I_\parallel(t)$ and $I_\perp(t)$ simultaneously to the Eqns (16) or (17) with the possibility to choose which cross term in the $s(t)r(t)$ product must be accounted for and which must be omitted. This program also uses subroutine ZXSSQ.

The quality of the fit is judged with visual inspection and with the help of various statistical functions and parameters, namely: the weighted residuals, the autocorrelation function of the weighted residuals, the number of sign changes in the autocorrelation function [32], the reduced χ^2 value and the Durbin-Watson parameter, DW [13]. The standard deviations of the fitted parameters can be estimated from the Hessian [20], which is one of the output parameters of subroutine ZXSSQ.

RESULTS AND DISCUSSION

Reference compounds

We have measured the fluorescence decays of *p*-terphenyl (λ_{em} = 345 nm) and POPOP (λ_{em} = 437 nm) upon 295-nm excitation. These two compounds are known to have a mono-

Table 1. *Fluorescence decay parameters for* p-*terphenyl and POPOP at 20°C*
f = frequency of detected photons

Sample	f	τ	χ^2	DW
	kHz	ns		
p-Terphenyl	5	1.061 ± 0.001	1.95	1.17
	15	1.063 ± 0.001	1.91	1.14
	30	1.068 ± 0.001	2.40	0.91
POPOP	5	1.360 ± 0.002	1.31	1.51
	15	1.355 ± 0.002	1.44	1.29
	30	1.360 ± 0.003	2.05	0.92

Table 2. *Fluorescence decay parameters of* $AcTrpNH_2$ *at 20°C*
f is the frequency of detected photons. The impulse response profile was measured either with a scatterer (S) or was obtained via fluorescence of *p*-terphenyl (Ph_3), as indicated under Method

f	Method	τ	τ_r	χ^2	DW
kHz		ns			
5	S	2.953 ± 0.004	–	1.18	1.69
15	S	2.937 ± 0.003	–	1.22	1.73
30	S	2.902 ± 0.002	–	1.35	1.34
5	Ph_3	3.011 ± 0.006	1.108 ± 0.005	1.01	2.02
15	Ph_3	2.985 ± 0.006	1.099 ± 0.004	1.05	2.03
30	Ph_3	2.977 ± 0.008	1.119 ± 0.005	1.29	1.50

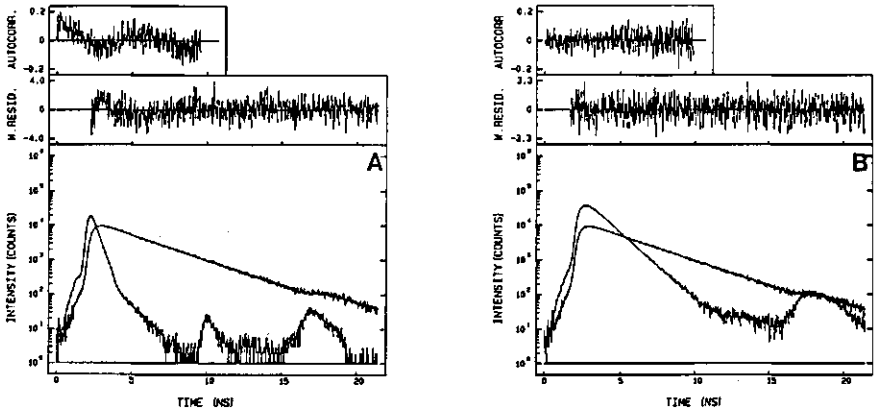

Fig. 1. *Fluorescence decay of* $AcTrpNH_2$ *at 20°C measured at 344 nm using 295-nm excitation.* (A) $AcTrpNH_2$ decay together with the impulse response profile which is obtained with a scatterer. (B) Decay curves of $AcTrpNH_2$ and of *p*-terphenyl, which are recorded under the same experimental conditions. The upper panels show the weighted residuals in each channel and the autocorrelation of these residuals. The decay parameters are listed in Table 2

exponential fluorescence decay [27]. Yet the fits with a single lifetime are very bad. Possibly these problems are due to pile-up effects. Usually we keep the frequency of the detected photons, f, at 15 kHz, which is 5% of the rate of the excitation photons. This time also $f = 5$ kHz and $f = 30$ kHz were tried. The results, presented in Table 1, show that the χ^2 and the Durbin-Watson parameter values (DW) for the 30-kHz fits are much worse than for the ones of the 5-kHz and 15 kHz decays. We may thus conclude that pile-up effects only occur at 30 kHz. The bad fitting of the results for 5 kHz and 15 kHz must have another origin, like a wavelength dependence of the detection system. When this dependence only results in a time shift, the quality of the fit should improve if we let this shift be an extra variable in the iteration [30]. No improvement was found, indicating that pulse-shape alterations with wavelength are dominant. In order to see whether these problems could be overcome with the use of the reference method, we have done some experiments with $AcTrpNH_2$ ($\lambda_{ex} = 295$ nm), measuring the impulse response profile directly with a scatterer or indirectly via the *p*-terphenyl fluorescence. These experiments were also done with the three start/stop pulse ratios. The results are listed in Table 2 and the 15-kHz decays are shown in Fig. 1. Excellent fits are obtained with the reference method at 5 kHz and 15 kHz. When the scatterer is used the quality of the fits is less, but not as bad as in the case of *p*-terphenyl and POPOP. The reason for this is that the $AcTrpNH_2$ lifetime is much longer and therefore the effect of the error in $P(t)$ using a scatterer is much less. We can conclude that, especially for short components in the fluorescence decay, the reference method yields more reliable results. Again 30 kHz was found to be too high and gave rise to pile-up effects. No difference is found between the results with at 5 kHz and 15 kHz. Consequently, it is better to use 15 kHz, because a better signal/noise ratio will be obtained in the same experimenting time.

During the analysis of the data with the reference method we let τ_r be an extra variable. Because the $AcTrpNH_2$ decay is also mono-exponential, this led to very good results for both the $AcTrpNH_2$ and the *p*-terphenyl lifetimes, which are in good agreement with values found by others [16, 25, 28].

The simultaneous analysis of the $AcTrpNH_2$ and *p*-terphenyl decays has also been performed on data obtained upon

300-nm excitation at two different emission wavelengths (337 and 350 nm) and three different temperatures (4, 20 and 30°C). The resulting lifetimes are presented in Table 3. The fluorescence lifetime of $AcTrpNH_2$ is found to be rather independent of the excitation or emission wavelength but there is a clear dependence on temperature. With increasing temperature the lifetime decreases. The *p*-terphenyl lifetime seems to be quite insensitive to temperature changes. This was also observed by Zuker et al. [16].

PROTEINS

Human serum albumin

Human serum albumin (HSA) is a protein ($M_r = 69000$) which contains a single tryptophan residue. The fluorescence decay of this protein has been analysed before ($\lambda_{ex} = 295$ nm) [18, 33]. Two lifetimes were found, one of 3.3 ns and one of 7.8 ns. Using 300-nm excitation, we found in addition to the 3.3-ns and 7.8-ns lifetimes a third, short component in the fluorescence decay. The values of the α_i's and the τ_i's are listed in Table 4. There is a relatively large difference in the values found for τ_i when using the scatterer or the reference method. As explained before the wavelength dependence of the detection system will have the most pronounced effect on short components in the decay and therefore it is believed that the numbers obtained with the reference method are the most reliable ones. The average lifetime $\langle\tau\rangle$, which is defined as:

$$\langle\tau\rangle = \frac{\sum_i \alpha_i \tau_i^2}{\sum_i \alpha_i \tau_i} \qquad (19)$$

is in both cases found to be 6.0 ns, which is in very good agreement with the results published before.

During the analysis of this three-exponential decay a fixed value for τ_r had to be used. If τ_r was not fixed, the iteration process was terminated because of entrapment of χ^2 in local minima of the χ^2 hyperspace, leading to poor fits and wrong

Table 3. *Temperature and wavelength dependence of the fluorescence parameters of $AcTrpNH_2$* and p-*terphenyl*
τ *is the lifetime of* $AcTrpNH_2$, τ_r *is that of p-terphenyl*

Temperature	λ_{em}	τ	τ_r
°C	nm	ns	
4	337	3.976 ± 0.010	1.060 ± 0.004
20		2.985 ± 0.006	1.064 ± 0.005
30		2.428 ± 0.004	1.057 ± 0.005
4	350	3.982 ± 0.010	1.071 ± 0.006
20		3.010 ± 0.007	1.069 ± 0.005
30		2.485 ± 0.004	1.073 ± 0.003

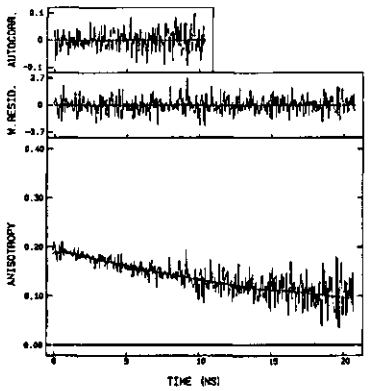

Fig. 2. *Anisotropy decay of HSA at 20°C measured at 344 nm upon 300-nm excitation.* The experimental anisotropy (Eqn 13) is shown. The quantities which are actually fitted are $I_{\parallel}(t)$ and $I_{\perp}(t)$ but the fit of the experimental anisotropy is easily obtained from these values. The weighting factors for the residues are $W_i = 3S(t_i)/[2 + 3R(t_i) - 3R(t_i)^2 - 2R(T_i)^3]$ [22]. The total fluorescence is fitted with a three-component decay (Table 4). The anisotropy parameters are: $\beta = 0.19 \pm 0.01$ and $\phi = 26 \pm 0.6$ ns. These results are obtained using *p*-terphenyl as a reference compound and fixing a value of $\tau_r = 1.1$ ns

Table 4. *Fluorescence decay parameters for HSA, LADH and lysozyme at 20°C*
The impulse response profiles was measured either with a scatterer (S) or obtained via *p*-terphenyl fluorescence (Ph_3) as indicated under Method

Protein	λ_{ex}	Method	α_1	τ_1	α_2	τ_2	α_3	τ_3	$\langle\tau\rangle$	χ^2	DW
	nm			ns		ns		ns			
HSA	300	S	0.19 ± 0.01	0.55 ± 0.05	0.46 ± 0.01	3.7 ± 0.08	0.35 ± 0.01	7.7 ± 0.07	6.0	1.09	1.85
	300	Ph_3	0.41 ± 0.01	0.11 ± 0.02	0.29 ± 0.01	3.7 ± 0.01	0.30 ± 0.01	7.3 ± 0.07	6.0	1.05	1.89
LADH	295	S	0.61 ± 0.01	3.31 ± 0.04	0.39 ± 0.01	6.51 ± 0.04	–	–	5.09	1.22	1.71
	295	Ph_3	0.57 ± 0.01	3.38 ± 0.05	0.43 ± 0.02	6.23 ± 0.05	–	–	5.04	1.08	1.97
	300	S	0.67 ± 0.01	3.44 ± 0.04	0.33 ± 0.01	6.39 ± 0.06	–	–	4.83	1.16	1.79
	300	Ph_3	0.61 ± 0.01	3.44 ± 0.04	0.39 ± 0.02	5.95 ± 0.05	–	–	4.74	1.09	1.90
Lysozyme	295	S	0.62 ± 0.01	0.72 ± 0.01	0.38 ± 0.01	2.53 ± 0.01	–	–	1.95	5.50	0.34
	295	S	0.46 ± 0.01	0.50 ± 0.01	0.50 ± 0.01	1.94 ± 0.02	0.04 ± 0.01	4.33 ± 0.06	2.00	1.19	1.94
	300	S	0.69 ± 0.01	0.98 ± 0.01	0.31 ± 0.01	2.89 ± 0.01	–	–	2.06	4.15	0.44
	300	Ph_3	0.75 ± 0.01	1.28 ± 0.01	0.25 ± 0.01	3.23 ± 0.02	–	–	2.17	3.03	0.61
	300	S	0.48 ± 0.01	0.55 ± 0.01	0.50 ± 0.01	2.08 ± 0.02	0.02 ± 0.01	5.94 ± 0.13	2.13	1.15	1.64
	300	Ph_3	0.42 ± 0.01	0.70 ± 0.02	0.56 ± 0.01	2.18 ± 0.02	0.02 ± 0.01	6.25 ± 0.16	2.22	1.03	1.83

τ_i values. Using 1.1 ns for τ_i as found with $AcTrpNH_2$ gave excellent results. The triple-exponential decay for the single tryptophan residue of HSA can be explained in terms of the modified conformer model as discussed in the introduction.

Analysis of the anisotropy decay of HSA at 20°C gave identical results for the scatterer and the reference methods, because no short components are present in this decay. Fig. 2 shows the experimental and the fitted anisotropy decays. A single-exponential with $\beta = 0.19 \pm 0.01$ and $\phi = 26.0 \pm 0.6$ ns is found. It is possible to estimate the value of ϕ for a rigid hydrated sphere according to an empirical relationship

$$\phi_{calc} = M(\bar{v} + h)\eta/RT \qquad (20)$$

in which M is the molar mass, $\bar{v}$ is the partial specific volume (0.735 cm^3/g), h the degree of hydration (0.2 cm^3/g), η the viscosity (cP), R the gas constant and T the absolute temperature. For HSA at 20°C Eqn (20) predicts a ϕ value of 26.5 ns, which is very close to the experimental value. This indicates that at 20°C the Trp residue rotates with the protein as a whole and has no internal mobility. Our results agree with those of Munro et al. [34] who have used 300-nm synchrotron radiation to measure the anisotropy decay of HSA at 8°C and at 41°C. At 8°C a mono-exponential decay was found with $\beta = 0.2$ and $\phi = 31.4$ ns. At 41°C a second, short correlation time appears and the overall protein rotation is much faster than predicted with Eqn (20). At this temperature the protein has probably gained internal flexibility and cannot be considered as a rigid sphere.

In a previous publication [18] a double-exponential anisotropy decay at 21°C was reported. These values were obtained by fitting the anisotropy without deconvolution. Upon reanalysis of these old data with our present method, we found that they also can be fitted with a single-exponential with the same correlation time as found with our new data. The after pulse, which is only taken into account when a deconvolution procedure is used, may have distorted the data.

Liver alcohol dehydrogenase

Liver alcohol dehydrogenase (LADH) is an ideal protein for time-resolved fluorescence because it is one of the best characterised proteins [35]. The active enzyme is a dimer made up of two identical ($M_r = 40000$) subunits. Each subunit contains two tryptophan residues. From X-ray data it is known that one of these residues (Trp-15) is located near the surface of the protein, while the other one (Trp-314) is buried inside the protein coil in a hydrophobic region, near the subunit interface. We have measured the tryptophan fluorescence lifetimes of LADH, using 295-nm or 300-nm excitation (Table 4). The differences between the results obtained with the scatterer and with the reference method are only small in this case, because the lifetimes are relatively long. From the χ^2 and DW values one may conclude that the fits with the reference method are slightly better than the ones with the scatterer method.

Similar experiments with LADH have been performed by other groups. Ross et al. [36] used 295-nm excitation and reported lifetimes which are comparable to ours. The small differences can be due to differences in the experimental conditions (i.e. buffer, temperature and emission wavelength). Based on KI quenching data, Ross et al. assign the short component to Trp-314 and the long one to Trp-15. Excitation at 300 nm is used by Barboy and Feitelson [37]. They report a single lifetime of 5 ns and interpret this by emission of Trp-314 only upon 300-nm excitation. Fitting of our data with a single exponential gave very bad results. A small decrease of the relative contribution of Trp-15 to the total fluorescence is found, but it does not totally disappear. This finding is supported by the steady-state quenching results of Ross et al. [36].

In the analysis of the anisotropy decay of LADH upon 295-nm and 300-nm excitation at 20°C no differences between the results obtained with the scatterer and the reference method were found. The decay can be described by a single-exponential and because the rotational correlation times are relatively long a small error in $P(t)$ does not affect the results significantly. Fig. 3 shows the anisotropy decays of the protein upon 295-nm and 300-nm excitation. Excitation at 300 nm yields a higher initial anisotropy as was expected, but there is another effect in addition. The rotational correlation time at $\lambda_{ex} = 300$ nm is longer than at $\lambda_{ex} = 295$ nm (36.0 ± 0.9 ns and 33.0 ± 1.0 ns respectively). This phenomenon can only be explained by means of the non-spherical shape of the protein. Indeed it has been reported that the LADH molecule can be considered as a prolate ellipsoid, with long and short semiaxes of 11 nm and 6 nm respectively [35]. Tao [38] has derived a general expression for the anisotropy decay of ellipsoids of revolution:

$$r(t) = \frac{2}{5} P_2(\cos\lambda)[\beta_1(\theta)\exp(-t/\phi_1) + \beta_2(\theta)\exp(-t/\phi_2) + \beta_3(\theta)\exp(-t/\phi_3)] \qquad (21)$$

where $P_2(\cos\lambda)$ is the Legendre polynomial of order 2, λ the angle between the absorption and emission dipoles and θ the angle that the emission transition dipole subtends with the main symmetry axis of the ellipsoid. Three correlation times are needed to describe the anisotropy of an ellipsoid of revolution and their values depend on the axial ratio. For LADH this ratio is about 1.8. This means that the three ϕ values are nearly identical; thus a mono-exponential decay with a rotational correlation time which is the weighted average of ϕ_1, ϕ_2 and ϕ_3 is observed. For molecules with one chromophore the amplitudes (β_i) are given by:

$$\beta_1(\theta) = (3/2\cos^2\theta - 1/2)^2$$
$$\beta_2(\theta) = 3\cos^2\theta\sin^2\theta \qquad (22)$$
$$\beta_3(\theta) = 3/4\sin^4\theta.$$

LADH has four tryptophans and there are two different electronic transitions (^1L_b is almost perpendicular to ^1L_a). As a result the expressions which describe the LADH anisotropy decay are very complex: however it can be argued that changing the excitation wavelength from 295 nm to 300 nm causes changes in the parameters which determine the β values and thus in the observed average of the three rotational correlation times.

Lysozyme

Lysozyme is, like LADH, a protein for which much structural information is available [39]. The analysis of the tryptophan fluorescence decay of this enzyme is difficult, because there are six different Trp residues (28, 62, 63, 108, 111 and 123). Imoto et al. [40] have measured the steady-state fluorescence of the native protein and of modified derivatives in which Trp-62 and/or Trp-108 are specifically oxidized. Their results indicate that more than 80% of the fluorescence comes from these two residues. Moreover in the native protein, energy transfer seems to occur from Trp-108 to Trp-

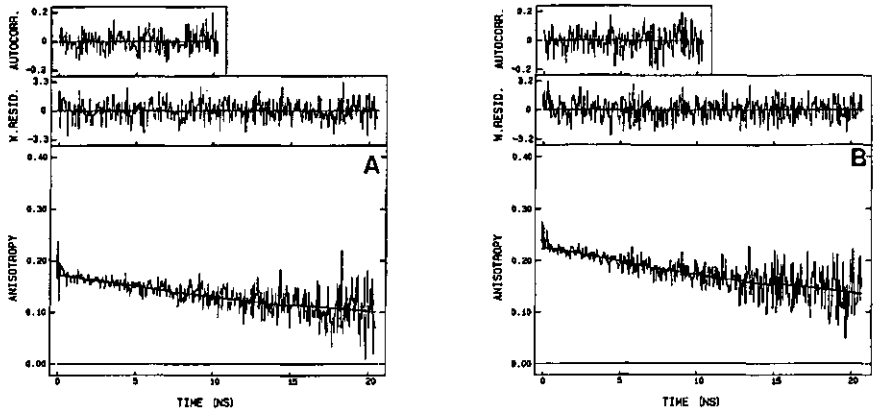

Fig. 3. *LADH anisotropy decay at 20°C.* Excitation wavelength is 295 nm (A) or 300 nm (B), emission wavelength is 344 nm. Fluorescence parameters are listed in Table 4. The anisotropies are fitted with a single exponential with $\beta = 0.17 \pm 0.01$ and $\phi = 33 \pm 1.0$ ns for $\lambda_{ex} = 295$ nm and $\beta = 0.22 \pm 0.01$ and $\phi = 36 \pm 0.9$ ns for $\lambda_{ex} = 300$ nm. *p*-Terphenyl was used as reference compound with $\tau_r = 1.1$ ns

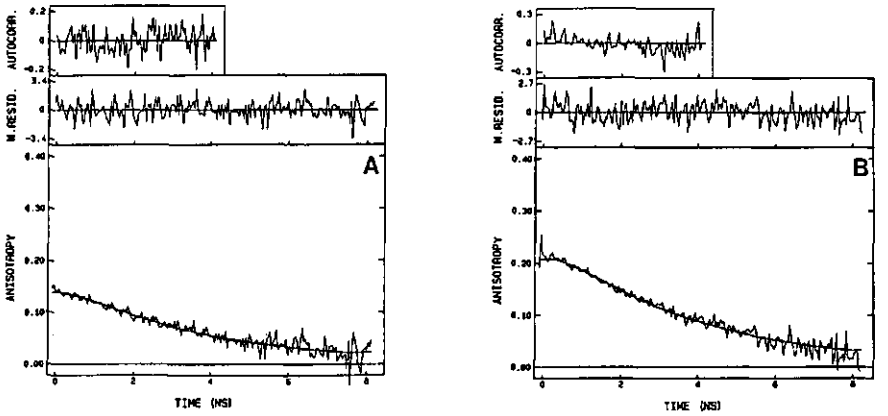

Fig. 4. *Anisotropy decays of lysozyme at 20°C, using 295-nm (A) and 300-nm (B) excitation.* Emission wavelength = 344 nm. The total fluorescence is fitted with three exponentials. Decay parameters are listed in Table 4. The anisotropy decays are described with a single exponential with $\beta = 0.14 \pm 0.01$, $\phi = 3.8 \pm 0.1$ ns and $\beta = 0.22 \pm 0.01$, $\phi = 3.8 \pm 0.1$ ns respectively

62. The lifetimes of the fluorescence have been measured by Formoso and Forster [41]. They find a double-exponential decay with lifetimes of about 0.5 ns and 2.26 ns at pH 8. Based on experiments with the modified derivatives, the 2.26-ns component was assigned to Trp-62 and the 0.5-ns component to Trp-108 and all other emitting Trp residues.

We have measured the native lysozyme decay upon 295-nm and 300-nm excitation. The lifetimes for the different fits are listed in Table 4 together with the χ^2 and DW values. The decay obtained with 295-nm excitation is analyzed using the impulse-response profile obtained with the scatterer. In this case the α_i and τ_i values obtained from a double-exponential fit are in very good agreement with the results of Formoso and Forster [41] but on the basis of the χ^2 and DW values and also of visual inspection of the plot of the weighted residuals these results have to be rejected. Fitting with three exponentials results in a considerable improvement. Analysis of the decay obtained with 300-nm excitation occurred both with the scatterer and the reference method. Again three exponentials are needed to obtain acceptable fits. The lifetimes are almost identical to the ones for $\lambda_{ex} = 295$ nm. The most important differences are found in the long component which becomes longer at $\lambda_{ex} = 300$ nm. It is not possible to assign the different lifetimes to specific residues on the basis of these experiments with the native enzyme only.

The anisotropy decays are shown in Fig. 4. Both decays are fitted with a single exponential, with a rotational correlation time of 3.8 ± 0.1 ns. With 300-nm excitation the initial

anisotropy is higher, as expected. A correlation time of 3.8 ns is low for a protein with a relative molecular mass, M_r = 13900. Chang et al. [42] have measured the fluorescence anisotropy decay of the eosin-lysozyme complex and they find a value of 5 ns for the overall rotational correlation time at 34°C. Assuming that ϕ is directly proportional to η/T (Eqn 20), this would correspond with 7.2 ns at 20°C. The same value is found from ^{13}C-NMR experiments [43]. A correlation time of 3.9 ns at 25°C was observed by Maliwal and Lakowicz [44] with their fluorescence depolarization technique. This value, which was also measured via tryptophan fluorescence, is very close to the one we find. Using an active-site inhibitor [*N*-acetyl-D-glucosamine or di(*N*-acetyl-D-glucosamine)], Maliwal and Lakowicz reported a significant increase in rotational correlation time. An explanation for these observations cannot easily be given. Internal motion of the tryptophan residues may influence the observed anisotropy decay. Molecular dynamics calculations [45] demonstrate the presence of picosecond internal movements of some tryptophan residues. However at present these oscillations cannot be observed with the single-photon counting technique. Nevertheless, they would result in a decrease of the initial anisotropy. Another possibility is that we observe the so-called hinge bending of lysozyme [46], that is the movement of two distinct domains of the protein relative to one another. This phenomenon could explain the increase in correlation time in the presence of active-site inhibitors [44], since it is known that binding of substrate reduces the hinge bending of lysozyme.

CONCLUDING REMARKS

Fluorescence lifetimes, obtained by the reference method, are in most cases very reliable. Only in the case that a lifetime component of the sample is too close to the reference lifetime will inconsistent results arise and in these cases other reference compounds or quenching of the reference fluorescence, as proposed by Löfroth [26], should be used.

The simultaneous analysis of the parallel and the perpendicular fluorescence components yields accurate rotational correlation times. Using this analysis technique, it is possible to distinguish between different correlation times of LADH upon 295-nm or 300-nm excitation. This observation indicates that the LADH molecule in solution does not behave as an isotropic rotor.

The relatively short correlation time found for lysozyme suggests that it is not the overall rotation of this protein that is observed but the hinge bending. This idea is supported by other experiments [44]. With our present equipment it is not possible to observe the picosecond internal motions of the tryptophan residues in proteins. However the fact, that the initial anisotropies at λ_{ex} = 300 nm never reach the value of 0.26, characteristic for totally immobilized tryptophans, suggests the presence of these motions. Implementation of a microchannel plate detector instead of a conventional photomultiplier tube improves the time resolution [47] and this is the first step to determine ultrafast motions experimentally in proteins.

We wish to thank Dr C. Laane, Dr J.-E. Löfroth and Prof. Dr C. Veeger for helpful discussions and Mrs J. C. Toppenberg-Fang and Miss Y. T. Soekhram for typing the manuscript. This work was supported in part by the Netherlands Foundation of Chemical Research (S.O.N.) with financial aid from the Netherlands Organization for the Advancement of Pure Research (Z.W.O.).

REFERENCES

1. Rigler, R. & Ehrenberg, M. (1973) *Q. Rev. Biophys. 2*, 139–199.
2. Cundall, R. B. & Dale, R. E. (eds) (1983) *Time-resolved fluorescence spectroscopy in biochemistry and biology*, Plenum Press, New York.
3. Beechem, J. M. & Brand, L. (1985) *Annu. Rev. Biochem. 54*, 43–71.
4. Grinvald, A. & Steinberg, I. Z. (1976) *Biochim. Biophys. Acta 427*, 663–678.
5. Szabo, A. G. & Rayner, D. M. (1980) *J. Am. Chem. Soc. 102*, 554–563.
6. Chang, M. C., Petrich, J. E., McDonald, D. B. & Fleming, G. R. (1983) *J. Am. Chem. Soc. 105*, 3819–3824.
7. Petrich, J. E., Chang, M. C., McDonald, D. B. & Fleming, G. R. (1983) *J. Am. Chem. Soc. 105*, 3824–3832.
8. Weber, G. (1960) *Biochem. J. 75*, 335–345.
9. Valeur, B. & Weber, G. (1977) *Photochem. Photobiol. 25*, 441–444.
10. Cross, A. J., Waldeck, D. H. & Fleming, G. R. (1983) *J. Chem. Phys. 78*, 6455–6467.
11. Szabo, A. (1984) *J. Chem. Phys. 81*, 150–167.
12. Lakowicz, J. R., Maliwal, B. P., Cherek, H. & Balter, A. (1983) *Biochemistry 22*, 1741–1752.
13. O'Connor, D. V. & Phillips, D. (1984) *Time-correlated single photon counting*, Academic Press, London.
14. Van Hoek, A. & Visser, A. J. W. G. (1985) *Anal. Instrum. 14*, 359–378.
15. Bebelaar, D. (1986) *Rev. Sci. Instrum. 57*, 1116–1125.
16. Zuker, M., Szabo, A. G., Bramall, L., Krajcarski, D. T. & Selinger, B. (1985) *Rev. Sci. Instrum. 56*, 14–22.
17. Morrisett, J. D., Pownall, H. J. & Gotta, A. M. (1975) *J. Biol. Chem. 250*, 2487–2494.
18. Van Hoek, A., Vervoort, J. & Visser, A. J. W. G. (1983) *J. Biochem. Biophys. Methods 7*, 243–254.
19. Visser, A. J. W. G., Ykema, T., Van Hoek, A., O'Kane, D. J. & Lee, J. (1985) *Biochemistry 24*, 1489–1496.
20. Bevington, P. R. (1969) *Data reduction and error analysis for the physical sciences*, McGraw-Hill, New York.
21. Wahl, Ph. (1977) *Chem. Phys. 22*, 245–256.
22. Wahl, Ph. (1979) *Biophys. Chem. 10*, 91–104.
23. Wahl, Ph., Auchet, J. C. & Donzel, B. (1974) *Rev. Sci. Instrum. 45*, 28–32.
24. Gauduchon, P. & Wahl, Ph. (1978) *Biophys. Chem. 8*, 87–104.
25. Wynaendts van Resandt, R. W., Vogel, R. H. & Provencher, S. W. (1982) *Rev. Sci. Instrum. 53*, 1392–1397.
26. Löfroth, J.-E. (1985) *Eur. Biophys. J. 13*, 45–58.
27. Berlman, I. B. (1971) *Handbook of fluorescence spectra of aromatic molecules*, 2nd ed, Academic Press, New York.
28. Chang, M. C., Courtney, S. H., Cross, A. J., Gulotty, R. J., Petrich, J. W. & Fleming, G. R. (1985) *Anal. Instrum. 14*, 433–464.
29. Gilbert, C. W. (1983) in *Time-resolved fluorescence spectroscopy in biochemistry and biology* (Cundall, R. B. & Dale, R. E., eds) pp. 605–606, Plenum Press, New York.
30. Cross, A. J. & Fleming, G. R. (1984) *Biophys. J. 46*, 45–56.
31. *International Mathematical and Statistical Library* (1985) IMSL Inc. Houston.
32. Ameloot, M. & Hendrickx, H. (1982) *J. Chem. Phys. 76*, 4419–4432.
33. Wahl, Ph. & Auchet, J. C. (1971) *Biochim. Biophys. Acta 285*, 99–117.
34. Munro, I., Pecht, I. Stryer, L. (1979) *Proc. Natl Acad. Sci. USA 76*, 56–60.
35. Brändén, C.-I., Jörnvall, H., Eklund, H. & Furugren, B. (1975) in *The enzymes* (Boyer, P. D., ed.) 3rd edn, vol. 11, pp. 103–190, Academic Press, New York.
36. Ross, J. B. A., Schmidt, C. J. & Brand, L. (1981) *Biochemistry 20*, 4369–4377.
37. Barboy, N. & Feitelson, J. (1978) *Biochemistry 17*, 4923–4926.
38. Tao, T. (1969) *Biopolymers 8*, 609–632.

39. Imoto, T., Johnson, L. N., North, A. C. T., Phillips, D. C. & Rupley, J. A. (1972) in *The enzymes* (Boyer, P., ed.) 3rd edn, vol. 7, pp. 665–868, Academic Press, New York.
40. Imoto, T., Forster, L. S., Rupley, J. A. & Tanaka, F. (1971) *Proc. Natl Acad. Sci. USA 69*, 1151–1155.
41. Formoso, C. & Forster, L. S. (1975) *J. Biol. Chem. 250*, 3738–3745.
42. Chang, M. C., Cross, A. J. & Fleming, G. R. (1983) *J. Biomol. Struct. Dyn. 1*, 299–318.
43. Dill, K. & Allerhand, A. (1979) *J. Am. Chem. Soc. 101*, 4376–4378.
44. Maliwal, B. P. & Lakowicz, J. R. (1984) *Biophys. Chem. 19*, 337–344.
45. Ichiye, T. & Karplus, M. (1983) *Biochemistry 22*, 2884–2893.
46. Karplus, M. & McCammon, J. A. (1983) *Annu. Rev. Biochem. 53*, 263–300.
47. Rigler, R., Claesens, F. & Kristensen, O. (1985) *Anal. Instrum. 14*, 525–546.

4 TIME-RESOLVED FLUORESCENCE AND CIRCULAR DICHROISM OF PORPHYRIN CYTOCHROME C AND ZN-PORPHYRIN CYTOCHROME C INCORPORATED IN REVERSED MICELLES

Kees Vos, Colja Laane, Stefan R. Weijers, Arie van Hoek, Cees Veeger and Antonie J.W.G. Visser

Reprinted from: European Journal of Biochemistry (1987) 169, 259-268.

Interactions between fluorescent horse heart cytochrome *c* derivatives (e.g. porphyrin cytochrome *c* and Zn-porphyrin cytochrome *c*) with surfactant interfaces in reversed micellar solutions have been studied, using different spectroscopic techniques. Anionic [sodium bis(2-ethylhexyl)sulfosuccinate, AOT] and cationic (cetyltrimethylammonium bromide, CTAB) surfactant solutions have been used in order to investigate the effects of charge interactions between proteins and interfaces.

Circular dichroism reveals that much of the protein secondary structure is lost in AOT-reversed micelles, especially when the molar water/surfactant ratio, w_o, is high ($w_o = 40$), whereas in CTAB-reversed micelles secondary structure seems to be preserved.

Time-resolved fluorescence measurements of the porphyrin in the cytochrome *c* molecule yields information about the changes in structure and the dynamics of the protein upon interaction with surfactant assemblies both in aqueous and in hydrocarbon solutions. With AOT as surfactant a strong interaction between protein and interface can be observed. The effects found in aqueous AOT solution are of the same kind as in hydrocarbon solution. In the CTAB systems the interactions between protein and surfactant are much less pronounced. The measured effects on the fluorescence properties of the proteins are different in aqueous and hydrocarbon solutions.

In general, the observations can be explained by an electrostatic attraction between the overall positively charged protein molecules and the anionic AOT interface. Electrostatic attraction can also occur between the cytochrome *c* derivatives and CTAB because there is a negatively charged zone on the surface of the proteins. From the fluorescence anisotropy decays it can be concluded that in the CTAB-reversed micellar system these interactions are not important, whereas in an aqueous CTAB solution the proteins interact with surfactant molecules.

Surfactant assemblies in organic media, called reversed micelles or, more general, water-in-oil microemulsions, have been investigated extensively over the past years. Many studies have been carried out towards the elucidation of structure and dynamics of reversed micelles [1–4] but also on the (bio)chemical and (bio)technological applications of these systems [2, 3, 5–9].

In our laboratory an important line of research consists of the incorporation of proteins in reversed micelles in order to perform bioconversions of apolar compounds or to isolate proteins [10–12]. At present, the effects of protein solubilization on both protein and micelle structure and dynamics are not very clear. Because reversed micellar solutions are optically transparent, spectroscopic and ultracentrifugation techniques can be applied to study these effects. Several systems have been the subject of this kind of investigation, some containing cytoplasmatic, others containing membrane proteins [5, 7–9].

Horse heart cytochrome *c* is a protein which *in vivo* is strongly associated via electrostatic interactions with the inner mitochondrial membrane. The sequence and X-ray structure of this 12.4-kDa heme protein are known [13]. The protein contains nineteen lysine residues, most of which are distributed on the two flanks of the protein molecule, giving it an overall positive charge at neutral pH, but there is also a region where nine of the twelve acidic residues are clustered, thus having a negative charge. The phenomenon of oppositely charged zones on the protein surface is found for cytochrome *c* from most sources and is assumed to be related to the peripheric interactions with the mitochondrial membrane.

Previous studies of cytochrome *c* incorporated in reversed micelles formed by the surfactant sodium bis(2-ethylhexyl)sulfosuccinate (AOT) dealt with the redox activity measured via chemical reductants [14] or hydrated electrons [15]. From these studies it was concluded that the activity is retained when the protein is incorporated. This does not necessarily imply a preserved secondary structure of the protein, because a direct reduction of the heme iron is also possible. Pileni and coworkers [16] conclude from a small-angle X-ray scattering study that cytochrome *c* is strongly associated with the AOT interface. They also find that the protein is still redox active. The steady-state fluorescence properties of the single tryptophan residue of cytochrome *c*, incorporated in AOT-reversed micelles were studied by Erjomin and Metelitza [17]. An increase of the fluorescence intensity together with a blue shift of the emission maximum was observed. These results

Correspondence to A. J. W. G. Visser, Laboratorium voor Biochemie der Landbouwuniversiteit, De Dreijen 11, NL-6703 BC Wageningen, The Netherlands

Abbreviations. AOT, Aerosol-OT [sodium bis(2-ethylhexyl)-sulfosuccinate]; CTAB, cetyltrimethylammonium bromide.

were interpreted in terms of an increased viscosity and a decreased polarity in the environment of the tryptophan residue, and therefore a change in protein conformation, because the tryptophan is buried in the protein coil near the heme group.

In the present study we have utilized derivatives of cytochrome *c* from which the heme iron was removed or replaced by a zinc ion, both giving rise to red fluorescence with a rather high quantum yield. The fluorescence and phosphorescence properties of porphyrin cytochrome *c* and Zn-porphyrin cytochrome *c* have been extensively described in a number of publications by Vanderkooi and coworkers [18–21]. The time-resolved and steady-state fluorescence properties of the porphyrin, which is covalently linked to the protein backbone, are very sensitive reporters of changes in the protein structure and environment. We have measured the fluorescence properties of both cytochrome *c* derivatives in aqueous solution and in reversed micellar systems. In addition the circular dichroic spectra in the far-ultraviolet were recorded in order to evaluate the secondary structural characteristics of these protein preparations. Two different surfactants were used for the reversed micellar solutions, an anionic (AOT) and a cationic (CTAB) one. In this way we have tried to elucidate the important role of charge interactions between protein and surfactant.

MATERIALS AND METHODS

Chemicals

AOT [sodium bis(2-ethylhexyl)sulfosuccinate] was obtained from Janssen Chimica and purified according to the method described by Menger and Yamada [22]. CTAB (cetyltrimethylammonium bromide) was from Serva and was used without further purification. Ruthenium tris(bipyridyl) and potassium ferricyanide, which were used for the size measurements of the reversed micelles, were from Strem Chemicals Inc. (Newburyport, MA, USA) and Merck respectively. Rose bengal, which was used as the reference component for the time-resolved fluorescence measurements, was from Eastman Kodak (certified grade) and was purified by thin-layer chromatography as described by Cramer and Spears [23]. Tetraphenyl porphyrin free base was a gift of Ing. R. B. M. Koehorst (Agricultural University, Wageningen). Isooctane (Uvasol, for fluorometry), hexanol (P.A.) and 2-methyl tetrahydrofuran (P.A.) were obtained from Merck. 2-Methyl tetrahydrofuran was distilled prior to use.

Preparation of porphyrin cytochrome c *and Zn-porphyrin cytochrome* c

Porphyrin cytochrome *c* was prepared according to a method which is a slight modification of the methods described by Flatmark and Robinson [24] and by Fisher et al. [25]. Anhydrous hydrogen fluoride (HF, 2–3 ml), obtained from Matheson (Oevel, Belgium), was distilled in a Teflon beaker, which was placed in a Dewar flask filled with liquid nitrogen. 100 mg of lyophilized horse heart cytochrome *c* (Sigma, type III) was added to the liquid HF and the solution was stirred with a Teflon rod. After 2–3 min, the reaction vessel was taken out of the liquid nitrogen and the HF was removed by applying a vigorous stream of nitrogen. When all the HF was removed a fluorescent, purple-colored, paste was left. This was dissolved in a small volume (3–4 ml) 0.1 M ammonium acetate pH 5.0.

The solution was dialysed against the same buffer for 24 h. To check that no alterations other than quantitative iron removal had occurred during this procedure, absorption, emission and circular dichroic spectra were measured of this preparation.

Zinc was incorporated by adding a tenfold molar excess of zinc acetate to a porphyrin cytochrome *c* solution in 0.1 M ammonium acetate pH 5.0. This solution was stirred for about an hour at room temperature in the dark (Zn porphyrin cytochrome *c* is reported to be light-sensitive [19]). The reaction was followed by the change of the visible absorption spectrum. After the reaction was completed the excess zinc acetate was removed by dialysis at 4°C in the dark.

Preparation of reversed micellar solutions

50 µl of a concentrated protein solution (0.3 mM) in 20 mM potassium phosphate pH 7.0 was injected into 2.5 ml of a 0.24 M solution of AOT in isooctane or CTAB in a 12% (v/v) hexanol/isooctane mixture and the solution was extensively Vortex-stirred until it became clear. Buffer was added until the desired w_0 (= $[H_2O]/[surfactant]$) value was obtained and after that the total volume of sample was adjusted to 3.0 ml with isooctane. In this way the samples had a final surfactant concentration of 0.2 M. The CTAB solutions contained 10% hexanol with respect to the total volume.

Fast protein liquid chromatography

Chromatographic comparison of porphyrin cytochrome *c* and Zn-porphyrin cytochrome *c* with the native protein was performed on a Pharmacia fast protein liquid chromatography (FPLC) system. This system consisted of a GP 250 gradient programmer, a V-7 injection valve and two P500 dual piston pumps. Detection occurred with a UV-1 monitor equipped with an HR flow cell. Detection wavelength was 280 nm.

Samples and buffers were filtered through 0.22-µm Millipore filters. Buffers were degassed under vacuum afterwards.

Gel permeation chromatography was performed on a Superose 12, HR 10/30 column; 50-µl samples of the protein in a 20 mM potassium phosphate, 150 mM potassium chloride pH 7.0 buffer were injected and eluted with the same buffer at a flow rate of 0.5 ml/min.

The cation-exchange experiments were done on a Mono S 5/5 column. Elution occurred with a 20 mM potassium phosphate buffer pH 7.0 with a gradient of 0–1 M potassium chloride. The flow rate was 1 ml/min. After each experiment the column was reequilibrated with 5 vol. starting buffer.

Absorption, steady-state fluorescence and circular dichroism measurements

Absorption spectra were recorded on a Cary-16 spectrophotometer. Fluorescence emission spectra were measured with an Aminco SPF-500 spectrofluorimeter. Slit widths were 4 nm for both the excitation and the emission monochromators. Circular dichroism was measured with a Jobin Yvon mark V Auto-dichrograph equipped with a Silex microcomputer for data aquisition. Concentrations for the CD measurements were 25 µM for the aqueous protein samples and 5 µM for the reversed micellar solutions. Cuvets with a path length of 0.5 mm were used throughout.

Time-resolved fluorescence measurements

Time-resolved fluorescence of ruthenium tris(bipyridyl) was measured with the mode-locked continuous-wave argon-ion laser and single-photon-counting set-up as described previously [26]. Excitation was performed with the 457.9-nm laser line. Pulses had nanojoule energies and widths of about 100 ps FWHM (full width at half maximum). The pulse repetition rate of 76 MHz was decreased to 300 kHz using an extra cavity electro-optic modulator set-up [27]. The cuvet holder was thermostatted and during the experiments temperature was kept at 25°C.

The fluorescence emission was detected perpendicular with respect to the direction of the exciting beam via tandemized 0.25-m (Jarrell Ash, 82-410) monochromators. Detection wavelength was 613 nm, bandwidth 3 nm. A sheet of Polaroid HN38 linear polarizer was placed at magic angle (54.74°C to the vertical) in front of the first monochromator slit. In order to prevent pile-up effects the excitation energy was reduced with neutral density filters so as to obtain a frequency of detected photons of 15 kHz [28], which is 5% of the excitation frequency. Data were collected in 512 channels of the multichannel analyzer and transferred afterwards to a MicroVax II computer for analysis.

For excitation of the protein samples a continuous wave dye-laser was used, synchronously pumped by the argon-ion laser, providing pulses of about 5 ps FWHM. The dye used was rhodamine 6G, giving tunable output from 580 nm to 630 nm. Excitation wavelengths used were 610 nm for the porphyrin cytochrome *c* and 590 nm for the Zn-porphyrin cytochrome *c* experiments. Emission was selected using a combination of an interference and a cut-off filter (Balzers B40, 625 nm plus Schott RG 630 for porphyrin cytochrome *c* and Balzers B40, 647 nm plus Schott RG 645 in the case of Zn-porphyrin cytochrome *c*). A sheet of linear polarizer (Polaroid HN22), mounted on a ball bearing holder, driven by two computer-controlled rotation magnets, was used to select emission, polarized parallel or perpendicular to the polarization direction of the exciting beam. Long-term fluctuations in the excitation power were averaged out by rotating the polarizer every 10 s.

Data of parallel and perpendicular polarized emission were collected in two subgroups (1024 channels each) of the multichannel analyzer. Analysis was performed with the reference convolution method described in a previous publication [28]. This means that the impulse response profile of the instrument was measured via the single-exponential fluorescence decay of a reference compound under exactly the same conditions as the other experiments. The reference compound used in this study was rose bengal, dissolved in water. To obtain a good value for the reference lifetime, τ_r, we have also measured the fluorescence decay of tetraphenyl porphyrin free base, dissolved in 2-methyl tetrahydrofuran. Simultaneous analysis of the two single-exponential decays [28] yielded lifetimes of 70 ± 2 ps for rose bengal and 11.00 ± 0.01 ns for tetraphenyl porphyrin at both excitation wavelengths used. In the rest of the experiments the τ_r value of 70 ps was fixed. All experiments were in duplicate.

RESULTS AND DISCUSSION

Characterization of the cytochrome c derivatives

The purity of the protein preparations was checked by gel permeation and ion-exchange chromatography using an FPLC apparatus. Samples of native Fe(III) cytochrome *c*, porphyrin cytochrome *c* and Zn-porphyrin cytochrome *c* were compared with these methods. On the Superose-12 molecular sieve column the three protein samples had exactly the same elution volume, indicating that the molecular mass of the protein does not change upon iron removal and zinc incorporation. At the detection wavelength of 280 nm some minor impurities in the protein solutions could be observed but the contribution of these never exceeded 1% and were no more important in the modified cytochrome preparations than in the native sample.

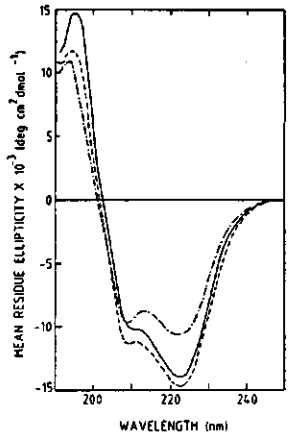

Fig. 1. *Circular dichroism of ferri (——), porphyrin (– – –) and Zn-porphyrin (–·–·–) cytochrome c at 25°C.* Protein concentration was 25 μM, cuvet path length 0.5 mm

When using the Mono S cation-exchange column a difference was observed between native Fe(III) cytochrome *c* and porphyrin cytochrome *c* on the one hand and Zn-porphyrin cytochrome *c* on the other. In a 0–1 M KCl gradient the first two proteins elute at 0.5 M KCl whereas the Zn derivative elutes at 0.4 M KCl. This means that charge interactions between Zn-porphyrin cytochrome *c* and column material are weaker than in the case of the other two proteins.

Porphyrin cytochrome *c* has the four-banded visible absorption spectrum characteristic for free base porphyrins. The two bands with maxima at 505 nm and 540 nm are due to the Q_y transition, the other ones (with maxima at 567 nm and 621 nm) to the Q_x transition [18]. The Soret peak has its maximum at 404 nm. Upon incorporation of Zn in the porphyrin, Q_y and Q_x become degenerate and the four bands collapse into two, with maxima at 550 nm and 586 nm. The Soret band shifts to 422 nm and sharpens.

The fluorescence emission spectra of the cytochrome *c* derivatives have been presented before [18, 19]. Upon 500-nm excitation porphyrin cytochrome *c* has emission maxima at 621 nm and 684 nm. Zn-porphyrin cytochrome *c*, excited at 550 nm, has emission maxima at 589 nm and 642 nm.

A good (qualitative) measure of the protein secondary structure is the circular dichroism (CD) in the far-ultraviolet region (190–250 nm). CD spectra of native Fe(III) cytochrome *c*, porphyrin cytochrome *c* and Zn-porphyrin cytochrome *c* are given in Fig. 1. The spectra of native Fe(III)

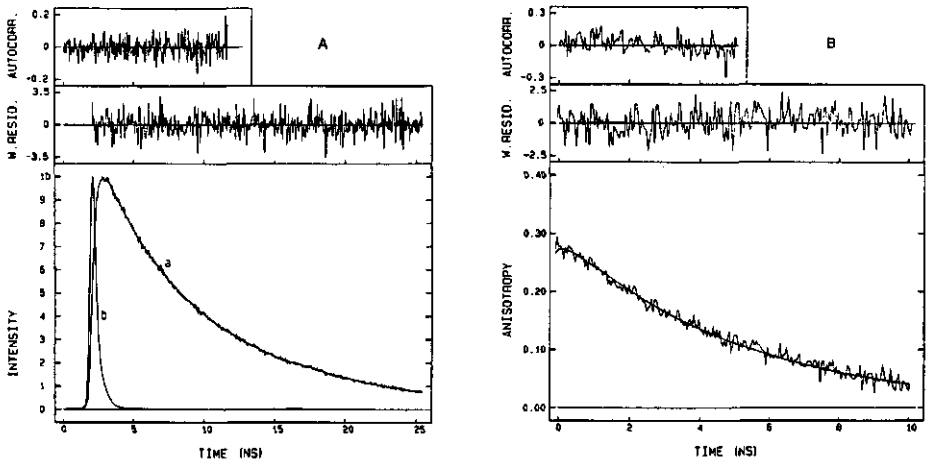

Fig. 2. *Fluorescence (A) and anisotropy (B) decay of porphyrin cytrochrome* c *in aqueous solution at 25°C.* (A) Excitation and emission wavelengths were 610 nm and 625 nm respectively. Time equivalence per channel was 0.046296 ns. The first 25 ns of the fluorescence is shown (a), together with the response of rose bengal (b), which was used as the reference compound. The decay was fitted with a triple-exponential function having the decay parameters $\alpha_1 = 0.16 \pm 0.01$, $\tau_1 = 0.54 \pm 0.01$ ns, $\alpha_2 = 0.22 \pm 0.01$, $\tau_2 = 4.1 \pm 0.1$ ns, $\alpha_3 = 0.62 \pm 0.02$, $\tau_3 = 9.4 \pm 0.1$ ns. The quality of the fit is indicated by the weighted residuals and the autocorrelation function, shown in the upper panels. Intensity is in arbitrary units. (B) The first 10 ns of the experimental anisotropy is shown together with the single-exponential fit. Anisotropy parameters are $\beta = 0.290 \pm 0.001$, $\phi = 5.00 \pm 0.05$ ns

cytochrome *c* and porphyrin cytochrome *c* are almost identical in shape and intensity except for the 190–200-nm region but in this region the experimental error is enhanced because of the increasing light absorption of protein and buffer and the decreasing output of the xenon arc. The CD spectrum of Zn-cytochrome *c* is significantly different. The peak at 222 nm has lost about 25% of the intensity in comparison with the other two spectra, while the peak at 208 nm is unchanged. Therefore, incorporation of the Zn ion in the porphyrin causes some changes in the secondary structure of the protein. This can be due to the fact that the Zn ion lies somewhat out of the plane of the porphyrin ring, which is usually the case with Zn-porphyrins [29], whereas it is known from Fe(III) cytochrome *c* that Fe lies almost exactly in the plane of the porphyrin [30]. Another difference is that Zn in porphyrins usually has five coordination bonds where Fe in Fe(III) cytochrome *c* has six (although the sixth coordination with methionine-80 is a weak one). The CD observation of a changing protein structure upon Zn incorporation is in good agreement with the FPLC results.

Time-resolved fluoresence of the proteins in aqueous solution

The fluorescence and anisotropy decays of porphyrin cytochrome *c* are shown in Fig. 2. Excitation was at 610 nm because of the high initial anisotropy at this wavelength [18, 31, 32]. The fluorescence decay must be described by a sum of at least three exponentials. Because the only emitting group in the protein is a free base porphyrin, which in a noninteracting environment is reported to have a single-exponential decay [33], the multi-exponential fluorescence decay must be explained by microheterogeneity in the porphyrin environment. A good parameter to characterize multiple exponential decays is the average lifetime $<\tau>$ [34], defined as:

$$<\tau> = \frac{\sum_i \alpha_i \tau_i^2}{\sum_i \alpha_i \tau_i} \qquad (1)$$

where α_i are the relative contributions of the exponential components to the decay and τ_i the fluorescence lifetimes. For porphyrin cytochrome *c* we find a $<\tau>$ value of 8.6 ns, which is substantially higher than the single lifetime of 6.5 ns reported by Vanderkooi et al. [19]. This difference is probably due to the fact that Vanderkooi et al. used a phase-modulation instrument, yielding modulation-frequency-dependent average fluorescence lifetimes [34].

The anisotropy decay is described by a single exponential. The high intial anisotropy, β, of 0.290 ± 0.001 allows an accurate determination of the rotational correlation time, ϕ. For porphyrin cytochrome *c*, ϕ is 5.00 ± 0.05 ns. From the rotational correlation time the hydrated radius, r_h, of the protein can be calculated according to the relationship:

$$\phi = \frac{4\pi r_h^3 \eta}{3kT} \qquad (2)$$

where η is the solvent viscosity (kg/m·s), k the Bolzman constant and T the absolute temperature. For $\phi = 5.00$ ns at 25°C the calculated $r_h = 1.77$ nm, which is in excellent agreement with X-ray data [13, 35].

For Zn-porphyrin cytochrome *c* the fluorescence and anisotropy decays upon 590-nm excitation are shown in Fig. 3. As can be seen the initial anisotropy is low. The use of a higher excitation wavelength to obtain higher anisotropies did not work because the excitation efficiency of the Zn-

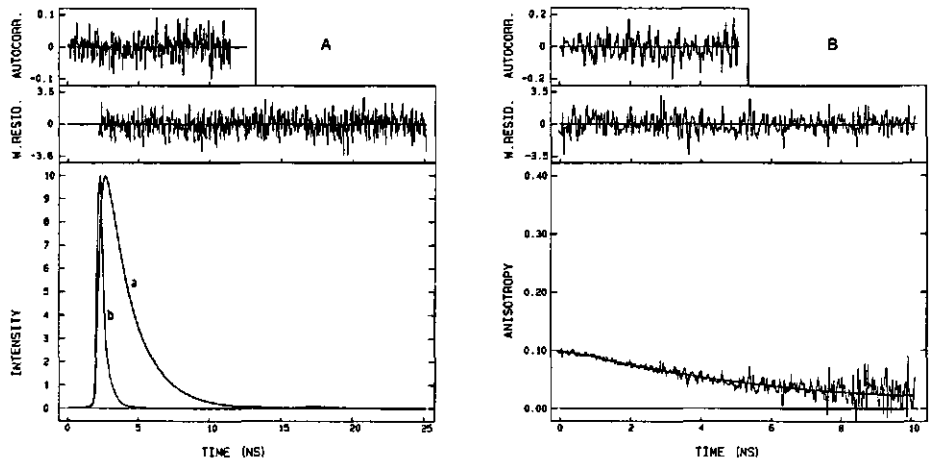

Fig. 3. *Fluorescence (A) and anisotropy (B) decay of Zn-porphyrin cytochrome c at 25°C.* (A) Excitation was at 590 nm; emission wavelength was 645 nm, time equivalence per channel 0.027932 ns. The fit is a double exponential having parameters $\alpha_1 = 0.18 \pm 0.01$, $\tau_1 = 0.49 \pm 0.02$ ns, $\alpha_2 = 0.82 \pm 0.02$, $\tau_2 = 1.92 \pm 0.03$ ns. (B) The anisotropy decay was fitted with a single-exponential function having $\beta = 0.100 \pm 0.002$, $\phi = 5.1 \pm 0.4$ ns. Other details as in Fig. 2

porphyrin becomes so low (low absorption coefficient) that impurities in the preparation (probably traces of free base porphyrin cytochrome *c*) disturb the measurements.

At least two exponentials are needed to describe the fluorescence decay, indicating that in the Zn-derivative also there is some microheterogeneity of the protein in the neighbourhood of the porphyrin. The average lifetime $<\tau> = 1.85$ ns. This is much shorter than the 3.2 ns reported by Vanderkooi et al. [19]. On the other hand Thomas et al. [36] have reported a lifetime of 2.0 ns of the Zn-substituted derivative of *Hansenula anomala* cytochrome *c* at 10°C, which is close to our value.

The analysis of the anisotropy decay is hampered by the combination of the short fluorescence lifetime and the low initial anisotropy of 0.100 ± 0.002 (Fig. 3). A rotational correlation time of 5.1 ± 0.4 ns is found. This value is in good agreement with the one found for porphyrin cytochrome *c* (note that the error in ϕ is much higher in the case of Zn-cytochrome *c*). From the measured rotational correlation time we can deduce that only monomers are present in our Zn-porphyrin cytochrome *c* preparation and no dimers as reported by Thomas et al. for the *H. anomala* Zn-porphyrin cytochrome *c* [37]. The same conclusion was derived from the FPLC results.

Size measurements of reversed micelles

To be able to interpret the anisotropy decay results of protein-filled reversed micelles, which will be discussed below, we need to obtain estimates of sizes and rotational correlation times of the empty micelles. For the AOT system literature values are available [38–40] but no reports have appeared yet about the CTAB system, to our knowledge. Therefore we have performed size measurements using the time-resolved fluorescence quenching technique described by Atik and Thomas [39]. As fluorophor we used ruthenium tris(bipyridyl) and as quencher potassium ferricyanide $[K_3Fe(CN)_6]$.

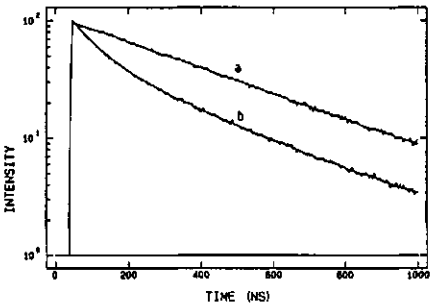

Fig. 4. *Fluorescence decays of ruthenium tris(bipyridyl) in CTAB-reversed micelles, $w_o = 20$, at 25°C.* Excitation wavelength 457.9 nm, emission wavelength 613 nm and time equivalence per channel 4.711 ns. The first 1000 ns of the decays is shown. The upper curve is the unquenched decay, fitted with a single-exponential function having $\tau = 374$ ns. Because of the long lifetime no deconvolution is needed. The lower curve shows the fluorescence decay in the presence of 1.0 mM potassium ferricyanide. This decay is fitted according to Eqn (3). Parameters are $\tau = 374$ ns, $k_q = 5.95 \times 10^6$ and [WP] = 0.92 mM

Assuming that exchange of probe and quencher molecules between the micelles is negligible during the fluorescence lifetime of the probe and that the quencher molecules have a Poisson distribution among the micelles, the quenching of the fluorescence can be described by (cf. [39]):

$$I(t) = I(0)\exp\{-t/\tau - n[1 - \exp(-k_q t)]\} \qquad (3)$$

with τ, the unquenched fluorescent lifetime of the probe in the reversed micelles, k_q, the intrawater pool quenching rate constant and n = [quencher]/[WP], the average number of quencher molecules per water pool. A typical example of an experiment is shown in Fig. 4.

From the water pool concentration the core radius of the micelles, r_c, can be calculated. If we want to obtain the rotational correlation times according to Eqn (2) we need to known the hydrodynamic radius, r_h, and the solvent viscosity. r_h is simply obtained by adding the average surfactant length to r_c. As lengths we have taken 1.2 nm for AOT [38] and 2.4 nm for CTAB [41]. The solvent viscosity is that of isooctane at 25°C in the case of AOT ($\eta = 4.74 \times 10^{-4}$ kg/m·s). In the CTAB system the continuous phase consists of a mixture of 1-hexanol and isooctane in a ratio of about 1:20 (v/v) according to Hilhorst et al. [11]. The measured viscosity of this mixture amounts to 5.00×10^{-4} kg/m·s. The results of the measurements and calculations are listed in Table 1. It must be noted that the r_h values and the rotational correlation times especially are only estimates because the surfactant lengths and, in case of the CTAB system, the composition of the continuous phase are not known exactly. Besides that, the micelles may interact mutually, which will also affect the rotational correlation times.

Circular dichroism of reversed micellar solutions

The effect of incorporation in two different reversed micellar systems, one containing an anionic (AOT) the other one a cationic (CTAB) surfactant on the two cytochrome *c* derivatives was measured by circular dichroism. For comparison also denaturating solutions of 5 M guanidine·HCl were measured. The results are summarized in Table 2. It should be noted that it is very difficult to measure circular dichroism of these samples because the protein concentrations are low (5 μM) and, in addition, there is much background signal from the solution due to the presence of the surfactants or the guanidine·HCl. Therefore we estimate the error in the reported values for the reversed micellar solutions to be about 20%. In the case of cyctochrome *c* the CD intensity at 222 nm, θ_{222}, is a measure of the amount of helix because this protein has no sheet structures [13, 30, 35]. Despite the high error in the CD data it is clear that the protein structure is more affected in AOT- than in CTAB-reversed micelles, whereas secondary structure is totally lost in the guanidine·HCl solution. An unexpected observation is that in the AOT micelles θ_{222} decreases with increasing w_o. This is the case for porphyrin and Zn-porphyrin cytochrome *c*. One would expect that in large micelles the protein structure resembles that in bulk water more than in small micelles, which is not the case.

Time-resolved fluorescence of the proteins in micellar solutions

The time-resolved fluorescence properties of the two proteins in aqueous solution have been discussed. Here we will concentrate on results obtained with micellar solutions. In this case the fluorescence decays of both proteins can be described with a sum of three exponentials. The average fluorescence lifetimes in the micellar systems as a function of w_o are displayed in Figs 5 and 6 for porphyrin and Zn-porphyrin cytochrome *c* respectively.

For porphyrin cytochrome *c* in AOT micelles a decrease of the average lifetime, $<\tau>$, is observed in comparison to the value in bulk water. This difference increases at higher w_o. This is the same unexpected phenomenon as has been noticed with the CD results. Above a w_o value of 30, the average lifetime becomes constant.

Table 1. *Sizes and correlation times of AOT- and CTAB-reversed micelles as a function of the water content at 25°C*

w_o	AOT-reversed			CTAB-reversed		
	r_c	r_h	ϕ	r_c	r_h	ϕ
	nm		ns	nm		ns
5	1.2	2.4	7	–	–	–
10	1.7	2.9	12	1.9	4.3	41
20	3.4	4.6	47	3.1	5.5	85
30	4.3	5.5	80	4.1	6.5	140
40	5.5	6.7	145	5.2	7.6	223
50	6.7	7.9	238	6.3	8.7	335

Table 2. *Circular dichroism of porphyrin cytochrome* c *and Zn-porphyrin cytochrome* c *in different solutions at 25°C*
KP_i = potassium phosphate; GuHCl = guadinium · HCl

Solution	w_o	θ_{222} for	
		porphyrin cytochrome *c*	Zn-porphyrin cytochrome *c*
		deg cm^2 dmol^{-1}	
20 mM KP_i pH 7.0	–	−14100	−10400
0.2 M AOT/isooctane	5	−12800	−8500
	10	−10700	−6500
	40	−6700	−3800
0.2 M CTAB/isooctane/hexanol	10	−12100	−10200
	40	−11900	−10100
20 mM KP_i, 5 M GuHCl pH 7.0	–	−2200	−2500

In the CTAB micelles the lifetimes of porphyrin cytochrome *c* are even shorter than in AOT. In this case there is almost no effect of w_o on $<\tau>$. Only at $w_o = 10$ is the average lifetime somewhat shorter. This observation agrees with the CD results where we also observe less dependence on the water content of the micelles in CTAB than in AOT. Apparently the interactions between protein and surfactant are stronger with AOT than with CTAB. This is in good agreement with the fact that *in vivo*, cytochrome *c* appears to be bound to negatively charged phospholipid cardiolipin [42].

We have also measured the fluorescence decays in aqueous surfactant solutions. For porphyrin cytochrome *c* in a 20 mM potassium phosphate 5 mM AOT pH 7.0 solution a $<\tau>$ value of 7.50 ns is observed. As in the reversed micellar solutions, this value is shorter than in normal buffer solution. Probably the interactions between the protein and the surfactant in the aqueous AOT solution are of the same nature as in the reversed micellar solutions.

In a 20 mM potassium phosphate 5 mM CTAB pH 7.0 solution the observed $<\tau>$ value is 9.20 ns, which is longer than the value found in buffer solution. In reversed micellar CTAB solutions a shortening of the average fluorescence lifetime was observed. So in case of CTAB the interactions between protein and surfactant in aqueous micellar solutions are different from those in reversed micellar solutions.

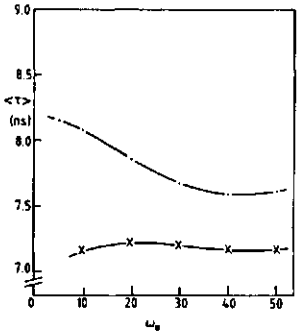

Fig. 5. *Average fluorescence lifetimes of porphyrin cytochrome* c *in AOT-reversed (–·–·–) and CTAB-reversed (–×–×–) micelles as a function of* w_o *at 25°C.* Experimental conditions were the same as described in the legend of Fig. 2. Fluorescence decays were fitted with a triple-exponential function

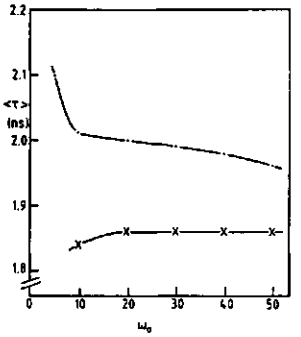

Fig. 6. *Average fluorescence lifetimes of Zn-porphyrin cytochrome* c *in AOT-reversed (–·–·–) and CTAB-reversed (–×–×–) micelles as a function of* w_o *at 25°C.* Experimental conditions were as in Fig. 3. Fluorescence decays were fitted with sum of three exponentials instead of two, which were sufficient in the case of Zn-cytochrome *c* in aqueous solution

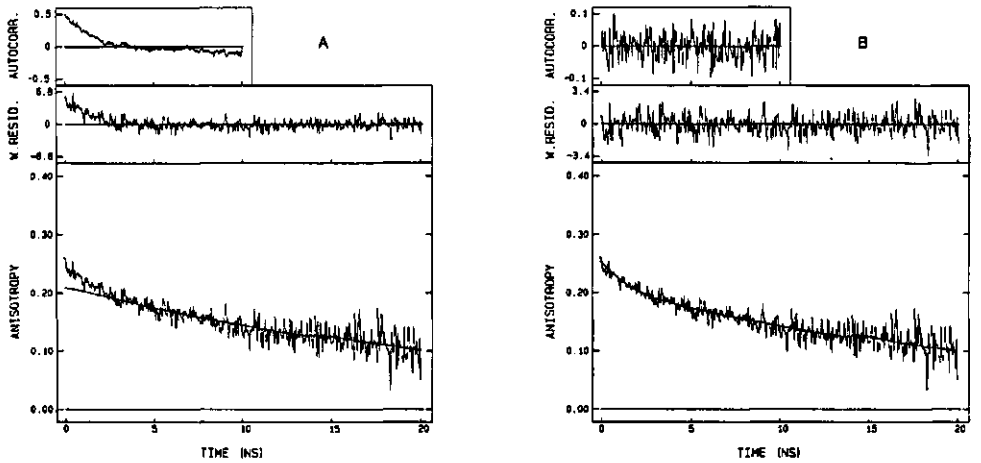

Fig. 7. *Fluorescence anisotropy decay of porphyrin cytochrome* c *in AOT-reversed micelles,* $w_o = 20$*, at 25°C.* Experimental conditions were the same as in Fig. 2. (A) Decay fitted with a single-exponential function having parameters $\beta = 0.21 \pm 0.003$, $\phi = 25.1 \pm 0.6$ ns. (B) Decay fitted with a double-exponential function having parameters $\beta_1 = 0.05 \pm 0.002$, $\phi_1 = 1.0 \pm 0.2$ ns, $\beta_2 = 0.21 \pm 0.002$, $\phi_2 = 25.4 \pm 0.7$ ns

In the case of Zn-porphyrin cytochrome *c* different effects are found. First, three fluorescence lifetimes are needed to describe the decays satisfactorily while in aqueous solution only two were needed. Second, the average lifetimes increase upon incorporation in the AOT-reversed micelles and are not significantly different from the value in aqueous solution and in CTAB-reversed micelles. The increase of $<\tau>$ is most strongly found in AOT micelles at $w_o = 5$. From $w_o = 10$ up to $w_o = 50$ the $<\tau>$ value hardly changes in AOT. In the aqueous surfactant solutions the changes are also small. $<\tau> = 2.02$ ns is found in 5 mM AOT and $<\tau> = 2.04$ ns in 5 mM CTAB. The only similarity between the results for porphyrin cytochrome *c* and those for Zn-porphyrin cytochrome *c* is that the lifetimes in aqueous and in hydrocarbon CTAB solutions differ while in AOT the effects of aqueous and hydrocarbon surfactant solutions are comparable. The different fluorescence behaviour of the two proteins is difficult to explain. Firstly, there is the effect of the Zn ion on the fluorescence properties of the porphyrin and, secondly, the alterations in the protein structure which are evident from CD spectra and FPLC experiments, both of which may play a role.

From the analysis of the anisotropy decays the first striking observation is that all decays of the proteins in (aqueous and hydrocarbon) surfactant solutions must be described by a sum of two exponentials, one with a rotational correlation time of about 1 ns, the other one longer. A typical experiment is shown in Fig. 7. The origin of the fast

Table 3. *Fluorescence anisotropy parameters of porphyrin cytochrome c and Zn-porphyrin cyctochrome c in different solutions at 25°C*

Solution	w_o	Porphyrin cytochrome *c*				Zn-porphyrin cytochrome *c*			
		β_1	ϕ_1	β_2	ϕ_2	β_1	ϕ_1	β_2	ϕ_2
			ns		ns		ns		ns
0.2 M AOT/isooctane	5	0.04 ± 0.003	1.0 ± 0.4	0.23 ± 0.003	30 ± 0.9	–	–	–	–
	10	0.04 ± 0.004	1.3 ± 0.4	0.22 ± 0.004	28 ± 1.2	–	–	–	–
	20	0.05 ± 0.002	1.0 ± 0.2	0.21 ± 0.002	25 ± 0.7	–	–	–	–
	30	0.05 ± 0.002	1.8 ± 0.2	0.20 ± 0.003	26 ± 1.0	–	–	–	–
	40	0.06 ± 0.002	1.1 ± 0.2	0.20 ± 0.003	28 ± 1.0	–	–	–	–
	50	0.06 ± 0.002	2.1 ± 0.2	0.19 ± 0.003	30 ± 1.1	–	–	–	–
20 mM KP_i, 5 mM AOT pH 7.0	–	0.04 ± 0.002	1.9 ± 0.2	0.23 ± 0.002	60 ± 12	–	–	–	–
0.2 M CTAB/isooctane/ hexanol	10	0.02 ± 0.002	0.9 ± 0.2	0.25 ± 0.002	15.3 ± 0.3	0.009 ± 0.004	2.0 ± 1.0	0.089 ± 0.004	20 ± 4
	20	0.03 ± 0.003	1.3 ± 0.2	0.25 ± 0.003	12.4 ± 0.2	0.009 ± 0.003	1.2 ± 0.4	0.092 ± 0.003	12 ± 1
	30	0.04 ± 0.004	0.6 ± 0.3	0.25 ± 0.006	9.7 ± 0.4	0.012 ± 0.009	2.0 ± 1.0	0.087 ± 0.009	10 ± 1
	40	0.04 ± 0.004	0.7 ± 0.2	0.26 ± 0.005	8.7 ± 0.4	0.008 ± 0.004	1.2 ± 0.5	0.093 ± 0.004	8 ± 1
	50	0.04 ± 0.004	0.7 ± 0.2	0.27 ± 0.005	7.8 ± 0.3	0.003 ± 0.005	1.6 ± 0.6	0.094 ± 0.004	7 ± 1
20 mM KP_i, 5 mM CTAB pH 7.0	–	0.04 ± 0.003	0.9 ± 0.1	0.26 ± 0.002	13.7 ± 0.2	0.009 ± 0.003	1.3 ± 0.5	0.080 ± 0.002	15 ± 2

component in the decay is not completely clear. Keh and Valeur [43] have proposed a model for the depolarization of the fluorescence in which the rotation of probe molecules within the micelles, characterized by ϕ_{int}, is coupled to the overall rotation of the micelles, represented by ϕ_{mic}. From this model the following expression for the anisotropy decay was derived:

$$r(t) = \frac{r_o}{\phi_{mic} - \phi_{int}} [\phi_{mic} \exp(-t/\phi_{int}) - \phi_{int} \exp(-t/\phi_{mic})]. \quad (4)$$

In this equation there is a combination of two exponentials, one of them having a negative preexponential factor. Attempts to fit the anisotropy decays of porphyrin cytochrome *c* and Zn-porphyrin cytochrome *c* in reversed micelles according to this model failed. Therefore we assume that the fast component in the anisotropy decay is caused by an enhanced mobility of the porphyrin group. Such a view is supported by the fact that this rapid component is also present in the aqueous surfactant solutions while its contribution is more important in AOT than in CTAB. The results of the analysis of the anisotropy decays are listed in Table 3.

In the case of porphyrin cytochrome *c* in AOT micelles we see a slight increase of the contribution of the fast component in larger micelles (Table 3). This implies that the mobility of the porphyrin within the protein becomes more important in larger micelles. This coincides with the CD results where we found that the protein structure is affected most strongly in AOT micelles with a high water content. The slowly decaying component in the fluorescence anisotropy, characterized by ϕ_2, reports on the overall motion of the protein, which is composed of the mobility of the protein within the micelles, represented by ϕ_{int}, and the mobility of the micelle as a whole, described by ϕ_{mic}. When these two components of the protein motion are independent ϕ_2, ϕ_{int} and ϕ_{mic} are related as follows (cf. [43]):

$$\frac{1}{\phi_2} = \frac{1}{\phi_{int}} + \frac{1}{\phi_{mic}}. \quad (5)$$

The observed ϕ_2 of porphyrin cytochrome *c* in AOT micelles are not very dependent on the water content. From $w_o = 5$ up to $w_o = 30$ a slight decrease of the rotational correlation time is observed and from $w_o = 30$ to $w_o = 50$ the values increase again. We have seen before that the other spectroscopic properties of this protein change with a variation of w_o (especially at w_o values below 20). Therefore we believe that there are two effects which have a compensating influence on the rotational correlation times. The first one is a decrease of ϕ_{int} with increasing w_o. When the size of the micellar water pools increases it can be expected that the mobility of the protein within the micelles also increases. The second effect is that ϕ_{mic} increases when the micelles grow. Comparing the rotational correlation times of the filled and the unfilled micelles we can conclude that at $w_o < 20$ the micelles have to expand upon incorporation of a protein molecule. This can be expected because the core radii of the unfilled micelles at $w_o = 5$ and at $w_o = 10$ are smaller than the radius of the protein molecule. For $w_o \geq 20$ it is not possible to make a statement about the size of the filled micelles. The measured ϕ_2 values are smaller in this case than the rotational correlation times of the empty micelles but this is probably due to the increasing mobility of the protein within the micelles.

Solubilization of cytochrome *c* in AOT-reversed micelles was also studied by Pileni and coworkers [16] with the small-angle X-ray scattering technique. A decrease of the micellar size at $w_o = 20$ upon protein incorporation was found, from which the authors argue that the protein is mainly located at the interface of the micelles and that addition of cyctochrome *c* has the same effect on the system as addition of surfactant, lowering the apparent w_o and thus causing a shrinking of the micelles. From our measurements we can only conclude that there are indeed important interactions between porphyrin cyctochrome *c* and the AOT-reversed micelles, even at the highest w_o value studied, but the statement of Pileni et al., that addition of the protein gives an increase of the interfacial area, cannot be positively affirmed.

In the aqueous AOT solution there are comparable interactions between protein and surfactant as was also concluded

from the fluorescence lifetimes. The anisotropy decay in this case also has two components. The contribution of the fast component is of the same order of magnitude as in the reversed micellar systems and the values found for ϕ_2 is, although high in standard error, much larger than the 5 ns found in normal aqueous solution. Apparently in an aqueous AOT solution also the protein interacts with surfactant aggregates.

In CTAB-reversed micelles the contribution of the fast component to the anisotropy decay is smaller than in the case of AOT (see Table 3). The measured ϕ_2 values are significantly shorter than in the case of AOT and decrease monotonically with increasing w_o. From this observation we conclude that porphyrin cytochrome *c* gains more internal mobility when the size of the reversed CTAB micelles increases. It is not expected that the size of the filled micelles decreases with increasing water content, thus causing the shortening of the rotational correlation time of the whole micelle. At $w_o = 50$ the value of ϕ_2 is quite close to that measured in normal aqueous solution. Because the empty CTAB micelle at $w_o \approx 50$ is very large, we do not expect that the overall rotation of the micelle has any contribution to the measured anisotropy decay. This indicates that the protein mobility within the micelle is almost the same as in bulk water.

In the aqueous CTAB solution a significant effect of the surfactant on the protein anisotropy decay is found. Again a fast component is found in the decay. The ϕ_2, which reflects the protein overall rotation, is nearly three times longer than in normal aqueous solution. Apparently, the interactions between protein and CTAB are more important in aqueous than in hydrocarbon surfactant solutions. Probably the changes in the fluorescence properties of the protein in the reversed micellar solutions are caused either by the high effective bromide concentration in the water pools or by interactions with surfactant-bound water molecules. Direct interactions between the protein and the surfactant interface are unlikely, because in that case the protein rotation would be more hindered, resulting in a longer rotational correlation time. The effects, which are observed in the aqueous CTAB solution, can only be explained in terms of direct interactions between the protein and the surfactant. The increase of the fluorescence lifetime can be explained if surfactant molecules interact with the protein, thus causing a shielding of the exposed part of the porphyrin ring. In the neighbourhood of this part of the porphyrin ring the protein has a zone where most of the acidic amino acid residues are clustered, which might lead to electrostatic attraction between the protein and CTAB molecules. In the reversed micellar system these interactions may be prevented by the high effective bromide concentrations in the water pools.

For Zn-porphyrin cytochrome *c* the dynamic properties are more difficult to obtain from the fluorescence anisotropy decay. The reason for this is, as we stated before, that the fluorescence lifetime is short and the initial anisotropy low (see Fig. 3). In the case of Zn-porphyrin cytochrome *c* in AOT micelles (aqueous and reverse) no meaningful values for the rotational correlation times can be obtained from the polarized fluorescence decay data. A good fit of the anisotropy decay can be obtained with every ϕ_2 value higher than 25 ns. Data are therefore omitted in Table 3.

In the case of CTAB-reversed micelles reliable values for the rotational correlation times can be obtained for Zn-porphyrin cytochrome *c*, although the standard error in the fitted parameters is much higher than in the case of porphyrin cytochrome *c*. The results are listed in Table 3 and they are comparable to those for porphyrin cytochrome *c*. Although the two proteins do not have exactly identical structures, the dynamic properties in CTAB aqueous and reversed micelles are almost the same.

We thank Miss Y. T. Soekhram for preparing the manuscript. Part of this work was supported by the Netherlands Foundation of Chemical Research (S.O.N.) with financial aid from the Netherlands Organization for the Advancement of Pure Research (Z.W.O.).

REFERENCES

1. Eicke, H. F. (1980) *Top. Curr. Chem. 87*, 85–145.
2. Fendler, J. H. (1982) *Membrane-mimetic chemistry*, Wiley-Interscience, New York.
3. O'Connor, C. J., Lomax, T. D. & Ramage, R. E. (1984) *Adv. Colloid Interface Sci. 20*, 21–97.
4. Vos, K., Laane, C. & Visser, A. J. W. G. (1987) *Photochem. Photobiol. 45*, 863–878.
5. Luisi, P. L. (1985) *Angew. Chem. (Int. Ed.) 24*, 439–460.
6. Luisi, P. L. & Laane, C. (1986) *Trends Biotechnol. 4*, 153–161.
7. Luisi, P. L. & Magid, L. J. (1986) *CRC Crit. Rev. Biochem. 20*, 409–474.
8. Martinek, K., Levashov, A. V., Klyachko, N., Khmelnitski, Y. L. & Berezin, I. V. (1986) *Eur. J. Biochem. 155*, 453–468.
9. Waks, M. (1986) *Proteins: Structure, Function and Genetics 1*, 4–15.
10. Hilhorst, R., Laane, C. & Veeger, C. (1983) *FEBS Lett. 159*, 225–228.
11. Hilhorst, R., Spruijt, R., Laane, C. & Veeger, C. (1984) *Eur. J. Biochem. 144*, 459–466.
12. Laane, C., Veeger, C. & Hilhorst, R. (1987) *Methods Enzymol.*, in the press.
13. Dickerson, R. E. & Timkovich, R. (1975) in *The enzymes* (Boyer, P. D., ed.) 3rd edn, vol. 11, pp. 397–549, Academic Press, New York.
14. Pileni, M. P. (1981) *Chem. Phys. Lett. 81*, 603–605.
15. Visser, A. J. W. G. & Fendler, J. H. (1982) *J. Phys. Chem. 86*, 947–950.
16. Pileni, M. P., Zemb, T. & Petit, C. (1985) *Chem. Phys. Lett. 118*, 414–420.
17. Erjomin, A. N. & Metelitza, D. I. (1984) *Biokhymia 49*, 1947–1954.
18. Vanderkooi, J. M. & Erecinska, M. (1975) *Eur. J. Biochem. 60*, 199–207.
19. Vanderkooi, J. M., Adar, F. & Erecinska, M. (1976) *Eur. J. Biochem. 64*, 381–387.
20. Dixit, B. P. S. N., Moy, V. T. & Vanderkooi, J. M. (1984) *Biochemistry 23*, 2103–2107.
21. Horie, T., Maniara, G. & Vanderkooi, J. M. (1984) *FEBS Lett. 177*, 287–290.
22. Menger, F. M. & Yamada, K. (1979) *J. Am. Chem. Soc. 101*, 6731–6734.
23. Cramer, L. E. & Spears, K. G. (1978) *J. Am. Chem. Soc. 100*, 221–227.
24. Flatmark, T. & Robinson, A. B. (1968) in *Structure and function of cytochromes* (Okunuki, K., Kamen, M. D. & Sekuzu, I., eds) pp. 383–387, University Park Press, Baltimore.
25. Fisher, W. R., Taniuchi, H. & Anfinsen, B. (1973) *J. Biol. Chem. 248*, 3188–3195.
26. Van Hoek, A. & Visser, A. J. W. G. (1985) *Anal. Instrum. 14*, 359–378.
27. Van Hoek, A. & Visser, A. J. W. G. (1981) *Rev. Sci. Instrum. 52*, 1199–1205.
28. Vos, K., Van Hoek, A. & Visser, A. J. W. G. (1987) *Eur. J. Biochem. 165*, 55–63.
29. Buchler, J. W. (1975) in *The porphyrins* (Dolphin, D., ed.) vol. 1, pp. 399–483, Academic Press, New York.
30. Timkovich, R. (1979) in *The porphyrins* (Dolphin, D., ed.) vol. 7, pp. 241–294, Academic Press, New York.
31. Weigl, J. W. (1957) *J. Mol. Spectrosc. 1*, 133–138.
32. Gouterman, M. & Stryer, L. (1962) *J. Chem. Phys. 37*, 2260–2266.

33. Benthem, L. (1984) Ph. D. Thesis, Agricultural University Wageningen.
34. Visser, A. J. W. G., Grande, H. J. & Veeger, C. (1980) *Biophys. Chem. 12*, 35–49.
35. Takano, K., Kallai, O. B., Swanson, R. & Dickerson, R. E. (1973) *J. Biol. Chem. 248*, 5234–5255.
36. Thomas, M. A., Gervais, V., Favaudon, V. & Valat, P. (1983) *Eur. J. Biochem. 135*, 577–581.
37. Thomas, M. A., Favaudon, V. & Pochon, F. (1983) *Eur. J. Biochem. 135*, 569–576.
38. Zulauf, M. & Eicke, H. F. (1979) *J. Phys. Chem. 83*, 480–486.
39. Atik, S. S. & Thomas, J. K. (1981) *J. Am. Chem. Soc. 103*, 3543–3550.
40. Robinson, B. H., Toprakcioglu, C., Dore, J. C. & Chieux, P. (1984) *J. Chem. Soc. Faraday, Trans. I 80*, 13–27.
41. Ekwall, P., Mandell, L. & Fontell, K. (1969) *J. Colloid Interface Sci. 29*, 639–646.
42. Vanderkooi, J. M., Erecinska, M. & Change, B. (1973) *Arch. Biochem. Biophys. 154*, 219–229.
43. Keh, E. & Valeur, B. (1981) *J. Colloid Interface Sci. 79*, 465–478.

5 TRIPLET-STATE KINETICS OF ZN-PORPHYRIN CYTOCHROME C IN MICELLAR MEDIA
MEASUREMENT OF INTERMICELLAR EXCHANGE RATES

Kees Vos, Daniel Lavalette and Antonie J.W.G. Visser

Reprinted from: European Journal of Biochemistry (1987) 169, 269-273.

The interactions of protein molecules with surfactant assemblies in aqueous and hydrocarbon media have been studied via the triplet-state kinetics of Zn-porphyrin cytochrome *c* in solutions containing an anionic [sodium bis(2-ethylhexyl)sulfosuccinate, AOT] or a cationic (cetyltrimethylammonium bromide, CTAB) surfactant.

In aqueous solution, the observed triplet state decay is single exponential with a lifetime of 8 ms.

In aqueous solutions of AOT and in AOT-reversed micellar solutions, biexponential triplet state decays were observed, indicating that interactions between the surfactant and the protein occur, resulting in a change in protein conformation near the porphyrin ring.

In CTAB-reversed micellar solutions, quenching of the Zn-porphyrin cytochrome *c* triplet state by ferricyanide and methyl viologen was studied. Because the quenching is exchange-limited under the conditions used, the exchange rate constants for the water pools can be obtained from these experiments. The observed exchange rate constants are in the range of $(1-5)\times 10^7\ M^{-1}s^{-1}$, depending on the water content of the reversed micelles and on the type of quencher used. These values are three orders of magnitude lower than the calculated collision rate of the reversed micelles.

The encapsulation of proteins in water droplets, separated from a hydrocarbon solvent by a layer or surfactant molecules (reversed micelles), has gained considerable and still increasing interest, because of the potential applications in conversions of apolar substrates or the enhanced stabilizing properties of reversed micelles (for review see [1–6]). Since reversed micelles are thermodynamically stable optically transparent solutions, spectroscopic techniques are the method of choice to characterize the structure of the entrapped protein and its interaction with the surfactant interface (see Vos et al. [7] for a survey). Small single polypeptides and well characterized proteins are the prime candidates to investigate the effect of surfactant assemblies on the structure and dynamics of the protein in more detail. Such an example is provided by the redox protein cytochrome *c*, which is one of the first proteins to be succesfully entrapped in the widely used reversed micellar system of the anionic surfactant sodium bis(2-ethylhexyl)sulfosuccinate (Aerosol OT or AOT) [8]. The spectroscopic properties of fluorescent derivatives of horse heart cytochrome *c*, incorporated in anionic (AOT) or cationic (cetyltrimethylammonium bromide, CTAB) reversed micelles have been described in the preceding paper [9]. In these derivatives the heme group, covalently linked to the polypeptide chain, was either depleted from the central iron ion or the iron replaced by zinc. Electrostatic attraction between the positively charged protein and the anionic AOT surfactant could be demonstrated. Time-resolved fluorescence of the more fluorescent, metal-free cytochrome *c* resulted in more conclusive results.

The photophysical properties of cytochrome *c* derivatives have been investigated and summarized by Vanderkooi and coworkers [10]. The incorporation of Zn in the heme moiety results in a more efficient triplet formation (90% efficiency [10]), which is manifested by a decreased quantum yield and shorter fluorescence lifetime as compared to metal-free cytochrome *c*. The high triplet yield enabled measurements of phosphorescence decay at room temperature to be made and the quenching of the phosphorescence by electron acceptors to be studied [11].

We have utilized the excited triplet state lifetime of Zn-porphyrin cytochrome *c* as a probe for specific interactions of the protein with anionic and cationic surfactant aggregates in aqueous and hydrocarbon solutions. Considering the sensitivity of triplet-state lifetimes towards environmental effects, any perturbation induced in the vicinity of the porphyrin ring must be sensed by this kinetic parameter. In addition, owing to the long lifetime of the unperturbed triplet state (in the order of 10 ms under anaerobic conditions), intermicellar exchange rates can be conveniently determined in a reversed micellar system, containing photoexcited electron-donating Zn-porphyrin cytochrome *c* and ionic electron acceptors which are initially hosted in separate micelles. Experiments of this kind have been performed with a wide variety of donor/acceptor couples [12–19]. The decay kinetics of the observed excited state species are well established for reactants which are confined to the water pools of the reversed micelles and have a Poissonian distribution among these water pools [12]. We have selected conditions under which the decay of the triplet state is determined by the exchange of molecules and ions between different reversed micelles. Exchange rates

Correspondence to A. J. W. G. Visser, Laboratorium voor Biochemie der Landbouwuniversiteit, De Dreijen 11, NL-6703 BC Wageningen, The Netherlands

Abbreviations. AOT, Aerosol-OT [sodium bis(2-ethylhexyl)-sulfosuccinate]; CTAB, cetyltrimethylammonium bromide; MV^{2+}, methyl viologen (1,1'-dimethyl-4,4'-bipyridinium ion).

could thus be determined for a system in which one of the reaction partners is the entrapped protein. According to our knowledge such measurements have not yet been performed with proteins.

MATERIALS AND METHODS

Chemicals

AOT [sodium bis(2-ethylhexyl)sulfosuccinate] was purchased from Janssen Chimica and was purified as described by Menger and Yamada [20]. CTAB (cetyltrimethylammonium bromide) was obtained from Serva and was used as received. Both surfactants were desiccated over P_2O_5. Methyl viologen (1,1'-dimethyl-4,4'-bipyridinium dichloride) was from Sigma. Potassium ferricyanide, isooctane (Uvasol, for fluorometry) and 1-hexanol (P.A.) were obtained from Merck. Cytochrome *c* was from Sigma (type III). Preparation and characterization of Zn-porphyrin cytochrome *c* has been described in the preceding paper [9].

Preparation of reversed micellar solutions

Reversed micellar solutions were prepared by injecting 50 µl of a concentrated Zn-porphyrin cytochrome *c* solution (0.3 mM) into 2.5 ml of a 0.24 M solution of AOT in isooctane or CTAB in 12% 1-hexanol/isooctane (v/v). The solutions were extensively Vortex-stirred until clarity. Buffer (20 mM potassium phosphate, pH 7.0) was added until the desired w_o ($[H_2O]/[surfactant]$) value was reached and finally the total volume was adjusted to 3.0 ml with isooctane. Samples had a final surfactant concentration of 0.2 M. The CTAB solutions contained 10% of 1-hexanol with respect to the total volume.

Transient absorption measurements

The instrument for the measurement of triplet-triplet absorption and/or ground state depletion has been described before [21]. The samples were excited by the second harmonic of a Q-switched Nd:Yag laser, providing 20-ns pulses with a maximum energy of 300 mJ at 532 nm. The triplet lifetimes were determined via ground state depletion, monitored at 422 nm. The overall protein concentration in the samples was 5 µM, which gave an $A_{530} = 0.02$ and an $A_{422} = 1.22$. Before measurement the samples were thoroughly degassed according to the method described in [21]. In the case of reversed micellar solutions, the argon was saturated with isooctane/water or with isooctane/hexanol/water. Temperature was kept at 25°C. An equilibration period of 15 min was maintained prior to the measurements.

The accuracy of the measurements is about 5% when one sample is flashed repeatedly. Intersample reproducibility is of the order of 10% due to unavoidable differences in outgassing procedure.

RESULTS AND DISCUSSION

Triplet state lifetimes of Zn-porphyrin cytochrome c

The triplet state lifetime of Zn-porphyrin cytochrome *c* was measured in different solutions. The results of these experiments are listed in Table 1. In 20 mM potassium phosphate buffer, pH 7.0 at 25°C we found repeatedly a lifetime $\tau = 8.0$ ms (Fig. 1), which is shorter than the 14 ms reported by Dixit et al. [10]. This difference may be accounted for by slight differences in the protein preparation, buffer, temperature or deoxygenation procedure.

In aqueous AOT solutions or in AOT-reversed micellar solutions non-exponential triplet state decays were observed. These decays can satisfactorily be described by a sum of two exponentials with one lifetime in the microsecond region and the other one in the millisecond region. In the 0.5 mM aqueous AOT solution the long lifetime was calculated and amounts to 6.0 ms, which is close to the value observed in normal aqueous solution. In the preceding paper [9] we reported that porphyrin cytochrome *c* and Zn-porphyrin cytochrome *c* have strong interactions with AOT interfaces in both aqueous and hydrocarbon solutions. This observation was made via time-resolved fluorescence and circular dichroic measurements. Here we observe the same phenomenon via the decay of the triplet state. The biexponential triplet state decay might be caused by the existence of two populations of protein molecules, one in a purely aqueous environment with similar characteristics as the protein in normal aqueous solution, the other population (consisting of at least 75% of the total number of protein molecules) being bound to the interface and having a changed conformation.

In the CTAB solutions, normal exponential decays of the triplet state were observed. In a 1.0 mM aqueous CTAB solution the triplet state is quenched. In reversed micellar solutions the observed decays are strongly dependent on w_o. At $w_o = 10$ a slight quenching of the excited triplet state is found, whereas at $w_o = 40$ the lifetime of the triplet state is even longer than in normal aqueous solution (Table 1). The lengthened lifetime at $w_o = 40$ may be related to differences in oxygen diffusion because of subtle changes in the micellar structure around the protein. A retarded oxygen diffusion results in a longer triplet state lifetime because of decreased oxygen quenching. From time-resolved fluorescence and circular dichroic experiments [9] we know, that the effect of CTAB interfaces on the characteristics of Zn-porphyrin cytochrome *c* is much less than that of AOT interfaces and also that, in aqueous CTAB solution, the interactions between protein and surfactant are more important than in reversed micellar solutions. The present experiments confirm these observations.

Quenching of the triplet state in reversed micellar solutions

Luminescence quenching experiments with probes which are located in reversed micellar water pools have been described in a number of publications [12–19]. A general assumption in this kind of experiment is that quencher molecules, which are restricted to the water pools, have a Poisson distribution among these water pools, i.e.

$$P_i = n^i \exp(-n)/i! \qquad (1)$$

where P_i is the probability of the occurrence of a water pool with i quencher molecules in it and $n = [\text{quencher}]/[\text{WP}]$, the average number of quencher molecules per water pool. When a probe is used, which decays exponentially in the absence of quencher, the time dependence of the luminescence can be described by (cf. [12, 22–25])

$$I(t) = I(0)\exp[-C_1 t - C_2\{1-\exp(-C_3 t)\}] \qquad (2a)$$

Table 1. *Triplet-state lifetimes of Zn-porphyrin cytochrome c in different solutions at 25°C*
KP_i = potassium phosphate

Solution	w_o	α_1	τ_1	α_2	τ_2
			ms		ms
20 mM KP_i pH 7.0	–	–	–	–	8.0
+ 0.5 mM AOT	–	0.74	0.25	0.26	6.0
+ 1.0 mM AOT	–	0.90	0.13	0.10	> 5
0.2 M AOT/isooctane	5	0.95	0.24	0.05	> 5
	40	0.80	0.22	0.20	> 5
20 mM KP_i pH 7.0 + 1.0 mM CTAB	–	–	–	–	2.0
0.2 M CTAB/isooct/hexanol	10	–	–	–	4.5
	40	–	–	–	11.7

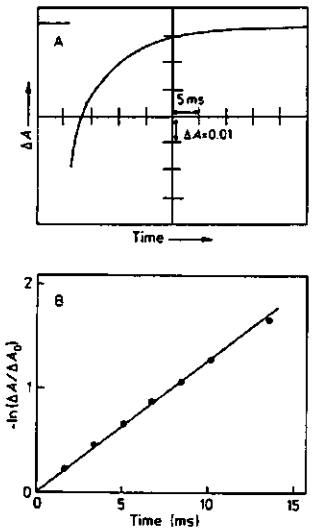

Fig. 1. *Transient bleaching at 422 nm of Zn-porphyrin cytochrome c in 20 mM potassium phosphate pH 7.0 at 25°C.* (A) Excitation wavelength was 532 nm, signal/noise ratio was around 500 and the response time for this particular picture was 100 μs. (B) Analysis of the oscilloscope trace in A, yielding a triplet-state lifetime of 8.0 ms

with:

$$C_1 = 1/\tau_o + k_q k_c[Q]/(k_q + k_c[WP]) \quad (2b)$$

$$C_2 = n k_q/(k_q + k_c[WP]) \quad (2c)$$

and:

$$C_3 = k_q + k_c[WP]. \quad (2d)$$

The parameters in this expression are: τ_o, the unquenched lifetime of the excited state; k_q, the intrawater pool first-order quenching rate constant and k_c, the bimolecular rate constant for the exchange process of the different water pools. The restriction of an exponential decay of the excited state at zero quencher concentration excludes the AOT-reversed micellar solutions with Zn-porphyrin cytochrome *c* as probe from this kind of experiment.

In CTAB-reversed micellar solutions we have measured quenching of the triplet state of Zn-porphyrin cytochrome *c* with two different quenchers, i.e. ferricyanide [$K_3Fe(Cn)_6$] and the methyl viologen ion (MV^{2+}). Quenching of the Zn-porphyrin cytochrome *c* triplet state by these compounds in aqueous solution has been described by Horie et al. [11] and is assumed to occur via an electron transfer mechanism. The apparent quenching constants in aqueous solution are reported to be 1.3×10^8 $M^{-1}s^{-1}$ and 1.0×10^7 $M^{-1}s^{-1}$ for $K_3Fe(CN)_6$ and MV^{2+} respectively [11].

From quenching experiments with tris(2,2'-bipyridine) ruthenium(II) dichloride as probe and ferricyanide as quencher, we know the water pool concentration in the CTAB-reversed micellar system to be about 2 mM at $w_o = 10$ and 0.4 mM at $w_o = 40$ [9]. These concentrations will only be very slightly altered upon protein incorporation because we have used a very low protein concentration (5 μM) resulting in a very low degree of occupancy at both $w_o = 10$ and $w_o = 40$. Since exchange rates of reversed micelles are in the order of $10^7 - 10^8$ $M^{-1}s^{-1}$ [12, 26] we can argue that $k_q \gg k_c[WP]$ (this means that quenching of the triplet state is exchange-limited). Besides that, we have used very low quencher concentrations (maximum quencher concentration used is 33 μM). Therefore we may state that $n \approx 0$. Under these conditions Eqns (2) reduce to:

$$C_1 = 1/\tau_o + k_c[Q]$$

$$C_2 = 0$$

and thus:

$$I(t) = I(0)\exp\{-(1/\tau_o + k_c[Q])t\}. \quad (3)$$

Eqn (3) predicts exponential decays for the excited state and a linear plot of $1/\tau$ versus [Q] with the slope yielding k_c. The decays we observe with Zn-porphyrin cytochrome *c* in CTAB-reversed micelles quenched with ferricyanide or with methyl viologen are indeed exponential. The $1/\tau$ versus [Q] plots are shown in the Figs 2 and 3. The exchange rate constants, k_c, for the different systems are listed in Table 2.

When the reversed micelles are considered as non-interacting particles the collision frequency, k_c, can be calculated from (cf. [27]):

$$k_c = \frac{2RT}{3\eta}\left(2 + \frac{r_1}{r_2} + \frac{r_2}{r_1}\right) \quad (4)$$

where R is the gas constant, T the absolute temperature, η the solvent viscosity (kg/m.s.), r_1 the (hydrodynamic) radius of a quencher-filled micelle and r_2 the radius of a protein-filled micelle. When $r_1 = r_2$, k_c is independent of the radius of the particles. In that case a collision frequency of 1.3×10^{10} $M^{-1}s^{-1}$ can be calculated for the CTAB-reversed micelles at

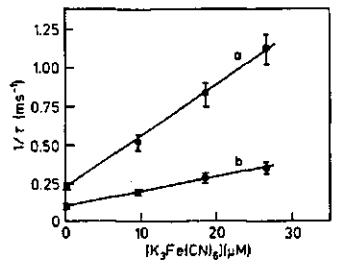

Fig. 2. *Plots of the reciprocal triplet state lifetimes of Zn-porphyrin cytochrome c in CTAB-reversed micelles at* $w_o = 10$ *(a) and* $w_o = 40$ *(b) versus* $[K_3Fe(CN)_6]$ *at 25°C.* Exchange rate constants, determined from the slopes are listed in Table 2

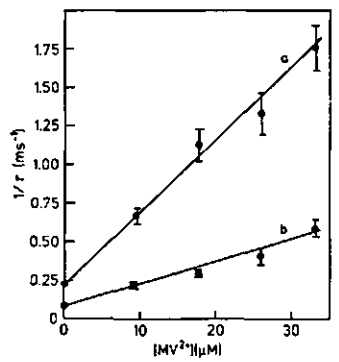

Fig. 3. *Quenching of the Zn-porphyrin cytochrome c triplet-state lifetime in CTAB-reversed micelles by methyl viologen.* Details as in Fig. 2

25°C, assuming, that the viscosity of the continuous phase is 5.00×10^{-4} kg/m · s [9]. The reported k_e values are a factor 250–1000 smaller than the calculated collision frequency. This phenomenon was also observed in the case of AOT-reversed micelles via luminescence [12] and rapid mixing [26] experiments.

There are two remarkable facts in our results. The first one is that with methyl viologen an exchange rate is observed which is higher than the one found with ferricyanide at both w_o values. This proves in our opinion that quenching of the Zn-porphyrin cytochrome *c* triplet state is indeed exchange-limited because in aqueous solution ferricyanide is the more effective quencher [11]. The explanation for this behaviour might be that ferricyanide, which is negatively charged, more or less sticks to the CTAB interface and thus less readily exchanges than methyl viologen, which has a positive charge. The second remarkable observation is that with both quenchers the exchange is three times faster at $w_o = 10$ than at $w_o = 40$. Possibly the collision rates at $w_o = 10$ and at $w_o = 40$ are different. This will be the case when the radii of the empty and the protein-filled micelles differ markedly at $w_o = 10$. To find a collision rate which is three times higher than at $w_o = 40$ the ratio r_2/r_1 must be about 10 at $w_o = 10$. This would imply that at $w_o = 10$ the radius of the protein-filled micelle is much larger than at $w_o = 40$, which is not likely. A more probable possibility is that the packing of the interface is less dense at $w_o = 10$ than at $w_o = 40$, caused by the stronger curvature. A less dense packing of the surfactant molecules will cause a more flexible interface and thus a higher exchange rate of the water pools. A similar tendency of increasing exchange rate constants at low w_o has been reported for AOT-reversed micelles in heptane [26].

Table 2. *Exchange rate constants of CTAB-reversed micelles at 25°C*

Quencher	w_o	$k_e \times 10^{-7}$
		$M^{-1}s^{-1}$
$K_3Fe(CN)_6$	10	3.3
	40	1.0
MV^{2+}	10	4.7
	40	1.5

CONCLUDING REMARKS

The triplet state decay of Zn-porphyrin cytochrome *c* is a very sensitive reporter of interactions of this protein with surfactant assemblies in aqueous and hydrocarbon solutions. In AOT solutions the protein molecules exhibit strongly affected triplet-state kinetics, indicating that interactions between surfactant and protein induce alterations in the conformation near the porphyrin macrocycle. In CTAB solutions the triplet state decays are less perturbed than in AOT solutions. Quenching experiments in CTAB-reversed micellar solutions allow the determination of the exchange rates of the water pools. The observed exchange rates are a factor of 250–1000 lower than the calculated collision frequency of the reversed micelles. The higher exchange rate with methyl viologen as quencher as compared to ferricyanide is best explained by an electrostatic attraction between the negatively charged ferricyanide and the positively charged surfactant headgroups. With both quenchers a higher exchange rate is found at $w_o = 10$ than at $w_o = 40$. Probably this is due to the stronger curvature of the surfactant interface at $w_o = 10$. Experiments with a small probe (Tb^{3+}) and a small quencher (Mn^{2+}) [28] which do not affect the size of the micelles might confirm this view.

The research described was supported by a *Centre National de la Recherche Scientifique* fellowship, granted to one of us (A.J.W.G.V.) by The Netherlands Organization for the Advancement of Pure Research.

REFERENCES

1. Fendler, J. H. (1982) *Membrane-mimetic chemistry*, Wiley Interscience, New York.
2. Luisi, P. L. (1985) *Angew. Chem. (Int. Ed.) 24*, 439–460.
3. Luisi, P. L. & Laane, C. (1986) *Trends Biotech. 4*, 153–161.
4. Luisi, P. L. & Magid, L. J. (1986) *CRC Crit. Rev. Biochem. 20*, 409–474.
5. Martinek, K., Levashov, A. V., Klyachko, N., Khmelnitski, Y. L. & Berezin, I. V. (1986) *Eur. J. Biochem. 155*, 453–468.
6. Waks, M. (1986) *Proteins: Structure, Function and Genetics 1*, 4–15.
7. Vos, K., Laane, C. & Visser, A. J. W. G. (1987) *Photochem. Photobiol. 45*, 863–878.
8. Douzou, P., Keh, E. & Balny, C. (1979) *Proc. Natl Acad. Sci. USA 76*, 681–684.

9. Vos, K., Laane, C., Weijers, S. R., van Hoek, A., Veeger, C. & Visser, A. J. W. G. (1987) *Eur. J. Biochem. 169*, 259–268.
10. Dixit, B. P. S. N., Moy, V. T. & Vanderkooi, J. M. (1984) *Biochemistry 23*, 2103–2107.
11. Horie, T., Maniara, G. & Vanderkooi, J. M. (1984) *FEBS Lett. 177*, 287–290.
12. Atik, S. S. & Thomas, J. K. (1981) *J. Am. Chem. Soc. 103*, 3543–3550.
13. Atik, S. S. & Thomas, J. K. (1981) *J. Am. Chem. Soc. 103*, 4367–4371.
14. Geladé, E. & de Schryver, F. C. (1982) *J. Photochem. 18*, 223–230.
15. Geladé, E. & de Schryver, F. C. (1984) in *Reverse micelles* (Luisi, P. L. & Straub, B. E., eds) pp. 143–164, Plenum, New York.
16. Furois, J. M., Brochette, P. & Pileni, M. P. (1984) *J. Colloid Interface Sci. 97*, 552–558.
17. Brochette, P. & Pileni, M. P. (1985) *Nouv. J. Chim. 9*, 551–555.
18. Almgren, M., van Stam, J., Swarup, S. & Löfroth, J.-E. (1986) *Langmuir 2*, 432–438.
19. Handa, T., Sakai, M. & Nakagaki, M. (1986) *J. Phys. Chem. 90*, 3377–3380.
20. Menger, F. M. & Yamada, K. (1979) *J. Am. Chem. Soc. 101*, 6731–6734.
21. Lavalette, D., Amand, B. & Pochon, F. (1977) *Proc. Natl Acad. Sci. USA 74*, 1407–1411.
22. Infelta, P. P., Grätzel, M. & Thomas, J. K. (1974) *J. Phys. Chem. 78*, 190–195.
23. Tachiya, M. (1975) *Chem. Phys. Lett. 33*, 289–292.
24. Atik, S. S. & Singer, L. A. (1978) *Chem. Phys. Lett. 59*, 519–524.
25. Atik, S. S. & Singer, L. A. (1979) *Chem. Phys. Lett. 66*, 234–237.
26. Fletcher, P. D. I. & Robinson, B. H. (1981) *Ber. Bunsenges. Phys. Chem. 85*, 863–867.
27. Cantor, C. R. & Schimmel, P. R. (1980) *Biophysical chemistry*, part III, pp. 920–921, W. H. Freeman, San Francisco.
28. Eicke, H.-F., Shepherd, J. C. W. & Steinemann, A. (1976) *J. Colloid Interface Sci. 56*, 168–176.

6 SPECTROSCOPIC PROPERTIES OF HORSE LIVER ALCOHOL DEHYDROGENASE IN REVERSED MICELLAR SOLUTIONS

Kees Vos, Colja Laane, Arie van Hoek, Cees Veeger and Antonie J.W.G. Visser

Reprinted from: European Journal of Biochemistry (1987) 169, 275-282.

Catalytic and spectroscopic properties of alcohol dehydrogenase from horse liver, incorporated in reversed micellar media, have been studied. Two different reversed micellar systems have been used, one containing an anionic [sodium bis(2-ethylhexyl)sulfosuccinate, AOT], the other containing a cationic (cetyltrimethylammonium bromide, CTAB) surfactant.

With 1-hexanol as substrate the turnover number of the enzyme in AOT-reversed micelles is strongly dependent on the water content of the system. At low w_o ([H_2O]/[surfactant]) ($w_o < 20$) no enzymatic activity can be detected, whereas at high w_o ($w_o = 40$) the turnover is only slightly lower than in aqueous solution. In CTAB-reversed micelles the dependence of the turnover number on w_o is much less. The enzymatic activity is in this case significantly lower than in aqueous solution and increases only slightly with an increasing water content of the reversed micelles.

Possible interactions of the protein with the surfactant interfaces in the reversed micellar media were studied via circular dichroism and fluorescence measurements. From the circular dichroism of the protein backbone it is observed that the protein secondary structure is not significantly affected upon incorporation in the reversed micelles since the far-ultraviolet spectrum is not altered.

Results from time-resolved fluorescence anisotropy experiments indicate that, especially in AOT-reversed micelles, interactions between the protein and the surfactant interface are largely electrostatic in nature, as evident from the dependence on the pH of the buffer used. In CTAB-reversed micellar solutions such interactions appear to be much less pronounced than in AOT.

Solubilization of biopolymers and especially of proteins in hydrocarbon media, via surfactant assemblies, called reversed micelles, has been extensively investigated during the last decade [1 – 7]. Structural information about these systems can be obtained via spectroscopic techniques, since reversed micelles form thermodynamically stable and optically transparent solutions. In two previous publications we have described some spectroscopic properties of fluorescent cytochrome *c* derivatives (from horse heart), incorporated in anionic- and cationic-reversed micelles [8, 9]. From these studies it became clear that electrostatic interactions between protein and surfactant interface are of considerable importance to the structure and dynamics of the encased cytochrome *c* molecules.

In this article, catalytic properties, fluorescence and circular dichroism results are presented of the well characterized protein alcohol dehydrogenase from horse liver (LADH) [10, 11], incorporated in reversed micelles, consisting of anionic sodium bis(2-ethylhexyl)sulfosuccinate (AOT) or cationic cetyltrimethylammonium bromide (CTAB) in isooctane. LADH consists of two identical subunits and has a relative molecular mass of 80000. Each subunit contains two tryptophan residues, which are very suitable intrinsic fluorescence probes for this study. From X-ray analysis [11] it is known that one tryptophan (Trp-15) is located near the surface of the protein, whereas the other (Trp-314) is buried inside the protein coil in a hydrophobic region near the subunit interface. The time-resolved fluorescence properties of the tryptophans in LADH have been described in a number of articles [12 – 16].

Incorporation of LADH in AOT-reversed micelles has been performed before by Meier and Luisi [17], and by Martinek et al. [18]. The group of Biellmann has recently reported on LADH catalysis in four-component reversed micellar systems with sodium dodecyl sulphate and cetyltrimethylammonium bromide as surfactants [19]. From the above-mentioned studies it was found that the enzymatic activity of the protein is preserved in the reversed micellar solutions and that in such systems both water-soluble and hydrocarbon-soluble substrates can be converted.

The aim of the present study is to obtain information about the structural and catalytic aspects of LADH incorporation in reversed micellar systems. In order to obtain information about charge effects, the spectroscopic properties of LADH incorporated in reversed micellar media have been studied with the protein dissolved in buffers of different pH (i.e. pH 8.8 and pH 7.0). The isoelectric point of the protein is about 8.7 [11], which means that at pH 8.8 the overall charge

Correspondence to A. J. W. G. Visser, Laboratorium voor Biochemie der Landbouwuniversiteit, De Dreijen 11, NL-6703 BC Wageningen, The Netherlands

Abbreviations. AOT, Aerosol-OT [sodium bis(2-ethylhexyl)-sulfosuccinate]; CD, circular dichroism; CTAB, cetyltrimethyl ammonium bromide; LADH, horse liver alcohol dehydrogenase.

Enzyme. Horse liver alcohol dehydrogenase (EC 1.1.1.1).

of the protein is almost zero, whereas at pH 7.0 there is an overall positive charge. Of course, the effective pH of the water pools of the reversed micelles is not known, but it can be expected that at pH 8.8 the protein is less positively charged than at pH 7.0. If electrostatic interactions between protein and surfactant interface influence the spectroscopic properties of LADH, differences between these two systems arising from pH variation are expected to be observed.

Detailed information in this study has been obtained with the time-resolved fluorescence depolarization technique, which is a very sensitive method to observe changes in the environment of the fluorescent probes [20–22]. The rotational dynamics of the LADH molecule in reversed micellar systems could be related to effects of pH, w_o and surfactant.

MATERIALS AND METHODS

Chemicals

LADH was obtained from Boehringer as a crystalline suspension in 20 mM potassium phosphate, 10% ethanol, pH 7.0. The crystals were centrifuged, dissolved in 20 mM sodium pyrophosphate/HCl, pH 8.8 or 20 mM potassium phosphate, pH 7.0 and dialyzed against the same buffer at 4°C for 24 h. The enzyme concentration was determined spectrophotometrically ($\varepsilon_{280\,nm} = 3.53 \times 10^4\ M^{-1}\ cm^{-1}$) [10]. The content of active sites was determined via a titration with NADH in the presence of 0.1 M isobutyramide [23] and amounted to about 95%. NAD^+ and NADH (both grade II) were purchased from Boehringer. AOT [sodium-bis(2-ethylhexyl)sulfosuccinate] was from Janssen Chimica and was purified according to the method of Menger and Yamada [24]. CTAB (cetyltrimethylammonium bromide; Serva) was used without further purification. Both surfactants were desiccated over P_2O_5. *p*-Terphenyl (scintillation grade) was obtained from BDH and was dissolved in ethanol (Merck, fluorescent grade). Isooctane (Uvasol, for fluorometry) and hexanol (P.A.) were from Merck.

Preparation of reversed micellar solutions

Stock reversed micellar solutions were 0.24 M AOT in isooctane and 0.24 M CTAB in a 12% hexanol/isooctane (v/v) mixture. To these solutions were added: concentrated protein (80 μM), or NAD^+ (60 mM) solutions, buffer and isooctane until the desired water and surfactant concentrations were reached. An important parameter for reversed micellar solutions is the molar ratio of water to surfactant, which we will denote as w_o. The final surfactant concentration was always 0.2 M, the protein concentration was 40 nM for the activity determinations and 1.3 μM for the spectroscopic measurements. All concentrations are given with respect to the total volume.

Activity measurements

Activity measurements were performed under saturating conditions for both substrate and cofactor. Oxidation of hexanol was performed with the enzyme dissolved in sodium pyrophosphate/HCl buffer, pH 8.8. The NAD^+ concentration was 0.5 mM ($K_{m,NAD^+} = 10.0$ μM in aqueous solution and ≈ 50 μM in AOT-reversed micelles [18]). The substrate concentration was 2 mM in aqueous solution and in AOT-reversed micelles ($K_{m,hexanol} = 0.4$ mM in water and ≈ 0.1 mM in AOT-reversed micelles [18]). Both for aqueous and AOT solutions 2.9 ml of sample, containing protein and cofactor, was prepared. The reaction was started by addition of 100 μl of a 60 mM solution of hexanol in buffer or in isooctane. In the CTAB system the substrate is also cosurfactant. In the case of CTAB two reversed micellar solutions were prepared, one containing protein, the other one NAD^+. The reaction was started by mixing equal amounts of these solutions. Initial reaction rates were determined by monitoring the absorbance changes at 340 nm. An absorption coefficient of 6.22 $mM^{-1}\ cm^{-1}$ was used to determine NADH concentration in both aqueous and hydrocarbon solutions. All experiments were carried out at 25°C.

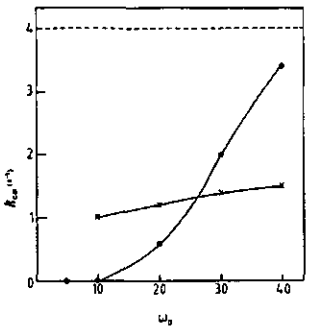

Fig. 1. *Turnover number of horse liver alcohol dehydrogenase with hexanol as substrate in AOT (–·–·–) and CTAB (–×–×–) reversed micellar solutions as a function of* w_o *at 25°C.* Buffer used is sodium pyrophosphate/HCl pH 8.8. Also shown is the activity of the dehydrogenase in aqueous pH 8.8 solution with hexanol as substrate (– – – –)

Spectroscopic measurements

Fluorescence emission spectra were recorded on an Aminco SPF-500 spectrofluorimeter. Slit widths were 4 nm.

Circular dichroism was measured with a Jobin Yvon Mark V Autodichrograph. Data were collected with a Silex microcomputer. Cuvets with 0.5 mm path length were used.

The experimental set up for the time-resolved fluorescence measurements has been described in previous publications [16, 25]. The excitation wavelength was 300 nm and the emission was selected with a 337-nm (10-nm bandpass) interference filter. Polarized fluorescence decay data were collected in two subgroups (1024 channels each) of the multichannel analyzer and transferred afterwards to a MicroVax II computer.

Analysis was performed with the reference convolution method, published before [16]. The reference compound was *p*-terphenyl dissolved in ethanol. For this compound fluorescence lifetimes of 1.064 ± 0.005 ns at 20°C and 1.057 ± 0.005 ns at 30°C have been reported [16]. In the analysis of the data presented here, a reference lifetimes, τ_r, of 1.06 ns was fixed. All experiments were carried out at 25°C and were duplicated.

RESULTS AND DISCUSSION

Enzymatic activity

The enzymatic activity of LADH, which was measured under saturating conditions for both hexanol and NAD^+, will

Table 1. *Fluorescence and anisotropy decay parameters of LADH at 25°C*

pH	α_1	τ_1	α_2	τ_2	$\bar{\tau}^a$	β	ϕ
		ns		ns			ns
8.8	0.69 ± 0.01	3.33 ± 0.05	0.31 ± 0.02	6.30 ± 0.03	4.25	0.25 ± 0.01	33.7 ± 0.8
7.0	0.70 ± 0.01	3.53 ± 0.04	0.30 ± 0.01	6.26 ± 0.05	4.36	0.24 ± 0.01	34.2 ± 0.8

[a] $\bar{\tau} = \sum_i \alpha_i \tau_i$.

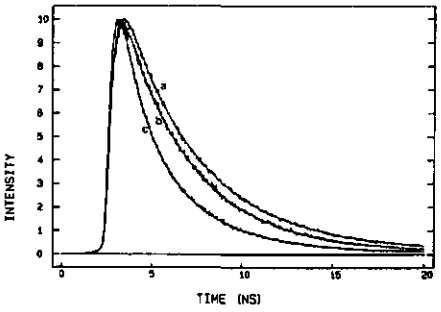

Fig. 2. *Fluorescence decay curves of horse liver alcohol dehydrogenase at 25°C in (a) aqueous solution, pH 8.8; (b) AOT-reversed micellar solution.* w_o *= 20, pH 8.8 and (c) AOT-reversed micellar solution* w_o *= 20, pH 7.0.* Excitation and emission wavelengths were 300 nm and 337 nm respectively. Time equivalence per channel was 0.030813 ns. The curve obtained for LADH in aqueous solution pH 7.0 (not shown) is almost identical to curve a. The fluorescence decay parameters are listed in Table 1 (curve a) and in Table 2 (curves b and c). Intensity is in arbitrary units

be presented here in terms of the turnover number; k_{cat}, which is the number of moles of NAD^+ reduced (mole enzyme)$^{-1}$ (second)$^{-1}$. For LADH in pH-8.8 buffer we have found k_{cat} = 4.0 s^{-1}. This value is substantially lower than the one reported by Martinek et al. [18] who found k_{cat} = 10 s^{-1} with hexanol as substrate. However, Boehringer reports a specific activity of LADH with ethanol of 2.7 U/mg, which corresponds to k_{cat} = 3.6 s^{-1}. In their article Martinek et al. show that there is almost no dependence of k_{cat} on an increasing chain length of the substrate when normal aliphatic alcohols are used from ethanol up to octanol, so we may conclude that the value we found is close to the Boehringer specifications.

The results, obtained in AOT and in CTAB-reversed micellar systems are shown in Fig. 1. In AOT micelles at w_o = 5 and at w_o = 10 no catalytic activity can be detected. At higher water contents there is activity, which increases monotonically with increasing w_o and at w_o = 40, k_{cat} is only slightly lower than in aqueous buffer solution. These results are in very good aggreement with the ones published by Martinek et al. [18]. The decreased activity at low w_o can be ascribed to changes in the microenvironment of the enzyme, like pH, ionic strength and H-bonding changes. In CTAB micelles there is enzymatic activity at the lowest water content studied (w_o = 10). This activity is strongly reduced in comparison to the aqueous LADH solution. With increasing w_o the activity slightly increases, but even at the highest water content (w_o = 40) there is still a large difference with the aqueous k_{cat} value. In a recent publication by the group of Biellmann [19], activity measurements of LADH in SDS and in CTAB-reversed micellar systems are presented. The CTAB system used in the latter work is quite different from ours. The buffer was 50 mM Tes pH 7.5, the organic solvent was cyclohexane and most results were obtained with 1-butanol as cosurfactant/substrate. However, the trend in the reported V_{max} values as a function of w_o is the same as found by us. V_{max} is considerably lower than in water and it is only slightly dependent on the water content of the system. The authors argue that the decreased activity is caused by a distorted binding of the coenzyme affecting its dissociation constant.

Fluorescence properties of LADH in aqueous solutions

The steady-state tryptophan fluorescence upon 300-nm excitation in aqueous solution is the same at pH 8.8 and at pH 7.0. The emission spectrum has a single peak with its maximum at 330 nm. Time-resolved fluorescence properties of LADH in aqueous solution, measured at 344 nm upon 300-nm laser excitation, have been presented in a previous publication [16]. The fluorescence decay can be described by a sum of two exponentials $\{\alpha_1 \exp(-t/\tau_1) + \alpha_2 \exp(-t/\tau_2)$, with α_i the preexponential factors and τ_i the fluorescence lifetimes). In this work the emission wavelength was 337 nm (337 nm was used instead of 344 nm because this is closer to the emission maximum of the protein fluorescence and thus more fluorescence intensity is obtained) and therefore the decay parameters differ slightly from the ones reported in [16]. The results from the analysis are presented in Table 1. The results obtained at pH 8.8 and at pH 7.0 differ only very little. The two lifetimes are believed to be independent, where the short one is due to Trp-314 and the long one to Trp-15 emission [12, 14]. In a recent paper by Demmer et al. [15] this simple model is opposed. Based on quenching experiments with potassium iodide the authors state that the fluorescence decay must be described by a sum of at least three exponentials. In the latter model a single lifetime of about 4 ns is assigned to Trp-314 and the two other ones ($\approx$ 1.7 ns and $\approx$ 6.5 ns) to Trp-15. The double exponential decay of Trp-15 is explained by conformational heterogeneity of this solvent-exposed residue. Fitting of our data with a sum of three exponentials is also possible and yields results which are quite comparable to the ones of Demmer et al. [15] but the quality of the fits as judged from the reduced χ^2 value, the Durbin Watson parameter, the plot of the weighted residuals and the autocorrelation function of the weighted residuals [26] does not improve upon introduction of the third exponential and therefore we will restrict ourselves to the double-exponential model.

The anisotropy decay of LADH has been reported to be dependent on the excitation and the emission wavelengths because of the non-spherical shape of the protein and the fluorescence originating from two different electronic tran-

Table 2. *Fluorescence decay parameters of LADH in AOT-reversed micelles at 25°C*

pH	w_o	α_1	τ_1	α_2	τ_2	α_3	τ_3	$\bar{\tau}^*$
			ns		ns		ns	
8.8	5	0.41 ± 0.01	3.2 ± 0.3	0.19 ± 0.03	5.7 ± 0.2	0.40 ± 0.03	0.11 ± 0.02	2.4
	10	0.39 ± 0.01	3.2 ± 0.2	0.16 ± 0.02	5.7 ± 0.2	0.45 ± 0.02	0.12 ± 0.01	2.2
	20	0.38 ± 0.01	3.1 ± 0.2	0.15 ± 0.02	5.7 ± 0.2	0.47 ± 0.03	0.07 ± 0.02	2.1
	30	0.38 ± 0.01	3.1 ± 0.3	0.14 ± 0.03	5.7 ± 0.3	0.48 ± 0.04	0.04 ± 0.01	2.0
	40	0.38 ± 0.01	3.1 ± 0.2	0.14 ± 0.03	5.7 ± 0.2	0.48 ± 0.04	0.04 ± 0.02	2.0
7.0	5	0.41 ± 0.01	2.2 ± 0.1	0.29 ± 0.02	4.9 ± 0.2	0.30 ± 0.01	0.21 ± 0.03	2.4
	10	0.45 ± 0.01	2.1 ± 0.1	0.26 ± 0.01	4.7 ± 0.1	0.29 ± 0.01	0.35 ± 0.03	2.3
	20	0.47 ± 0.01	2.1 ± 0.1	0.20 ± 0.03	4.7 ± 0.1	0.33 ± 0.02	0.40 ± 0.03	2.0
	30	0.47 ± 0.01	2.1 ± 0.1	0.20 ± 0.03	4.7 ± 0.1	0.33 ± 0.02	0.41 ± 0.03	2.0
	40	0.47 ± 0.02	2.1 ± 0.1	0.20 ± 0.02	4.7 ± 0.2	0.33 ± 0.01	0.42 ± 0.05	2.0

* See Table 1 for definition.

sitions (^1L_a and ^1L_b) [16]. An influence of the non-spherical protein shape on the rotational dynamics of LADH was also observed by Beechem et al. [13] via multiple dye fluorescence anisotropy experiments. The observed anisotropy decays can be fitted with a single-exponential function [$\beta \exp(-t/\phi)$, with β the preexponential factor and ϕ the rotational correlation time]. Parameters are listed in Table 1. Again the results at the two different pH values are almost identical.

Spectroscopic properties of LADH in reversed micellar solutions

The far-ultraviolet (190–250 nm) circular dichroic spectrum of LADH does not change significantly upon changing the pH of the aqueous solution from 8.8 to 7.0, indicating, that the overall protein structure is nearly identical at both pH values. This agrees well with our observation that the time-resolved fluorescence properties hardly change at varying pH. CD spectra obtained in reversed micellar solutions are, within the experimental error (which is about 10% for these solutions), identical to the ones in the aqueous solutions. Therefore we conclude that no significant changes of the overall protein conformation occur upon incorporation of LADH into the reversed micelles. A similar observation was made by Meier and Luisi [17], who have measured circular dichroism of LADH in pH 8.8 buffer and in AOT-reversed micelles.

Analysis of the fluorescence decays of LADH in AOT-reversed micelles reveals complex decay patterns. Three fluorescence lifetimes are needed to describe the observed decays satisfactorily. Typical examples are shown in Fig. 2. The parameters for the unconstrained fits of the data are presented in Table 2.

First the results, obtained at pH 8.8 will be discussed. At this pH the values of τ_1 and τ_2 are quite close to each other. It has been noted by O'Connor et al. [27] that recovery of decay parameters is not always straightfoward when the decay times do not differ by more than a factor of 2. Acceptable fits are also obtained when τ_1 is fixed at a value of 3.33 ns, which is also found in the aqueous solution. It is tempting to conclude that the fluorescence from the buried tryptophan residue (Trp-314) does not change upon incorporation in the reversed micelles but, if this were so, the preexponential factor α_1 should also be of the same order of magnitude as in the aqueous solution, which is not observed. Therefore we believe that the best explanation of the observations is that both

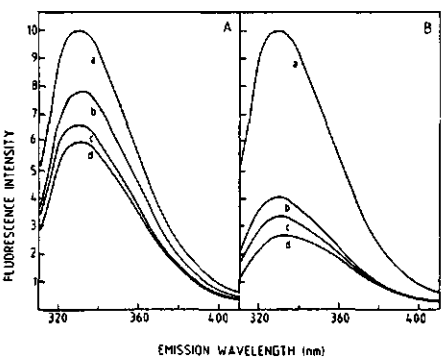

Fig. 3. *Uncorrected fluorescence emission spectra of horse liver alcohol dehydrogenase upon 300-nm excitation at pH 8.8 (A) and at pH 7.0 (B) (25°C).* Curve a is the spectrum obtained of LADH in aqueous solution; curves b, c and d are obtained in AOT-reversed micellar water pools at w_o = 5, w_o = 10 and w_o = 40 respectively

tryptophan residues have a contribution to the third lifetime. For Trp-15 this can be due to a solvent effect because this residue is exposed but for Trp-314 it is more likely that a change in the conformation of the protein in its neighbourhood causes the alterations. This conformational change can only be a subtle one because it was not observed via the circular dichroism of the protein. Circular dichroism of the aromatic residues of the protein might yield more information about the changes in the neighbourhood of the tryptophans but even at the highest possible protein concentration in the reversed micellar systems we were not able to detect any signal in this spectral region. The fluorescence lifetimes are only very slightly dependent on the water content. So the interactions between the protein and the micelles, which cause the change of the fluorescence lifetimes, are not very much dependent on the water pool size.

The same conclusion can be reached when the emission spectra are considered (Fig. 3A). Upon incorporation into AOT micelles the emission is quenched and with increasing w_o this effect gets stronger. We do not find a shift of the emission maximum in the spectra. These observations contradict with the ones reported by Meier and Luisi [17] who found

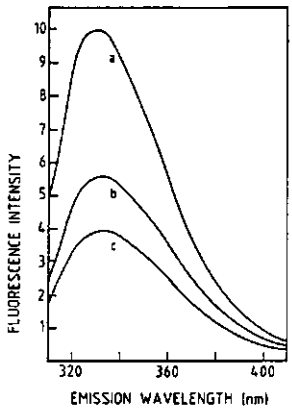

Fig. 4. *Uncorrected fluorescence emission spectra of horse liver alcohol dehydrogenase in aqueous AOT solutions (pH 7.0) at 25°C.* Excitation wavelength was 300 nm. Curve a corresponds to the spectrum obtained at [AOT] = 0 and 0.1 mM. Curve b is measured at 0.5 mM AOT and curve c is the spectrum at 1.0 mM, 2.0 mM and 5.0 mM AOT

a blue shift of the emission maximum and a quenching which is stronger at w_o = 19 than at w_o = 42. The reason for this discrepancy is not clear.

When the protein is dissolved in pH-7.0 buffer the overall charge will be more positive than at pH 8.8 and thus stronger interactions are expected with negatively charged AOT interfaces. At pH 7.0 it is not possible to obtain good fits of the observed fluorescence decays with τ_1 fixed at the value found in aqueous solution; therefore it is obvious that both tryptophan residues are affected. The differences between the fluorescence properties in aqueous solution and in reversed micelles are indeed more pronounced at pH 7.0 than at pH 8.8. This is also observed via the emission spectra, which are shown in Fig. 3B. In addition to the quenching of the fluorescence a red shift of the emission maximum, which varies from 2 nm at w_o = 5 to 8 nm at w_o = 40, is found at pH 7.0.

A good explanation for the unexpected increasing changes of the fluorescence of LADH in reversed-AOT micelles with increasing w_o cannot be given at this moment. The changes of the fluorescence properties are apparently not correlated to the enzymatic activity, because k_{cat} is most close to the value in aqueous solution at w_o = 40.

Emission spectra were also measured of LADH in aqueous surfactant solutions at different surfactant concentrations. The spectra obtained in AOT solutions at pH 7.0 are shown in Fig. 4. At an AOT concentration of 0.1 mM the spectrum is identical to the one in normal aqueous solution. At 0.5 mM AOT the emission is quenched and the maximum is shifted about 4 nm to the red. The spectra obtained at 1.0, 2.0 and 5.0 mM AOT are identical. The red shift is the same as at 0.5 mM but the quenching is stronger. This stepwise change of the emission spectrum is an indication that also in aqueous AOT solutions LADH interacts with surfactant aggregates. The changes take place when the surfactant concentration is raised above the critical micellar concentration. At pH 8.8 similar observations were made.

In CTAB-reversed micelles the results of the fluorescence decay experiments (Table 3) are easier to interpret. Three exponentials are also needed to fit the data but the values of α_1 and τ_1 are almost identical throughout the whole w_o range to the ones in aqueous solution. This is found both at pH 8.8 and at pH 7.0. Examples of decay curves are shown in Fig. 5. The tabulated values are obtained from unconstrained fits of the data. It can be concluded that the fluorescence of Trp-314 is not affected in this case and that the third fluorescence lifetime is due to Trp-15 emission only (probably caused by conformational heterogeneity). The fact that there are almost no differences in the properties of the protein at the two different pH values is an indication that electrostatic interactions between LADH and the CTAB interface are much less pronounced than with AOT.

Both at pH 8.8 and at pH 7.0 the steady-state fluorescence of the protein is quenched upon incorporation in the CTAB-reversed micelles. At low w_o the quenching is stronger than at high w_o. The maximum of the fluorescence is at the same wavelength as in the aqueous solution. In aqueous CTAB solution no effect on the LADH fluorescence can be observed up to surfactant concentrations of 5 mM. This is different from the case of AOT where comparable effects are found in aqueous and in hydrocarbon micellar solutions, indicating that the changes in the fluorescence properties in the CTAB-reversed micellar system are not due to direct interactions between the protein and the sufactant. Some properties of the water pools like the high local bromide concentration may cause the quenching of the fluorescence in the reversed micelles.

Rotational dynamics of LADH in reversed micellar solutions

The rotational dynamics of LADH, as measured via the fluorescence anisotropy decay, change markedly upon incorporation of the protein in reversed micellar media, especially when AOT is the surfactant. The anisotropy decay parameters, obtained in AOT micelles at pH 8.8 and at pH 7.0 are given in Table 4. In most cases, the observed decays must be described by a sum of two exponentials. A typical example of a double exponential anisotropy decay is shown in Fig. 6. The same phenomenon was observed with fluorescent cytochrome *c* derivatives, incorporated in AOT or in CTAB-reversed micelles [8]. With LADH, the appearance of the second (fast) component in the decay can be explained by a rapid internal motion of a tryptophan residue, superimposed on the overall rotation of the protein. When this component is due to motion of only one of the tryptophans, a model must be used to fit the data, in which the fluorescence of the other tryptophan residue is not coupled to this fast component [16]. With the application of such a model it should in principle be possible to determine which tryptophan is involved in this fast motion. However, it was not possible to distinguish between the different possibilities of coupling fluorescent lifetimes with rotational correlation times. The reason for this is that the relative contribution of the fast component to the total anisotropy decay is only very small.

At pH 8.8 the fast component is only observed at $w_o < 30$. From w_o = 5 up to w_o = 20 the preexponential factor, β_1, associated with the fast component, decreases and the concomitant rotational correlation time gets shorter. At pH 7.0 a double exponential decay is observed up to the highest w_o value studied (w_o = 40). The value of the rotational correlation time at pH 7.0 also decreases with increasing w_o but the preexponential factor, β_1, is less dependent on w_o than

Table 3. *Fluorescence decay parameters of LADH in CTAB-reversed micelles at 25°C*

pH	w_o	α_1	τ_1	α_2	τ_2	α_3	τ_3	$\bar{\tau}^a$
			ns		ns		ns	
8.8	10	0.75 ± 0.06	3.5 ± 0.2	0.14 ± 0.08	5.2 ± 0.5	0.11 ± 0.04	0.07 ± 0.04	3.3
	20	0.71 ± 0.03	3.6 ± 0.3	0.19 ± 0.06	5.0 ± 0.4	0.10 ± 0.04	0.05 ± 0.03	3.5
	30	0.70 ± 0.05	3.6 ± 0.2	0.21 ± 0.05	5.2 ± 0.5	0.09 ± 0.04	0.05 ± 0.02	3.6
	40	0.69 ± 0.05	3.7 ± 0.4	0.20 ± 0.05	5.4 ± 0.5	0.11 ± 0.03	0.06 ± 0.03	3.6
7.0	10	0.72 ± 0.07	3.5 ± 0.1	0.13 ± 0.07	5.3 ± 0.4	0.15 ± 0.04	0.09 ± 0.03	3.3
	20	0.74 ± 0.07	3.5 ± 0.1	0.16 ± 0.07	5.2 ± 0.4	0.10 ± 0.03	0.09 ± 0.03	3.5
	30	0.73 ± 0.08	3.5 ± 0.1	0.17 ± 0.08	5.2 ± 0.4	0.10 ± 0.03	0.09 ± 0.04	3.5
	40	0.74 ± 0.08	3.6 ± 0.1	0.17 ± 0.08	5.3 ± 0.4	0.09 ± 0.03	0.09 ± 0.04	3.6

[a] See Table 1 for definition.

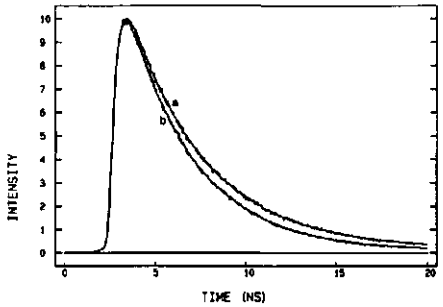

Fig. 5. *Fluorescence decay curves of horse liver alcohol dehydrogenase at 25°C in (a) aqueous solution pH 8.8 and (b) CTAB-reversed micellar solution* $w_o = 20$, *pH 8.8.* Experimental conditions were identical to the ones described in the legend of Fig. 2. The curves, obtained at pH 7.0 are not shown because they are almost identical to the ones shown here. Decay parameters are given in Table 1 (curve a) and in Table 3 (curve b)

Table 4. *Fluorescence anisotropy decay parameters of LADH in AOT-reversed micelles at 25°C*

pH	w_o	β_1	ϕ_1	β_2	ϕ_2
			ns		ns
8.8	5	0.05 ± 0.01	1.3 ± 0.5	0.200 ± 0.003	190 ± 47
	10	0.04 ± 0.01	0.9 ± 0.2	0.204 ± 0.002	132 ± 33
	20	0.02 ± 0.01	0.6 ± 0.2	0.220 ± 0.003	90 ± 21
	30	–	–	0.239 ± 0.001	58 ± 4
	40	–	–	0.241 ± 0.001	35 ± 2
7.0	5	0.05 ± 0.01	1.7 ± 0.6	0.222 ± 0.002	203 ± 64
	10	0.04 ± 0.01	1.1 ± 0.3	0.216 ± 0.003	201 ± 44
	20	0.04 ± 0.01	1.2 ± 0.4	0.207 ± 0.004	115 ± 19
	30	0.04 ± 0.01	0.9 ± 0.5	0.205 ± 0.003	71 ± 12
	40	0.04 ± 0.01	0.9 ± 0.3	0.204 ± 0.003	62 ± 10

at pH 8.8. The shortening of the rotational correlation time with increasing water pool size can be due to a decreasing viscosity in the neighbourhood of the protein, which is expected when the micelles grow.

The slow decaying component of the anisotropy represents the overall rotation of the protein, which is determined by the motion of the protein within the micelle and the motion of

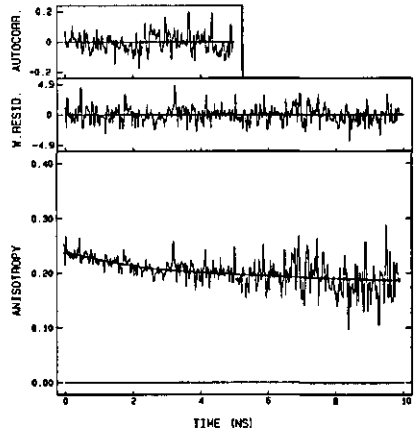

Fig. 6. *Fluorescence anisotropy decay of horse liver alcohol dehydrogenase in AOT-reversed micellar water pools,* $w_o \approx 20$, *pH 7.0 at 25°C.* Shown are the first 10 ns of the decay. Experimental conditions were the same as in Fig. 2. The decay is fitted with a double-exponential function. The quality of the fit is indicated by the weighted residuals and the autocorrelation of these residuals, shown in the upper pannels of the plot. The anisotropy parameters are listed in Table 4

the micelle in the organic solvent. Assuming that these motions are independent, the observed rotational correlation time, ϕ_2, is composed of ϕ_{int} (describing internal motion within the micelle) and ϕ_{mic} (describing overall micellar rotation) as follows (cf. [8, 28]):

$$\frac{1}{\phi_2} = \frac{1}{\phi_{int}} + \frac{1}{\phi_{mic}}. \quad (1)$$

Especially at low w_o values, where the observed rotational correlation times are long, the error in the reported ϕ_2 values is very large. The reason for this is that, on the time scale of the fluorescence experiment (≈ 20 ns), there is almost no decay of the anisotropy (Fig. 6). When the rotational correlation times get shorter the accuracy of the parameters improves.

At both pH values in AOT-reversed micelles the trend is that ϕ_2 decreases monotonically when the size of the water pools increases. Because it is not likely that ϕ_{mic} decreases with increasing w_o, the latter observation must be related to

Table 5. *Core radii (r_c) and rotational correlation times (ϕ) of AOT and CTAB-reversed micelles at 25°C*

w_o	AOT		CTAB	
	r_c	ϕ	r_c	ϕ
	nm	ns	nm	ns
5	1.2	7	–	–
10	1.7	12	1.9	41
20	3.4	47	3.1	85
30	4.3	80	4.1	140
40	5.5	145	5.2	223

Table 6. *Fluorescence anisotropy decay parameters of LADH in CTAB-reversed micelles at 25°C*

pH	w_o	β	ϕ
			ns
8.8	10	0.230 ± 0.002	135 ± 21
	20	0.231 ± 0.002	111 ± 21
	30	0.233 ± 0.002	105 ± 15
	40	0.229 ± 0.001	73 ± 8
7.0	10	0.228 ± 0.002	123 ± 19
	20	0.229 ± 0.002	86 ± 9
	30	0.229 ± 0.001	77 ± 7
	40	0.227 ± 0.001	67 ± 6

an increased mobility of the protein within the micelles. At pH 8.8 the observed rotational correlation times are shorter than at pH 7.0. Sizes and rotational correlation times of empty AOT- and CTAB-reversed micelles as earlier determined with time-resolved luminescence quenching [8] are presented in Table 5. Since the LADH molecule can be considered as a prolate ellipsoid with long and short semiaxes of 11 nm and 6 nm respectively, we may conclude that only at $w_o = 40$ is the water pool of an empty AOT micelle large enough to accomodate the protein. This means that up to $w_o = 30$ the micelles have to grow to be able to solubilize a protein molecule. When the protein is totally immobilized in the micelle ($1/\phi_{int} = 0$) the size of the micelle can be calculated from ϕ_2 [8]. The diameter of the water pool at $w_o = 5$, pH = 8.8 is then about 12 nm, which is close to the largest dimension of the LADH molecule (11 nm). The decreasing rotational correlation times at higher w_o can then only be explained if the micelles are larger than expected and if there is some internal mobility of the protein in the water pool. At $w_o = 40$ a rotational correlation time of 145 ns is calculated for the empty AOT micelles. Substituting this value for ϕ_{mic} in Eqn (1), values of 46 ns and 108 ns can be calculated for ϕ_{int} at pH 8.8 and at pH 7.0, respectively. These numbers are only valid when the size of the micelle does not increase upon incorporation of a protein molecule but, even if there is a considerable expansion of the micelle, the internal mobility of the protein is markedly higher at pH 8.8 than at pH 7.0. Such a result strongly suggests that at pH 7.0 the interactions between the protein and the AOT interface are much more important than at pH 8.8, providing evidence for an electrostatic nature of these interactions. It is noteworthy that the activity of the enzyme follows the same tendency as observed for the rotational dynamics in AOT-reversed micelles.

In CTAB-reversed micelles, single-exponential anisotropy decays are found at both pH values (decay parameters listed in Table 6). As with AOT as surfactant, the rotational correlation times, which represent the overall rotational dynamics of the protein, decrease monotonically with increasing w_o. The observed rotational correlation times in the CTAB-reversed micelles are somewhat longer at pH 8.8 than at pH 7.0 (especially at $w_o = 20$ and at $w_o = 30$). So it seems that in the cationic micelles also (local) electrostatic interactions play a role and that at pH 8.8 the protein is more associated with the interface than at pH 7.0. This effect was not observed with the fluorescence lifetime measurements.

The rotational correlation times in the CTAB-reversed micelles at $w_o = 10$ of 135 ns and 123 ns at pH 8.8 and at pH 7.0, respectively, can not be explained by the existence of a spherical reversed micelle with a core diameter of 11 nm (being the largest dimension of the LADH molecule) and the protein totally immobilized in it because in that case a rotational correlation time, ϕ, of about 250 ns would be expected [8]. Internal mobility of the protein within the micelle or a non-spherical micelle shape could explain the observed rotational correlation times. The present experiments do not allow us to distinguish between these two possibilities. For empty CTAB-reversed micelles at $w_o = 40$ we have calculated a rotational correlation time of 223 ns (Table 5). When this value is substituted in Eqn (1) for ϕ_{mic} we can calculate ϕ_{int} for the protein in CTAB-reversed micelles. At pH 8.8 a value of 109 ns is found and at pH 7.0 $\phi_{int} = 96$ ns. These values, which are valid when the micelles do not expand upon protein incorporation, are similar, in contrast to those determined in AOT micelles. So at least at $w_o = 40$ the electrostatic interactions are less important in CTAB than in AOT. The observed effects in the reversed micellar media agree well with what could be expected, based on charge effects of the protein and the surfactant interface.

CONCLUDING REMARKS

The interactions between LADH in reversed micellar systems and surfactant interfaces are largely electrostatic in nature. This can be concluded from the fact that a change of pH from 8.8 to 7.0 causes differences in the structural and dynamic properties of the protein molecule especially in AOT-reversed micellar water pools.

The overall structure of LADH is only very little affected upon incorporation in the reversed micellar systems. The circular dichroism of the protein backbone hardly changes in the reversed micelles. On the other hand, the time-resolved fluorescence properties are markedly different in aqueous solution and in reversed micellar solutions. This means that the fluorescent lifetimes especially are mainly dependent on local changes in the environment of the tryptophan residues in the protein and do not report on the overall properties of the protein molecule.

With increasing w_o, both the activity and the rotational mobility of LADH in reversed micellar water pools increase. In AOT solutions the differences between low and high w_o are larger than in CTAB solutions.

Part of this work was supported by the Netherlands Foundation of Chemical Research (S.O.N.) with financial aid from the Netherlands Organization for the Advancement of Pure Research (Z.W.O.).

REFERENCES

1. Fendler, J. H. (1982) *Membrane-mimetic chemistry*, Wiley-Interscience, New York.

2. Luisi, P. L. (1985) *Angew. Chem. (Int. Ed.) 24*, 439–460.
3. Luisi, P. L. & Laane, C. (1986) *Trends Biotech. 4*, 153–161.
4. Luisi, P. L. & Magid, L. J. (1986) *CRC Crit. Rev. Biochem. 20*, 409–474.
5. Martinek, K., Levashov, A. V., Klyachko, N., Khmelnitski, Y. L. & Berezin, I. V. (1986) *Eur. J. Biochem. 155*, 453–468.
6. Waks, M. (1986) *Proteins: Structure, Function and Gentics 1*, 4–15.
7. Vos, K., Laane, C. & Visser, A. J. W. G. (1987) *Photochem. Photobiol. 45*, 863–878.
8. Vos, K., Laane, C., Weijers, S. R., van Hoek, A., Veeger, C. & Visser, A. J. W. G. (1987) *Eur. J. Biochem. 169*, 259–268.
9. Vos, K., Lavalette, D. & Visser, A. J. W. G. (1987) *Eur. J. Biochem. 169*, 269–273.
10. Sund, H. & Theorell, H. (1963) in *The enzymes* (Boyer, P. D., ed.) 2nd edn, vol. 7, pp. 25–57, Academic Press, New York.
11. Brändén, C.-I., Jörnvall, H., Eklund, H. & Furugren, B. (1975) in *The enzymes* (Boyer, P. D., ed.) 3rd edn, vol. 11, pp. 103–190, Academic Press, New York.
12. Ross, J. B. A., Schmidt, C. J. & Brand, L. (1981) *Biochemistry 20*, 4369–4377.
13. Beechem, J. M., Knutson, J. R. & Brand, L. (1986) *Biochem. Soc. Trans. 14*, 832–835.
14. Eftink, M. R. & Hagaman, K. A. (1986) *Biochemistry 25*, 6631–6637.
15. Demmer, D. R., James, D. R., Steer, R. P. & Verrall, R. E. (1987) *Photochem. Photobiol. 45*, 39–48.
16. Vos, K., van Hoek, A. & Visser, A. J. W. G. (1987) *Eur. J. Biochem. 165*, 55–63.
17. Meier, P. & Luisi, P. L. (1980) *J. Solid-Phase Biochem. 5*, 269–282.
18. Martinek, K., Khmelnitski, Y. L., Levashov, A. V. & Berezin, I. V. (1982) *Dokl. Akad. Nauk SSSR 263*, 737–741.
19. Samama, J. P., Lee, K. M. & Biellmann, J. F. (1987) *Eur. J. Biochem. 163*, 609–617.
20. Rigler, R. & Ehrenberg, M. (1973) *Q. Rev. Biophys. 2*, 139–199.
21. Cundall, R. B. & Dale, R. E. (eds) (1983) *Time-resolved fluorescence spectroscopy in biochemistry and biology*, Plenum Press, New York.
22. Beechem, J. M. & Brand, L. (1985) *Annu. Rev. Biochem. 54*, 43–71.
23. Theorell, H. & Tatemoto, K. (1971) *Arch. Biochem. Biophys. 142*, 69–82.
24. Menger, F. M. & Yamada, K. (1979) *J. Am. Chem. Soc. 101*, 6731–6734.
25. Van Hoek, A., Vervoort, J. & Visser, A. J. W. G. (1983) *J. Biochem. Biophys. Methods 7*, 243–254.
26. O'Connor, D. V. & Phillips, D. (1984) *Time-correlated single-photon counting*, Academic Press, London.
27. O'Connor, D. V., Ware, W. R. & Andre, J. C. (1979) *J. Phys. Chem. 83*, 1333–1343.
28. Keh, E. & Valeur, B. (1981) *J. Colloid Interface Sci. 79*, 465–478.

7 SUMMARIZING DISCUSSION

In this thesis a number of spectroscopic studies on reversed micellar systems has been presented. From these studies much information about the physical properties of these systems can be obtained. Parameters like for instance the size, viscosity and polarity of the water pools or the dynamics of water pool exchange have been accessed using different techniques, like scattering, magnetic resonance and not in the last place optical spectroscopy. In Chapter 2 of this thesis an overview of spectroscopic studies of reversed micellar systems is presented.

The main part of this thesis deals with the characterization of protein-containing reversed micellar systems. In order to put the results of such studies into the right context one must have detailed knowledge of the properties of the host system. A very important parameter is the size of the reversed micellar water pool. When the volume of the water pool is initially orders of magnitude larger than the volume of the protein molecule, it may be expected, that the incorporation of the protein has little effect on the micelles. On the other hand, when the volume of the water pool has about the same size or is even smaller than that of the protein a considerable redistribution of water and surfactant molecules over the system can occur, leaving a system with two different kinds of micelles: the empty ones and the protein containing ones. A study about hydrodynamic radii of protein containing reversed micelles has recently been published by the group of Waks [1]. The radii are measured by fluorescence recovery after fringe photobleaching. The results indicate, that the radius of AOT micelles at w_o=5.6 considerably increases after uptake of the myelin basic protein, whereas at w_o=22.4 the protein-filled and the empty micelles have similar radii.

We have used two different micellar systems. The first one consisted of an anionic surfactant (i.e. AOT), the second one contained a cationic surfactant (CTAB) and also a cosurfactant (i.e. n-hexanol). The cosurfactant in the second system had to be used to obtain thermodynamically stable solutions. For these reversed micelles we have measured the water pool sizes as a function of the molar water to surfactant ratio, w_o, using the time-resolved fluorescence quenching technique, introduced by Atik and Thomas [2]. In the w_o range from 5 to 50, the radii of the water pools vary from about 1 nm to about 6.5 nm for both micellar systems. This means, that ini-

tially the size of the water droplets is in the same range as the size of the incorporated protein molecules. Therefore introduction of protein molecules in the reversed micelles is likely to have a considerable impact on the properties of these systems.

A totally different situation arises when small molecules, e.g. fluorescent probes, are introduced in the micelles. In this case the system will only be slightly perturbed by the presence of the probes. Recently two publications of our group, describing such studies have appeared [3,4].

In the first one [3], spectral and time-resolved fluorescence properties of an amphiphilic flavin, dispersed in AOT reversed micelles are presented. The aim of this study was to investigate the dynamic properties of the interface of AOT reversed micelles. The results suggest, that the flavin occupies a position within the surfactant boundary layer. This could be expected because of the amphiphilic nature of the probe. Furthermore the fluorescence anisotropy of the flavin indicates, that the flexibility within the interface enhances when the size of the water droplets becomes larger.

The other paper [4] reports on time-resolved fluorescence experiments conducted on (octadecyl) rhodamine B, incorporated in AOT micelles. In this case a system in which glycerol was entrapped instead of water was also studied. From comparison of the properties of the dye molecules in micellar media with those of the dye in homogeneous solution a qualitative estimate of the polarity of the probe environment in the micellar interior could be inferred. In addition, fluorescence anisotropy studies provide information about the dynamics of this reversed micellar system.

During the last few years, several publications describing studies like the two mentioned above have appeared. A combination of the results presented in these papers provides us with a better insight into the dynamic behaviour of these empty micelles, which can assist in the interpretation of phenomena observed in protein-containing reversed micellar systems.

Effects of proteins in reversed micelles.

The main part of this thesis deals with the effects that incorporation of proteins into reversed micellar media can have on structure and dynamics of both proteins and reversed micelles. The determining factors are the

size, shape and charge distribution of the protein molecules, in addition to properties like the charge of the surfactant and the nature of the entrapped water.

In the Chapters 4 and 5 the behaviour of cytochrome c in AOT and in CTAB reversed micelles is described. This behaviour was studied via the spectroscopic properties of the iron-free and the zinc substituted derivatives of this protein. The far UV circular dichroism and time-resolved fluorescence of both derivatives have been described in Chapter 4. The former technique shows, that the secondary structure of the proteins undergoes changes upon incorporation into the reversed micelles. This is a well known phenomenon and it can easily be explained by the fact, that the protein senses an environment, totally different from bulk water, due to the limited space available and the proximity of the charged surfactant interface. In a study by the group of Pileni [5] it was shown, that in AOT micelles the cytochrome c molecule is located at the micellar interface. From other studies [6,7] it is known, that the redox properties of the native cytochrome c, incorporated in AOT reversed micellar water pools is not too different from the ones in aqueous solution, indicating that the protein conformation near the active site is not drastically changed.

Fluorescence anisotropy experiments provide information about the rotational motion of the fluorophore. For the characterization of protein-containing reversed micellar systems this can be an important parameter. The anisotropy experiments, performed with the cytochrome c derivatives in AOT and CTAB reversed micelles, show some interesting results. In the first place, fluorescence anisotropy decays of the proteins become non-exponential, whereas in aqueous solution exponential decays are observed. The reason for this is believed to be a fast motion of the porphyrin, superimposed on the protein overall rotation. The fact, that this fast motion is only observed in the reversed micellar systems is another indication, that the protein structure changes upon incorporation in the micelles. The second interesting observation is related to the measured overall rotation of the protein. In AOT reversed micelles the overall rotation is retarded in comparison with that in water and this effect is almost independent on the water content of the micellar system unlike the other properties. These results strongly suggest, that the measured overall rotation consists of two components, namely: the component arising from the rotation of the protein within the micellar water pool and the rotation of the whole micelle

in the hydrocarbon solvent. When the water content of the system increases the first component will become faster because of the increasing size of the water pool, but the second component will slow down for the same reason. In the case of porphyrin cytochrome c in AOT micelles these two effects almost compensate and therefore the net effect on the measured rotational motion is almost zero. From size measurements of the micellar water pools with the time-resolved fluorescence quenching technique it is known, that at the highest water content the water droplet is large enough to provide complete rotational freedom of the protein molecule. The retardation of the rotation can then only be explained if there exists a considerable interaction between the protein and the negatively charged surfactant interface even when the water pool is large enough to accomodate the protein molecule. This is in agreement with the fact, that in vivo cytochrome c is bound to negatively charged mitochondrial membranes (cardiolipin). With CTAB as surfactant this effect is not found. In the CTAB micellar system with the highest water content the rotational motion is almost as fast as in water, which means, that in that case there is almost no interaction between the protein and the surfactant interface. Fluorescence anisotropy measurements allowed us to show the presence of charge interactions between protein and surfactant in the AOT system.

Chapter 5 describes the triplet state kinetics of the zinc substituted cytochrome c derivative in micelles in the absence and presence of quenching molecules. The results of this study also indicate, that there is considerable interaction between the protein and AOT interfaces impeding the measurements of intermicellar exchange kinetics. On the other hand, exchange of water pools in the CTAB reversed micellar systems could be demonstrated. It was shown, that the exchange rate depends on the water content of the reversed micelles and on the charge of the exchanged component. At low water content the exchange is faster. This is most likely due to the stronger curvature of the interface in small micelles, giving rise to a greater flexibility of the interface. Furthermore in the CTAB system a component which is negatively charged exchanges less readily than a positively charged quencher. Electrostatic attraction between the negative quenching molecule and the positive surfactant molecules is thought to cause this effect. Irrespective of charge and size considerations it is

found, that the exchange rate of the water pools is about three orders of magnitude lower than the collisional rate of the reversed micelles. Therefore only one out of about every thousand collisions results into exchange of the water pools.

In Chapter 6 studies of a totally different protein (i.e. alcohol dehydrogenase from horse liver, LADH) in the same micellar systems are described. The LADH molecule is about six times larger than the cytochrome c molecule and, in vivo, it has no considerable interactions with membranes like cytochrome c. The fluorescence properties of the two tryptophan residues, which are also described in Chapter 3, are very sensitive to environmental changes. Large effects on these properties are observed upon incorporation of the protein into the reversed micelles. These changes are not caused by significant alterations of the protein secondary structure because the circular dichroism of the protein backbone is identical in aqueous solution and in the reversed micellar water pools. Therefore small changes in the neighbourhood of the tryptophans must be the cause of the changed fluorescence properties. The studies with LADH have been performed with two different buffer pH values (i.e. pH 8.8 and pH 7.0). This was done to obtain more information about possible charge effects. At pH 8.8 the protein overall charge is almost zero whereas at pH 7.0 there is an overall positive charge. Especially the anisotropy decay results of AOT reversed micelles show, that charge effects play an important role. At both pH-values a monotonic increase of the rotational mobility of the protein molecules with increasing water pool size is observed. The difference lies in the fact, that at pH 8.8 the rotational mobility at the highest w_o-value is almost identical to that in water, whereas at pH 7.0 the rotation in the same micelles is considerably retarded.

The importance of charge effects was also found for cytochrome c containing AOT micelles. In the CTAB micellar system these effects are less pronounced. Only marginal differences in the rotational dynamics of the protein at the different pH-values are observed. This can be due to the fact, that in neither case the LADH molecule and surfactant have opposite charges but it is also possible, that with CTAB as surfactant the charge of the interface plays a less important role on the properties of the micellar interior than in the AOT micelles.

Literature

1. Chatenay,D., Urbach,W., Nicot,C., Vacher,M. & Waks,M. (1987) J. Phys. Chem. **91**, 2198-2201.

2. Atik,S.S. & Thomas,J.K. (1981) J. Am. Chem. Soc. **103**, 3543-3550.

3. Visser,A.J.W.G., Vos,K., Santema,J.S., Bouwstra,J. & van Hoek,A. (1987) Photochem. Photobiol. **46**, 457-461.

4. Visser,A.J.W.G., Vos,K., van Hoek,A. & Santema,J.S. (1988) J. Phys. Chem. **92**, 759-768.

5. Petit,C., Brochette,P. & Pileni,M.P. (1986) J. Phys. Chem. **90**, 6517-6521.

6. Pileni,M.P. (1981) Chem. Phys. Lett. **81**, 603-605.

7. Visser,A.J.W.G. & Fendler,J.H. (1982) J. Phys. Chem. **86**, 947-950.

SAMENVATTING

Omgekeerde micellen kunnen worden beschouwd als waterdruppeltjes in een apolair oplosmiddel, die worden gestabiliseerd door de aanwezigheid van zeepmoleculen. In deze druppeltjes kunnen eiwitmoleculen worden opgelost, die normaal gesproken niet stabiel zijn in een overwegend apolair milieu. Voor dergelijke systemen zijn de afgelopen jaren verschillende toepassingen beschreven.

In dit proefschrift is het onderzoek naar de eigenschappen van enkele eiwitten in omgekeerde micellen beschreven. Bij dit onderzoek heeft de nadruk gelegen op de fysische eigenschappen van de eiwitten zoals die kunnen worden bestudeerd m.b.v. bepaalde spectroscopische technieken (b.v. fluorescentie en circulair dichroisme). Deze technieken kunnen worden toegepast dankzij het feit, dat omgekeerd micellaire oplossingen thermodynamisch stabiel en optisch transparant zijn.

Hoofdstuk 2 van dit proefschrift geeft een overzicht van dergelijke spectroscopische studies van omgekeerde micellen, waarbij ook systemen waarin geen eiwitten zijn opgenomen uitgebreid aan de orde komen. Eigenschappen zoals grootte, viscositeit, polariteit en uitwisselingssnelheid van de waterdruppeltjes zijn bepaald m.b.v. verschillende technieken, zoals verstrooiing, magnetische resonantie, en optische spectroscopie. Deze informatie is van groot belang bij de interpretatie van meetgegevens, die worden verkregen over in micellen opgeloste eiwitmoleculen.

Bij het in de hoofdstukken 4, 5 en 6 beschreven onderzoek is gebruik gemaakt van twee verschillende micellaire systemen. Het eerste systeem bevatte een negatief geladen zeep n.l. AOT (Aerosol-OT of natrium bis (2-ethylhexyl) sulfosuccinaat). In het tweede systeem was de zeep het positief geladen CTAB (cetyltrimethylammonium bromide). Op deze manier was het mogelijk om ladingsinteracties tussen het zeep/water grensvlak en de eiwitmoleculen in de waterdruppeltjes te onderzoeken.

In de hoofdstukken 4 en 5 is het gedrag van cytochroom c in deze micellare systemen beschreven. Dit gedrag is bestudeerd aan de hand van de spectroscopische eigenschappen van de ijzervrije en zink gesubstitueerde derivaten van dit eiwit. Meting van het circulair dichroisme van deze derivaten geeft informatie over de secondaire structuur van de eiwitmoleculen in de omgekeerde micellen. Het blijkt, dat in AOT omgekeerde micellen de secondaire structuur van cytochroom c bijna volledig verdwijnt.

In CTAB micellen wordt dit effect niet waargenomen. Tijdopgeloste fluorescentie metingen verschaffen inzicht in zowel structurele als dynamische aspecten van de systemen. Uit dergelijke metingen blijkt, dat er sterke interacties bestaan tussen cytochroom c moleculen en AOT grensvlakken. In CTAB micellen komen deze interacties veel minder tot uitdrukking. Deze resultaten kunnen worden verklaard door een electrostatische aantrekking tussen positief geladen cytochroom c en negatief geladen AOT. Electrostatische interacties tussen cytochroom c en negatief geladen grensvlakken komen ook in vivo voor. Het eiwit is namelijk gebonden aan het negatief geladen phospholipide cardiolipine in het mitochondriaal binnenmembraan.

In hoofdstuk 5 wordt de kinetiek van de triplettoestand van zink gesubstitueerd cytochroom c in omgekeerde micellen beschreven. Omgevingsfactoren en de aanwezigheid van quenchermoleculen kunnen de levensduur van triplettoestanden sterk beinvloeden. De resultaten van dit werk duiden evenals de bovenbeschreven resultaten op sterke interacties tussen cytochroom c moleculen en AOT grensvlakken. In CTAB micellen is deze interactie veel minder sterk. Door middel van quenching studies is het mogelijk om de uitwisselingssnelheid tussen de waterdruppeltjes van de CTAB micellen te meten. Het blijkt, dat deze uitwisselingssnelheid ongeveer duizend maal lager is dan de berekende botsingsfrequentie van de omgekeerde micellen. Blijkbaar is er een behoorlijke energiebarriere die genomen moet worden voordat een botsing tussen twee micellen tot uitwisseling van de inhoud ervan leidt.

In hoofdstuk 6 komt een ander eiwit aan de orde n.l. alcohol dehydrogenase uit paardelever (LADH). Het LADH molecuul is ongeveer zes maal groter dan cytochroom c en in vivo heeft LADH geen belangrijke interactie met membranen. De fluorescentie eigenschappen van de twee tryptophaan residuen in het eiwit zijn zeer gevoelig voor veranderingen in de omgeving van het molecuul. Een sterke verandering van deze eigenschappen wordt waargenomen als het eiwit in omgekeerde micellen wordt opgenomen. Circulair dichroisme wijst uit, dat deze veranderingen niet veroorzaakt worden door grote wijzigingen in de eiwitstructuur. De experimenten met LADH zijn uitgevoerd bij twee verschillende pH waarden (pH 7.0 en pH 8.8). Op deze manier is het mogelijk om meer informatie te krijgen over ladingseffecten. Bij pH 7.0 is het eiwit netto positief geladen terwijl het bij pH 8.8 netto vrijwel geen lading heeft. Het blijkt, dat vooral in AOT micellen het

effect van de lading van het eiwit invloed heeft op de interacties tussen eiwit en grensvlak. In CTAB is het ladingseffect veel minder sterk. Dezelfde trend werd waargenomen bij cytochroom c. Waarschijnlijk zijn de eigenschappen van het grensvlak in CTAB micellen anders dan in AOT micellen zodat ladingseffecten een minder belangrijke rol spelen.

CURRICULUM VITAE

Kees Vos werd op 3 juni 1960 geboren in Lopik. In 1978 behaalde hij het diploma Atheneum aan de Chr. Scholengemeenschap Oude Hoven in Gorinchem, waarna hij begon met de studie Moleculaire Wetenschappen aan de Landbouwuniversiteit in Wageningen.

In Januari 1983 legde hij het kandidaatsexamen af. De doctoraalfase van zijn studie omvatte de hoofdvakken Kolloidchemie en Biochemie. In januari 1985 studeerde hij met lof af.

Van januari 1985 tot april 1987 verrichtte hij, in dienst van de Landbouwuniversiteit, het onderzoek, dat leidde tot dit proefschrift. Vanaf april 1987 werkt hij in de technische automatisering bij BSO (Buro voor systeemontwikkeling) in Eindhoven.